وزارة التعليم العالي و البحث العلمي

BADJI MOKHTAR – ANNABA UNIVERSITY جامعة باجي مختار–عنابة

UNIVERSITE BADJI MOKHTAR – ANNABA

FACULTE DES SCIENCES DE L'INGENIEUR Année 2010

DEPARTEMENT DE GENIE MECANIQUE

THESE

Présentée en vue de l'obtention du diplôme de

DOCTORAT D'ETAT

Surface finish generation in machining stainless steel

Option: PRODUCTIQUE

Par

Nehal Abdelaziz

DIRECTEUR DE THESE : HAIAHEM A Pr Université de Annaba

DEVANT LE JURY

PRESIDENT :	**Ali Rachedi M.**	**MC**	**EPST Annaba**
EXAMINATEURS :	**Assas Mekki.**	**M.C**	**Université de Batna**
	Bouchelaghem. A.	**M.C**	**Université de Annaba**
	Khenfar Khadidja	**M.C**	**Université d'USTHB**
Invité	**Boutaba Smail**	**MC**	**Université de Guelma**

ABSTRACT:

The project is designed to examine the surface finish achieved on stainless steel when machining is a lathe using a cemented carbide tool. The finish forces and the ship thickness have been measured and observed using the talysurf 5 and the scanning electron microscope.
A wide range of parameters were considered.

The relationship between the measured parameters and the surface geometry were defined, some of which have been defined as primary (introduced by tool shape) and others as secondary (introduced by metallurgical interaction). The materials were 247 165 annealed and cold drawn, AISI 304, free cutting BS970.303 S21.

It was found at although no tool wear was seen in these test, sponzipfel accounted for the variation of the surface finish and that if the forces were reduced a better finish could be expected. This was especially true on the 303 S21. The surface finish measurements were shown to be highly being withing+10% off a specific surface and closer to +40% off two surfaces machined under apparently the same condition. Tool geometry to give feed marks with an enhanced squeezing effect was produced. A great amount of sponzipfel was observed no wear was noticed. It has been found that sponzipfel is the phenomenon that is probably the major cause of the variable readings on measured surfaces.

RESUME:

Le travail traite l’analyse des surfaces finies lors de l’usinage de l’acier inoxydable en tournage en utilisant un outil en carbure métallique. La surface finie et la surépaisseur du copeau ont été mesurées et contrôlées en utilisant un rugosimétre et un microscope électronique. Un grand nombre de paramètres ont été considérés.

La relation entre les paramètres mesurés et la géométrie de la surface a été évaluée.

Plusieurs types de géométrie ont été définis, parmi lesquelles quelques une ont été considérées comme primaires introduites par la forme de l'outil et d'autres comme paramètres secondaires introduites par les interactions métallurgiques.
Les paramètres utilisées sont k'acier de nuance 247165 recuit et étiré a froid de référence AISI304, de décolletage BS970.303.S21.

Il a été constaté qu'aucune usure de l'outil n'a été apparente durant ces testes, par contre il a constate un écrasement de matière sur la pièce lorsque les forces sont réduites, un meilleur état de surface peut être attendu, cela a été vérifié pour l'acier 303S21.

L'analyse des surfaces finies a montrée une variation avec un intervalle de 100% à 40% avec les mêmes conditions de coupe. De larges empreintes sont produites par la géométrie de l'outil avec la formation du coupeau et la poussée du métal qui sont observées et aucune usure importante n'as été constatée sur l'outil.
Il a été conclu que la variation de l'état de surface ne peut être due a l'usure de l'outil, mais très possible a l'écrasement de la matière.

الملخــص

يهدف البحث إلى اختبار السطوح المشطبة المحصل عليها تشغيل الفولاذ المقاوم للصدأ على المخرطة بأداة كربيدية. ثم قياس و ملاحظة قوى القطع و سمك الحدادة باستعمال ميكروسكوب إليكترون ماسح.

هناك عوامل عديدة تم أخذها بعين الاعتبار. ثم قياس العلاقة الرابطة بين العوامل التي تم قياسها و هندسة السطح, ثم تعريف أنواع هندسة عديدة بعضها ابتدائي نتج من تشكل الأداة و البعض الأخر ثانوي نتج من التداخل المعدني.

المواد هي 277165 مدنه تم تبريدها AISI 304 تشغيل حر BS 970.303.521 .

تم التأكد من خلال الاختبارات بعدم وجود تتام الأداة « Sponzipfel ».

فسر التفاوت للسطح المشطب و إذا خفضت القوى يمكن تشطيب افشل.

و على وجه الخصوص كان حقيقيا بالنسبة للمادة 303521. تظهر قياسات السطح المشطب مرتفعة ب 10 % بالنسبة النوعية و قريبة من 40% من سطحين مشغلين تحت نفس الظروف ظاهريا.

الشكل الهندسي للأداة أثاره بسبب التعدية بوجود تأشيرة متدبدبة.

كمية كبيرة من « Sponzipfel »تم ملاحظتها و لم يلاحظ أي تثلم.

لقد وجد « Sponzipfel » و هو ظاهر .يحتمل ان يكون السبب الرئيس للقراءات المتغيرة علي السطح الذي تم قياسه.

CONTENTS

ACKNOWLEDGEMENTS

LIST OF FIGURES.

SYNOPSIS

List of Figures

REMERCIEMENTS.

Au terme de cette thèse, j'aimerai remercier les personnes qui ont participé de prés ou de loin à la réalisation de ce travail et qui m'ont aidé et soutenu pendant la préparation de ce travail.

Tout d'abord, j'exprime toute ma reconnaissance à Mr Ammar Haiahem, Professeur et directeur du Laboratoire L.M.I mon directeur de Thèse qui a dirigé mon travail avec beaucoup de soin et de disponibilité qu'il soit remercie pour tout le temps qu'il ma consacré ainsi que pour les précieuses remarques et conseils dont il ma fait bénéficier.

Je remercie vivement Mr Mahieddine Ali Rachedi qui m'a fait l'honneur de présider le jury de soutenance de ce travail. Mr A. Bouchelaghem maitre de conférences à l'Université de Annaba.

Mr Ellias Hadjadj Maitre de conférences est remercié pour tous son soutien et ses conseils très avisés.

Je remercie également Mr Assas Mekki Maitre de conférences à l'Université de Batna. Mr Boutaba Smail Maitre de conférences à l´université de Guelma. Mme Khenfar Khadidja Maitre de conférences à l'Université des sciences technologiques Haouri Boumediene Alger d'avoir accepter d´être membre de jury et pour avoir pris toute la peine pour se déplacer .Je tiens à leur exprimer toute ma gratitude.

J'aimerai saluer tous les membres du département de Génie Mécanique de Annaba, particulièrement ceux du L.M.I et précisément Mr Kamel Bey Maitre de conférences et chef de département, Mr B. Bouzitouna,A ,Mr Kallouche pour leur soutien lors de la réalisation de ce travail.

Enfin je ne pourrai conclure ces remerciements sans évoquer ma famille et particulièrement mon père, ma femme et mes enfants Ahlem , Ramy et Akram pour leur patience leur soutien et leur compréhension qui m'ont été si bénéfiques pendant la rédaction de cette thèse.

CHAPTER I

INTRODUCTION

INTRODUCTION:

Metal cutting is the term intended to include operations in which a thin layer of metal is removed by wedge shaped tool from a larger body [110]. The principle used in all machine tools is one of generating the surface required by providing relative motions between the cutting tool and work piece. The cutting tool removes a layer of work material. The removed material is called a shaving or a chip. This has been a technology and a craft since the process ring work of Taylor, shop floor personnel had made considerable achievements before that time which made a major contribution to the success of the industrial revolution [111].

The technology of metal cutting has been improved by the developments in tool materials and understanding of the surface finish, today metal cutting is a very large segment of most industries , production of domestic equipment and the machine tool industry itself, all having large machine shops with many thousands of employees engaged in machining [112].

Progress in the technology of machining has been achieved by ingenuity and experience, the intuition and logical thought of many thousands of practitioners engaged in the many-sided arts of metal cutting[113],[114]. The workers operating the machine, the tool designer, the lubrication engineer metallurgist, the information technologist, are all constantly probing to find answers to new problems; these are created by the necessity to machine novel materials, and by the incentives to reduce costs, by increasing rates of metal removal, and to achieve greater precision or improved surface finish.

It is the search for mathematical parameters controlling the surface finish and its effect on the performance of the product in operation, to make possible improved surface values and thus reduce a cost which has been responsible for some of the developments in the past[115].

CHAPTER II

LITERATURE SURVEY

2. Literature Survey:

2.1 Terminology used machining:

Turning in one of the commonly employed operations in experimental work on metal Cutting. The work piece is held in the headstock of the lathe and rotated about an axis parallel to the lathe bed. The tool is rigidly held in a tool post and moved at a constant rate along the axis of the work material [4][1].

Three parameters associated with the cutting conditions must always be defined.

a) Cutting speed, this is the relative rate of movement of tool and work piece, it is usually expressed in terms of meters /min.
b) The depth of cut is the thickness of metal removed from the bar, measured perpendicular to the axis of rotation of the work piece.
c) The feed, this is the relative incremental movement of the tool into the work piece and it is usually measured in mm/rev.

The product of these three variables gives the material removal rate, a quantity which is used to measure the efficiency of cutting. As machining proceeds the face of the tool over which the chip passes in order to be discarded is the rake face.fig1.(b).This face is inclined at an angle to the axis of the work piece.

The angle formed between the rake face and a line parallel to the axis of the work piece is known as the side rake angle (α).

This angle is variable but is often of the order of $6\text{-}10^0$. A “negative rake” angle turns the chip through an angle greater than 900 causing the chip to flow back against the rotation of the bar. (fig1. (c), fig1. (d)).

The tool terminates in an end clearance face, which also is inclined at such an angle as to avoid rubbing the freshly cut surface.

The nose of the tool is at the intersection of three faces and may be sharp, but more frequently there is a “nose radius” between the two faces. The secondary cutting edge is formed by the intersection of the end clearance face. The flank face and the rake together form the primary cutting edge. (Fig 1. (a)).

Turning may be divided into the three major categories, orthogonal, semi orthogonal and non orthogonal (Fig2).

In the first case only the primary cutting edge is used and this is typified by turning on the end of a tube. The speed, feed and primary cutting edge are all at right angles. In semi orthogonal cutting the nose radius and secondary cutting edge are used and this is typified by turning on the outside bar. The vectors of the cutting speed and feed are mutually perpendicular. For non orthogonal cutting any or all the variables above may be altered but the most typical is that of using an approach angle on the primary cutting edge which means that this edge is inclined to the axis of rotation(Fig3).

The type of chip produced during metal cutting depends on the material being machined and the cutting conditions used.

2.2Cutting forces and chip formation process:

The forces acting on the tool are an important aspect of machining. The component of the force acting on the rake face of the tool normal to the cutting edge is called the cutting force F_c. This is usually the largest of the three components and acts in the direction of cutting velocity. The force required to form the chip is dependent on the shear yield strength of the work material under the cutting conditions used and the area of the shear plane (Fig4).

Two other forces, the shear force and the radial force also act on the tool and all three of these have their origin in the ship formation process.

Types of chip formed by cutting generally fall into one of three main groups:

a) Continuous without built up edge.
b) Discontinuous without built up edge.
c) Continuous with built up edge

In practice there is a gradual change from one distinctive type to another. The distinction between different chip types is not always obvious.

(a) Continuous chip without built up edge (Fig 5).a, a continuous chip formed by steady plastic deformation in the primary shear zone. Use of ductile materials, high speeds and unlubricated conditions gives rise to this type of chip.

(b) Discontinuous chip without built up edge Fig (5).c,a discontinuous chip Which is formed by unsteady plastic deformation and periodic fracture on the shear plane. Conditions which give rise to this type are use of an efficient cutting lubricant, low speed and brittle material.

(c) Continuous chip with built up edge (Fig 5).b, continuous chip which forms over a built up adhering to the rake face. Higher values of feed low speed and also poor properties of the lubricants give rise to this type of continuous chip.

2.3 The effect of cutting conditions on chip formation:

The built up edge is a structure formed at relatively low speeds and feeds when cutting many alloys. (fig6).

It is well known that built up edge has a large effect on surface roughness. The top of the built up edge is only semistable and this leads to the formation of scales on the workpiece surface.Fig7.Increasing either speed or feed gives rise to eventually no build up edge formation. The workpiece is still bonded to the tool rake face and shear is now confined to a narrow zone known as the secondary shear zone. This condition results from seizure at the tool workpiece interface.(Fig8).

At very low cutting speeds the interface is contaminated with oxide oil, air, etc, and the metal machined behaves in a brittle, manner as the primary shear plane exhibits low compressive stress, the chips produced are often discontinuous and slide easily along the rake face with low forces which encourages segmentation. Discontinuous chip formation results in irregular variation in tool forces .workpieces machined under these conditions show relatively smooth areas where cutting has occurred and fractured areas. In the

fractured areas segments of the work material have been removed from the surface leaving cavities. At higher speeds the contaminant layer is removed and bonding of the chip to the tool can take place and a built up may form.

Takeyamma and Ono have reported that mechanical bonding was caused by physic-chemical adhesion on an atomic or molecular scale. This adhesion is caused by one of the following:

- Metallic interlocking.
- Diffusion across the interface.
- Alloy production at the interface.
- Metallic compounds produced at the interface.

These workers also reported that the built up edge (B.U.E) was temperature sensitive only.

Williams, Smart and Milner have shown that a two phase material is required for B.U.E formation and several other workers have shown that two phase materials deform they do so unhomogeneously. Ashby has reported that even under a compressive stress, a shear stress may cause cracks to originate from a second phase particle where non deformable inclusions are considered.

From this, it may be seen that the surface is very dependent upon the deformation characteristics of the shear zone. It has been shown by Williams and Rollason [9] that the B.U.E. was formed with both a softer or harder second phase and the tool material had no effect on the B.U.E. except for resulphurised high speed steel. This may have been caused by the formation of a sulphide layer on the tool inhibiting seizure. It was suggested by Hovinga, [10] that flow from the deformation zone was of particular importance.

Shear around the built up edge had been observed by Dynes [11] to occur in narrow bands but the structure of these shear bands was irresolvable.

The shear zone was not resolvable optically but interpretation of the resulting structure aided by the use of two stage replicas in the electron microscope, this showed heavy cold working [12]. As previously state at low cutting speeds, the tool intermittently cuts and fractures the chip from the bar and hence a surface containing a fracture and a cut component exists. As the

speed increase the temperature generated by shearing is such that the cracking becomes shortened, ductility increases chip to tool contact and compression minimizes cracking. Smaller areas of fracture are left with the material.

At higher speeds the surface layer of the tool is cleaned and the bonding forces are high. These conditions give rise to a continuous chip. Continuous chip is formed by steady plastic deformation in the primary shear zone. Increasing speed gives rise to eventually no B.U.E. formation. Wallbank [13] has suggested that the built up edge is a fracture process aided by inhomogeneous deformation around inclusions.

2.4 The nature of the flow zone seizure at the chip/tool interface:

When speeds and temperatures exceed those at which the built up edge is stable, a secondary shear zone commonly known as the flow zone is formed at the chip/tool interface.

The existence of this second zone of shear has long been recognized but the conditions at the chip/tool interface necessary for its formation have not been fully understood.

The work material and tool material do not rub together as the standard friction theories but seizure occurs at the interface and shearing of the chip material takes place in a region close to the rake face over much of the contact area.

Wallbank [13] has shown, when a flow zone is present the work material wraps itself around a sharp cutting edge and the new surface is formed where the work material contact with the tool flank a short distance below the cutting edge.

The formation of the secondary shear zone and material behavior within it can be satisfactory explained by considering the conditions under which the seizure occurs. These conditions were first proposed and discussed in considerable detail by Trent [14, 15] (Fig9).

Under the conditions existing in metal cutting where a continuous chip is formed the stress on the rake face is so high that the real area of contact of work material with the tool becomes a large promotion of the apparent contact area. In the extreme case, where the two surfaces are completely in contact the force

parallel to the interface becomes independent of the normal force. The force required to move one surface over the other becomes that necessary to shear the weaker of the two materials across the whole area. This relationship is thus directly opposed to that of classical concepts of friction where the coefficient of friction is independent of the sliding area of the two surfaces [16].

Trent [17] has suggested when cutting mild steel at high speeds the flow zone is only 25μm thick. The flow zone appears to be of constant thickness even if the workpiece velocity changes by two or three hundred/min.

Over the chip/tool contact length the material at the top of the zone will be moving at a velocity close to the bulk chip speed, whilst the material near the tool surface will have zero velocity.

The resulting structure is nearly irresolvable using optical metallographic because of the intense deformation zone.

Some workers have used transmission electron microscopy to examine the structure of steel in the floor zone [16].Looking at the flow lines in a continuous chip and its measurement Zorev [18] has shown that the strain rate in secondary shear zone can be of the order of 4×10^4 per sec.

The strain rates are is accompanied by high temperatures (caused by the adiabatic heat generated in secondary shear).

Review of the results obtained in laboratory high- speed tension and shear tests at elevated temperatures in thus worthwhile[19,20].

Using different materials Nadai and Manjoine[19] have constructed graphs for final tensile strength versus temperature for particular strain tests. The ultimate tensile stress has got a distinct maximum and the temperature at which this occurred was a function of strain rate.

Campbell and Ferguson [21]; working with mild steel (0.12%C), show similar trends but their results are more applicable to the conditions that exist in

the secondary shear zone. Since they consider the yield stress in stress in shear (Fig 10).

The curves demonstrate that (a) for a fixed value of temperature, shear strength increases with increasing strain rate, and (b) for a fixed value of strain rate, shear strength decreases with increasing temperature.

Zorev [18] proposes that there is insufficient time for the metal in the secondary shear zone to recrystallise even at a temperature of 1000^{o}C.Other workers [20] however, believe that chip softening and recrystallisation is possible.

Sturne, [23] indicates that recovery process determine the strength of the material when hot working conditions at high deformation rates are present.

Trent [24], observed that, under severe working of the structure the heat generated in the flow zone caused recrystallisation on a scale visible by optical microscopy.

Dines [11] also observed such a structure present in a flow zone produced from 0.19%C steel cut at 46m/min with H.S.S tools.

Working over a range of materials Shelbourne [16] observed the final flow zone structure in all these materials are basically very similar consisting largely of equiaxed between 0.25-1.5μm in diameter. These are the product of dynamic recovery or recrystallisation processes in zones of thermoplastic instability where strains are extremely rapid.

He concluded that the contact area between the tool and work surface is so nearly complete over a large part of the total area of the interface that sliding at the interface is impossible under most cutting conditions.

2.5 Surface roughness:

The new surface generated during machining operations may be considered as the sum of two independent effects.

1. The ideal surface roughness which is the result of the geometry of the tool and the feed rate.

2. The natural surface roughness, which is a result of the irregularities in the cutting operation.

2.5.1 The ideal surface roughness:

The ideal surface roughness represents perfect replication of the tool geometry on the workpiece surface which may be calculated for a given tool shape and feed. This finish can only be achieved if defects such as built up edge, chatter, inaccuracies in the machine tool movement are eliminated completely. This is represented in (fig 11).

For the purposes of characterization, analysis and quantitative comparisons it is useful for a practical determination to be able to specify in meaningful way the roughness of machined surfaces using a single factor or index. The most common is Ra. This value could be obtained as follows:

From (fig 2) which shows a cross section through the surface under consideration, a mean line is first drawn parallel to the general surface direction which divides the surface in such a way that the sum of the areas formed above the line is equal to the sum of the areas formed below the line. The surface roughness value Ra is now given by the sum of absolute values of the areas above and below the mean line divided by the sampling length.

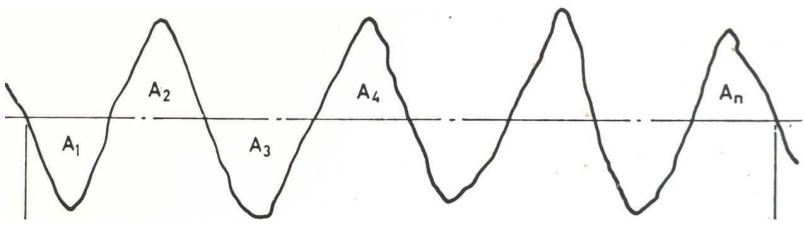

Thus, for example in Fig2,the surface roughness value is given by

$$Ra = \frac{\sum(Area A3 + A4)\,2}{f}$$

Where f is the feed, since the area A1+A2, A3+A4 are equal. For a round nose tool the following provides a good approximation: $Ra = \frac{32f^2}{Re}$.

Where f is the feed rate and Re is the nose radius. Equation 3 shows that the surface roughness value for such a surface is closely related to the feed and corner radius. The theoretical relationship between the surface roughness value and the feed are given by equation 2 tabulated in tables 2.

2.5.2 Natural surface roughness:

In practice, it is not usual to succeed in achieving the ideal surface described above, and normally the natural surface roughness form is a large contributor of the actual roughness.

One of the main factors contributing to natural surface roughness is the occurrence of a built up edge. Thus it would be expected that the larger the built up the rougher would be the surface produced.

In order to improve the surface finish we should reduce the built up edge. such factors would therefore be an increase in cutting speed, or the introduction of free machining materials such as resulphurized steels, the application of the correct cutting lubricant at low cutting speed.

Other factors which could contribute to natural surface roughness in practice are:

1) The occurrence of chatter or vibrations of the machine tool.
2) Inaccuracies in machine tool movement or the saddle on a lathe.
3) Irregularities in the feed mechanism.
4) Defects in the structure of the work material.
5) Discontinuous chip formation when machining brittle materials.
6) Tearing of the work material when ductile metals are cut at low cutting speed.
7) Surface damage caused by chip flowed.

The above discussion has been confined to the surface roughness produced by single point tool operations. The other surface finish parameters used in this thesis are:

- **Ra**: It is the arithmetic mean of the departures of the profile from the mean line. Fig1.
- **Rq**: Is the rms parameter corresponding to Ra. Fig 1.
- **Rmax**: Is the maximum peak to valley height of the profile within the sampling length L.(Fig 2).
- **Rt**: Is the maximum peak to valley height of the profile within the assessment length. (Fig 2).
- **Rtm**: Is the average of the Rmax of five consecutive sampling lengths.
- **R3tm** is the height difference between the third highest peak and the third lowest valley. (Fig 2).
- **Rp** is the maximum height of the profile above the mean line within the assessment length.(Fig3).
- **Rsk**: Skewness is measure of the asymmetry of the amplitude distribution curve about the mean line.Fig3a.
- **λa**: This is the arithmetic shape of the profile throughout the assessment length.
- **Δa**: This is the arithmetic mean shape of the profile throughout the assessment length.
- **Sm**: This is the mean spacing between profile peaks at the mean line, measured over the assessment length.(Fig4a).
- **Hsc**: The high spot count is the number of complete profile peaks projecting above the mean line. (Fig 3b).

2.5.3 Measurement of surface finish:

Surface finish is a complex parameter which is very difficult to specify in meaningful way. Many methods and numbers of instruments have been developed to measure surface finish. One of these instruments can be used by semi or unskilled operators but more complex instruments should be used by experienced and qualified operators in order to minimize errors.

The most simple are visual or touch comparator methods where a surface is compared with one of a series of standard surfaces. Methods using sophisticated equipment which will measure Rq, Ra and other parameters accurately and quick are also available. The most accepted measure of surface finish is the surface roughness value Ra. (Fig 12(a)).There are several main methods for surface texture, these are explained briefly below.

2.5.4Types of machine and information obtained:

The Taylor Hobson Talysurf:

The Taylor Hobson Talysurf is a surface finish measuring instrument which provides a wide range of parameters. The traverse unit houses, the motor and variable gearbox for traversing the pick up across the surface to be measured. It uses a processor to provide a selection of roughness and waviness parameters. The results are then selectable from the stored information and a surface finish graph. Fig12(b) or roughness value. [Table 3].

Several different methods are frequently used in measuring surface finish and the most common are described here.

Non instrumental methods:

Comparison with a roughness standard. Work produced is compared visually and by “feel” with sample surfaces acting as standards.

Interferometry method:

The method is useful for looking very highly finished surfaces. It is a technique suffering from a limited depth of field at high magnifications, interpretation difficulties may also be observed if the surface is rough.

Depth of field method:

This method utilizes the depth of field limitations mentioned above. At high magnifications fraction of a micron may possibly be resolved in height. This method seems to be compromise between rough and smooth surface usage. For very smooth surfaces the technique would show little detail and for very rough surfaces only small area would be in focus at any one time. This is a simple method and relatively quick.

Absorption method:

This method uses a replica of the surface which is transparent to light. This replica is placed against a glass cover slip and some translucent liquid sandwiched between the two. When viewed in the microscope using transmitted light the surface is seen to be darkest where the most liquid is.

This gives a contour effect. Large areas of rough surface may be viewed by this method and although not demonstrated smooth areas should show good results.

Brightness measurements:

This method may be subjective or made more accurate by the use of a photometer and controlled light source. The correlation between reflectivity and Ra values is not good and is expected to vary in a complex manner with surface geometry.

2.5.5Meaning of indices used to measurement of surface finish:

Surface roughness is measured by the heights of the irregularities with respect to an average line as shown in (Fig 11).These measurements usually are expressed in micrometers .In most cases the surface roughness value Ra is used but also it is identified by centre line average previously known as CLA or Rq (the root mean square average).

Surface roughness value:

The surface roughness value previously known as CLA (AA) is the standard adopted in Great Britain and USA since 1955.It is defined as the average height from a mean line of all ordinates of the surface, regardless of sign. It is frequently calculated from Ra=$\frac{\sum A}{l}$

∑A=sum of areas above and below the mean line in mm^2 L is the length over which A is calculated i.e. the sampling length.

L=Length of trace in mm.

This is sometimes known as the arithmetic average height.

Root mean square (Rms):

This is defined as the square root of the squares of the ordinates of the surface measured from a mean line.

This measure was standard until it changes to CLA value.

If equally spaced ordinates are erected at 1, 2, 3, 4, k, whose height are h1, h2, h3, h4, then:

$$h.r.m.s = \frac{1}{l}\int_0^l h^2 dl^{\frac{1}{2}}$$

Where h is a ordinate from the centre line and l is the sampling length.

Roughness, waviness and errors of form:

Waviness and errors of form are characteristics of surface geometry which are not classified within the roughness category. Two classes of these arise: “Errors of form” are generally associated with deflection with incorrectly set up workpiece or irregularities in the feed mechanism. “Roughness” is generally associated with chatter (periodic tool/workpiece deflection), feed marks

(produced by the impression of the nose radius of the tool on each revolution) and fine scale surface damage to these feed marks.

The information obtained from the Talysurf has the widest application in quality control in industry. The most common pieces of information used are the RMS and CLA values of the surface and these have been found to correlate of performance criteria.

It must be noted that these are not the only way of characterising surfaces and that others may prove more advantageous.

2.5.6 Mechanisms of surface finish production:

There are six basic mechanisms which contribute to the production of a surface which has been machined [25]. These are:

1. The basic geometry of the cutting process.
2. Too1 wear and the influence of this factor on squeezing (sponzipfe1).
3. The efficiency of the cutting operation.
4. The stability of the machine too1.
5. The effectiveness of removing swarf.
6. The effective clearance angle on the cutting too1.

2.5.6.1 The basic geometry of the cutting process:

In a single point turning the tool will advance a constant distance axially per revo1ution of the workpiece. The resu1tant surface will have on it when viewed perpendicular1y to the direction of tool feed grooves replicating the shape of the tool (Fig II.) These are known as feed marks and their formation is included in the ideal surface finish.

2.5.6.2 Tool wear and the influence of this factor on squeezing (sponzipfel) effect:

Too1 wear has an effect on surface roughness. Of the three main forms of wear which are known to occur (Flank wear, crater wear, notch wear). Flank wear is,

the most commonly observed form. This is caused by the rubbing action of the newly machined workpiece surface the clearance face (flank) of the tool.

It has been known that during fiÎish turning surface metal is disp1aced in a direction opposite to the feed. Smal1 grooves are often formed on the too1 at the feed mark. The disp1acement of metal is cal1ed the squeezing effect (Fig 13). The large local pressures generated between the flank of the too1 and the workpiece surface which is being generated allows the metal to flow sideways. This hypothesis is supported by the fact that a newly sharpened tool squeezed less than a worn too1 [26].

It had been known for some time that grooving wear occurred when cutting various materials and several theories have been proposed.

Pekelharing [27]: Describes the formation of small grooves on the end cutting edge. He has suggested that squeezing of metal in the chip formation process leads to an increase in the height of the feed marks and this may, in tom have some effect on groove formation.

2.5.6.3 The efficiency of the cutting operation:

Under some cutting conditions feed marks may not be the most significant effect. Two significant variations can occur related to the type of chip formation:

- Cutting under conditions, using large feeds, low cutting speeds (but not conditions which lead to unstable B.U.E. production), the cutting process itself can become unstable. Instead of continuous shear occurring in the shear zone. Tearing takes place and a discontinuous chip forms. Discontinuous chips are produced by fracture on the primary shear plane. The result is a poor surface finish.
- Cutting with an unstable built up edge will produce a surface which contains hard built up el1ge fragments which will result in an increase in surface roughness.

a) Surface generated by a discontinuous ship:

A discontinuous chip is formed by unsteady plastic deformation and periodic fracture on the shear plane. These are produced at low speeds. The mechanism has

been investigated by many authors[28.29.30] The tool intermittently cuts and fractures the chip from the bar, therefore a surface:

Containing a fracture and a cut component exists (Fig 14).

The work of Shaw, on free machining steels, dealt with both leaded and resulphurised steels. It was shown that at low speeds an increase in sulphur content improved the surface finish. This was attributed to the sulphide inclusions acting as crack nuclei thus enabling the discontinuous chips to break in smaller pieces and produce a less fractured surface.

JA. Bailey [29] using the S.E.M. saw that during the propagation of this crack, microcracks and voids may occur. This intermittent cutting action also left chatter marks on the surface.

Furthermore [31], he observed that a fracture started near the nose of the tool and travelled into the metal. Secondary cracks could occur once the primary fracture had been formed. It was suggested that bending of the chip produced fracture. Long grooves have been identified in the area between fractures.

An increase in speed leads to an increase in ductility. The chip seizes to the tool and compression minimizes cracking. Resulting in material left behind on the area fractured. Finally a continuous chip is produced and in two phase metals a built up edge can form.

b) Surface generated when B.U.E. is present:

The built up edge has a large effect on the machined surface. At intervals a discontinuous shear process occurs at the top of the built up edge producing a 'scale' on the workpiece and the chip surface. The built up edge has been investigated by many workers but its instability is largely unexplored.

Williams and Rollason [32] suggest that this occurs because the built up edge is essentially a fracture process which is aided by the addition of possible crack nuclei.

Dynesll found that thermoplastic shear occurred in this area in 0.2% C and O.4%C steel. It was suggested that these were nucleated by inhomogeniety in the structure

such as a cementite plate or sulphide inclusions.

c) Surface produced when machining with a continuous chip:

A continuous chip is formed by steady plastic deformation in the primary shear zone. The chip flowing over the tool clearance face is in contact with the tool over a certain distance beginning at the cutting edge.' Laudherer, and Zaat [33] have shown a system whereby material flowing down a smooth surface contacts an asperity and deformation takes place. This deformation causes a localised build-up which may break away from the asperity by deformation or fracture. These deformations on the surface were termed microchips. Their size being determined by the stability of the system.

The number of microchips present is stated to be dependent on many factors some of them are:

a) The roughness of the 1001 Bank surface.

b) The inherent roughness of the freshly generated surface.

c) The hardness and *Bow* characteristics of the workpiece material and their variation with temperature.

d) Meta1lurgical compatibility to weld.

e) Contamination effects of lubricants.

Templeblack and RamaHngham [34] have shown that the use of replicas in the transmission electron microscope is a valuable way of studying surfaces. Velar types of damage have been seen and described by other workers [35].

Microcracking was observed in the surface region which was explained as resulting from a tensile stress field which exists below the cutting edge of the too1. . Ridges on the workpiece surface after cutting, were reported as resulting from grinding scratches on the tool during its preparation.

J.A. Bailey [36] investigated the formation of microchips on machining of AISI 4340 steel (a medium carbon low alloy steel). Using a carbide tool and viewing surface features in an S.E.M. microchips and surface ridges were easily seen.

Surface damage was observed to decrease with increased speed. The number of grooves was also found to increase. Four different types of microchip were noted all of which were formed by similar mechanisms:

1) Standard microchip and groove.
2) Microchip removed but groove visible.
3) Microchip redeposited on surface after
4) Microchip associated with tool fragment.

The last one was also seen by Nishina [37] working on an annealed 18% managing steel at low speeds (6m/min).

Bailey also observed a number of other surfaces features in other works [31.37].

a) Cavities.
b) Micro cracks.
c) Plastic deformation.
d) Voids.

An increase in speed produced a decrease in void and cavity formation and also the long straight grooves became discontinuous and ill defined. These grooves are again attributed to grinding marks on the tool and their disappearance at higher speeds is attributed to the higher temperature causing a burnishing effect.

Using lubricants on further tests he showed that the general trends were as for unlubricated condition except that the amount of plastically deformed debris was considerably reduced. In all these experiments chatter marks were noted as well.

2.5.6.4 The stability of the machine tool:

Under some cutting conditions (workpiece size, method of setting and cutting tool rigidity relative to the machine tool structure). Instability can be set up in the tool which causes it to vibrate. These vibrations result in a waveform on the surface. This phenomenon is known as chatter in the machined surface.

2.5.6.5 The effectiveness of removing swarf:

In discontinuous chip production, machining such as tuning of brittle materials, the chip breaks and slides easily onto the rake face because the surface is contaminated by cutting fluid or other substances.

Leaving the cut surface the chip is likely to encroach on and mark the surface generated and the result is a poorer surface finish.

2.5.6.6 The effective clearance angle on the cutting tool:

Due to the cutting tool wear a combination of minor cutting edge relief and clearance angles it is possible to cut on the major cutting edge and burnish on the minor cutting edge. This can produce a good surface finish.

2.6 Tool Wear Mechanisms:

Introduction:

Cutting tools are subjected to constant wearing during machining. Wear resistance, toughness and hot hardness are essential properties of a cutting tool material. High speed steels are, tougher than cemented carbide and ceramic tools, but they are still sufficiently hard to cut most metals. The original shape of a tool is altered over the machining time. The wearing process involved being time dependent. The work of Taylor showed that an empirical relationship exists between cutting speed and tool life (fig 15), namely:

$$\frac{v}{v_r} = \frac{t_r}{t^n} \qquad (38)$$

Where:

v = cutting speed

t = tool life

n = constant

t_r= measured tool life for a given cutting speed v_r

The Taylor tool life equation has been applied in the form:

$$v_t^{\,n} = c \qquad (39)$$

Where:

v is measured in meter per minute, t in minute.

Equation 2 can be expressed as:

$$LogV = LogC - nLogT \qquad (40)$$

If different values of $Log\ T$ are plotted against corresponding values of $Log\ V$, and if cutting speed is neither too low nor too high, it is found that the resulting curve is linear, as a graph similar to that shown in (fig 15[6]).

In almost all machining operations the action of cutting gradually changes the shape of the tool and it ceases to cut efficiently, or fails completely [41]. Catastrophic failure is avoided by using the tool until a certain predetermined magnitude of wear which is sufficiently lower than a wear level that would initiate complete fracture. End of tool life may also be related to surface finish. The tool may be reground or replaced when it fails or ceases to cut. The length of time during which the tool is actually engaged in cutting before this maximum allowable magnitude of wear is exceeded is known as the tool life. Often the skill of the operator is required to detect symptoms of the end of tool life, to avoid the damage caused by total tool failure making tool life very subjective. Tool wear manifests itself in different forms on different parts of the too1. There are four regimes of tool wear: flank wear, cratering, gross tool fracture, and notcbing (Fig 16a,b).

Metallographic sections have been taken from the worn surfaces and prepared in order to study the wear of tools, usually either normal to the cutting edge or parallel with the rake face. Observations have shown that the shape of the tool edge may be changed by plastic deformation as well as by wear. The distinction is that a wear process always involves some loss of material from the tool surface though it may also include plastic deformation

locally so that there is no sharp line separating the two.

Most data from tool-life testing has been compiled by carrying out simple lathe turning tests in continuous cutting, using tools with a standard geometry, and measuring the width of the flank wear land and sometimes the width, depth and position of any crater found on the rake face.

The results of one such test programme, cutting steel with high speed steel tools over a wide range of speed and three feed rates is .given by Opitz and Konig [42] and (figure 17) is taken from these results. For crater wear the results are simple, the wear rate being very low up to a critical speed, above which cratering increased rapidly. This critical speed is lowered as the feed is increased. This may be related to the built up edge on the tool face during cutting which can affect the tool wear rate in various ways, sometimes decreasing the life of a cutting tool and sometimes increasing it. With an unstable built up edge the highly strain-hardened fragments, which adhere to the chip under surface and the new workpiece surface, can increase the tool wear rate by abrading the tool faces. However when materials such as cast iron are cut, the presence of a stable built up edge can be beneficial43. A stable built up edge protects the tool surface from wear and performs the cutting action itself fig 7a. A built up edge can also contribute to sudden tool failures when tools with carbide inserts are used (Fig 7b).

For flank wear also the wear rate increases rapidly at about the same speed and feed as for cratering. It is in this region that the temperature dependent wear mechanisms control tool life.

Below this critical speed range, Bank wear rate does not continue at a low level but often increases to a high value as attrition and other wear mechanisms become dominant.

Classification:

The wear and deformation process which have been observed to change the shape of high speed steel tools were classified by Trent [44] into the

following divisions:

1. Superficial plastic deformation by shear at high temperature.
2. Plastic deformation under compressive stress.
3. Diffusion wears.
4. Attrition wears.
5. Abrasive wear.
6. Wear under sliding conditions. Also failure can occur by processes such as.
7. Thermal fatigue.
8. Corrosion/oxidation and atmosphere attack.

2.6.1 Superficial plastic deformation by shear at high temperature:

When cutting steel at high rates of speed and feed, a characteristic form of wear is the formation of a crater, a hollow in the face behind the cutting edge. The extremely intense shear[9] strain and very high strain rates generate much heat in a small volume of metal greatly increasing its temperature such that the flow zone becomes the major heat source raising the tool temperature.

Besides the centre of the hot spot, the surface layers of the tool may be sheared in the direction of chip flow to form a shallow crater, with tool material swept to the back to form a ridge [45].

This phenomenon occurs also when cutting titanium and its alloys, and nickel and its alloys.

When cutting the stronger alloys it occurs at much lower cutting speeds than when cutting the commercially pure metals. It has been found46 that nearly pure iron may shear away layers of high-speed steel. The temperature increases from 6500 C near the cutting edge to about 9000 C.
Where the tool surface is being sheared to form the crater. Therefore it is possible that the pure iron can shear high speed steel. This is because the yield stress of high speed steel is greatly lowered at high temperature and low strain rate. The rate of strain of pure iron in the flow zone is very high and this leads to an increased strength in this material.

ô: stress (flow)

E: Strain

E: strain rate

n and m are constants

At low temperatures n are high and m is low. As the temperature rises n decreases and m increases. Therefore at high temperatures a high strain rate can offset the basic low strength of pure iron against a low strain rate in the high speed steel.

This wear mechanism forming deep craters, is not frequently observed under industrial cutting conditions, but it is a form of wear which high speed tools. This mechanism is not the only one responsible for crater formation.

2.6.2 Plastic deformation under compressive stress:

The shape of the tool may be changed by plastic deformation resulting from the high stress and temperature nears the edge during cutting. The compressive stress acting on the rake face tends to deform the tool, and a basic requirement of a cutting material is a high yield stress in compression. The upper limit to the rate of metal removal may occur when the tool is no longer able to resist the stress and temperature near the edge.

Wright and Trent [48] observed that stress and temperature distribution did not give rise to plastic deformation when cutting low carbon iron. However, it was further observed that cratering along the rake face took place as a result of plastic deformation.

Cutting cast iron and Nimonic 75 [5] Wright found that the temperature of the cutting edge was high and the edge was thermally weakened and

deformed by the compressive stresses. With cemented carbide tools cratering by plastic deformation has not boon observed but they do exhibit plastic deformation near the cutting edge [49]. It is most commonly observed when cutting at higher speeds and food rates than with high-speed[11] steel-tools [50] because of their much higher proof stress at temperature.

2.6.3 Diffusion wears:

The study of the structure of metals provides evidence that conditions exist where diffusion across the tool work interface is probable. Seizure occurs at the interface and the temperature is high enough for diffusion. Beyond the edge of this contact there is a region where visual evidence suggests that contact is intermittent [51] (Fig 8). The tool surface may be dissolved by the work material flowing over il. The basic requirements for diffusion wear are: [52]

- Metallurgical bonding of the two surfaces so that atoms can move freely across the interface
- Temperatures high enough to make rapid diffusion possible.
- Solubility of the tool material phases in the work material or vice-versa.

This is a wear mechanisms that becomes important when cutting relatively high melting point[12]metals and alloys at high cutting speeds where high temperatures are generated.

A white layer has been observed [52,53,54] under certain conditions at the interface between tool and work-piece material and this suggests that diffusion may make a contribution to tool wear.

Diffusion wear is observed in ceramic tools, although it is of lesser magnitude compared to other tool materials. Pure alumina ceramics are said to have better resistance to diffusion wear as compared to mixed ceramics. At high cutting speeds, it has been found that wear due to plastic deformation can be observed. A study on the wear mechanisms of sialon tools has verified this

[57].

Evidence for diffusion-wear is circumstantial since direct observation of the process is not possible by optical metallographic, but by examining the worn surfaces, it is possible to infer that the mechanism occurs. When cutting steel with cemented carbide tools at high speeds, temperature of 1000° C or more may occur on the tool rake face at the position of the crater. Metallographic examination of 100 is used in this way reveal that a crater is worm in the rake face but that the surface of this crater is smooth.

Observation of flank wear on **wc-co** tools used to cut steel at high speeds show that they wear more rapidly than tools containing mixed carbides resulting from an addition of **TiC** or **TaC**..

Others suggests that wear on the flank under these conditions is also mostly caused by diffusion
process [58].

Trent has suggested that a crater is formed as the atoms of the Tungsten carbides diffuse out of the tool to be carried away by the chip.

At low speeds tool wear rates by diffusion become insignificant because interface temperatures are too low, tool life should become effectively infinite at low speeds, if based purely on a diffusion wear mechanism.

The problem of machining steel at high speeds with cemented carbide tools was improved by addition in the tool material of one' or more of the cubic carbides **TiC**, **Tac** and **Nbc**. When cutting a medium-carbon steel with a tool containing **TiC WC** and **Co** one with just **WC+Co**, although cratering wear starts at about the same speed with the tool containing **TiC**, the wear rate increases only very slowly with cutting speed.

For many steel-cutting applications coated tips pennit higher cutting speeds or give much longer too life at the same cutting speed.

High-speed steel tools are also worn by a diffusion process when cutting steel and other metals at high speed. In the case of steel tool it is the atoms from the matrix that diffuse across the interface are carried away in the work materia1 [58].

"Throw-away" tool tips have been developed consisting of a cemented carbide substrate coated with TiC and a very thin layer of Al_2O_3 over this.

These are claimed to give longer tool life than TiC-coated tools, probably by making use of the resistance of $A1_2O_3$ to diffusion wear, without the sensitivity to mechanical and thermal stresses which limits the use of alumina tools [58].

2.6.4 Attrition wear:

Attrition is a wear mechanism that usually occurs at relatively low cutting speeds and temperatures. At low cutting speeds, the flow of metal past the cutting edge of the tool is irregular and less streamlined. Under these conditions a built up edge may occur and contact between the tool and work material might become less continuous. Under these conditions. and others that give rise to fluctuating forces and temperatures, fragments of a microscopic size may be plucked mechanically from the tool surface and this is known as attrition [59]. Worn surfaces of the tool caused by attrition are usually irregular compared with the smooth surfaces resulting from diffusion.

It has been found [60] that the rate of wear by attrition decreases as the speed is raised. Using high speed steel tools, attrition is usually a slow form of wear. More rapid destruction of the cutting edge occurs when cutting is discontinuous or may be aggravated by poor machine conditions such as lack of rigidity.

In the presence of a stable built up edge tool life may be very variable. It can act as a protective cover, preventing contact between tool and work material as in cutting steel with **H.S.S.** tools, but under some conditions (e.g. when cutting cast iron with **WC-Co** cemented carbide tools), attrition wear is often found to be severe when a build up is present.

The **WC-Co** alloy tools are usually more resistant to attrition wear than are those containing the cubic carbides (titanium, tantalum etc). Ceramics are less resistant to attrition wear. The finding of many experimental works suggest that ceramic tools suffer attrition wear at low cutting speeds [61.62,63] and also high speeds when a continuous chip is present This indicates that the border the tool material the more likely it is to suffer from attrition wear.

2.6.5 Abrasive wear:

In abrasion, material is removed from a softer surface by border particles by processes sometimes referred to as repeated ploughing, or the formation of microchips. Abrasive wear may occur when machining work materials containing bard inclusions such as carbides, oxides and silicates. The majority of workpieces are less than half the hardness of the tool, making abrasion by the bulk of the workpiece unlikely. For abrasive wear to take place, it is generally assumed that the abrading substance must be considerably border than the surface that is worn.

In high speed steel tools, the particles are border than the matrix and retain this hardness to higher temperature.

Trent found [64] that in cast iron and steel particles of a few microns size, consisting of carbides of iron, chromium, titanium, radium, etc, and also oxides in particular AL_2O_3 but also silica and some silicates are as bard or harder than the carbides used as the basis for cemented carbide tools. Such particles in the work material may cause abrasion. However direct evidence for this mechanism in the literature is bard to find but it may account for the high wear rate when fatigue cracks mainly propagate along grain and phase boundaries. Oxidation and wear have an obvious influence on the mechanisms leading to thermal fatigue. These phenomena increase with decreasing titanium carbide content and even more with increasing Cobalt-content in cemented carbide tools. This mechanism tends to be prevalent around the edges of contact of the chip with the tool.

Corrosion is used to describe the eating way of a solid material by its environment; it is most commonly applied to the deterioration of metals due to chemical attack which is oxidizing in nature, and this can produce changes in properties, without necessarily causing any alteration in dimension or appearance [70].

When machining a low carbon steel at low feed using carbon tetrachloride,

as a lubricant, severe tool wear was noticed by Wallbank [13]. He suggested that corrosion may occur on bath equally as quickly because they are chemically similar. However the areas of the two surfaces are very different and hence it only appears that the tool is suffering preferential corrosion.

2.7 Influence of non metallic inclusions on machine ability:

In some materials, a deliberate addition is made, to provide isolated particles which will improve the machinability of a structure.

Thus in free machining steels, the presence of high sulphur contents and excess manganese, above that required for dioxidation cause free globules of manganese sulphide to form which are scattered throughout the structure.

Free machining steels with additions of 0.1 to 0.3% sulphur or 0.1 to 0.35% lead or combinations of both are common. Free cutting steels with up to 0.2% sulphur require up to 1.0% manganese to ensure that all of the sulphur is present as isolated globules of manganese sulphide.

These additions reduce cutting forces, cutting temperatures and tool wear rates.

2.7.1 Inclusions beneficial to machinability:

It is now well known that non-meta1lic inclusions are a major factor in determining the machinability of steel. Depending on their type, size, shape, distribution and volume fraction, on metallic inclusions are either beneficial or detrimental to machinability.

Kiessling [71] has listed four parameters that a non-metallic inclusion should have in order to improve the machinability of a steel.

a) The inclusions should act as stress raisers in the shear plane of the swarf (chip) so initiating crack formation and embrittling the chips. The chip-tool contact length then decreases which is an advantage. They should not, however, be such strong stress-raisers that the workpiece cracks.

b) The inclusions should participate in the flow of the metal in the flow zone,

decreasing the shear of the matrix, but should not cut through the plastic flow of the metal and thus damage the tool surface.

c) The inclusions should form a diffusion barrier on the rake face of the tool at the temperature of the tool chip interface. This temperature depends on several variables, especially the cutting speed.

d) The inclusions should give a smooth workpiece surface and not act as abrasives on the flank face of the tool.

The machinability of steel is enhanced primarily by free machining additives such as sulphur, phosphorus, lead, bismuth, selenium and tellurium [72].

During recent years, attention has been given to the development of structural steels having improved machinability and it was found by Wicker [73] that steels deoxidised using calcium exhibit improved machinability.

Calcium deoxidation has emerged as a viable means of improving the machinability of certain grades of steels. Unlike the free machinability additives, calcium deoxidation does not derive its machinability enhancement by increasing the volume fraction of beneficial non metallic inclusions.

Calcium deoxidation primarily modifies the oxide inclusions resulting from deoxicdation.

The enhancement in machinability by calcium deoxidation can be derived, therefore, even when the sulphur level is low and other free machining additives are not present unlike steels containing additions of sulphur and lead the calcium-deoxidised steels, when machining do not have an improved chip form.

Into and al [74] have shown that small additions of sulphur (up to 0.075%) and/or lead up to 0.06% to calcium-deoxidised steels have a profound beneficial effect on machinability. Further sulphur and lead appear to act independently and their effects on improving machinability are additive.

The best known and Most used free machining additive in use today is sulphur - sulphur is present in steel in amounts ranging from 0.04% in plain carbon steel up 10 0.40% in the rephosphorised and resulphurised free machining steels. The effect of sulphur on machinability is related to the

oxygen content in the steel [75].

At high oxygen contents, the MnS inclusions remain globular rather than stringing out during hot working and therefore are more efficient in their role as crack nucleation sites.

Moore [76] has suggested that larger inclusions are squeezed more easily onto the tool rake face to form a lubricating layer between the chip underside and the tool.

Opitz and Konig [77] found layers of manganese sulphide on the rake face of cemented carbide tools after cutting a medium carbon steel.

ln some worker's experience [78, 79, 80] the layers form more rapidly on cemented carbide tools containing titanium carbide. There are certain features which are characteristic of all free machining steels when compared to non free machining grades. The action of sulphides during cutting is dependent on the tool material as much as the properties of the workpiece [81.82].

The characteristics are:

- Lower cutting forces.
- Reduced chip/tool contact area.
- Higher shear plane angle.
- Reduced chip thickness.
- Less collar formation.
- Increased chip curl, longer tool life, less tool wear

The precise way in which manganese sulphide inclusions are effective during cutting steel is not resolved.

Metallographic evidence presented by Trent showed that sulphides are elongated on passing through the primary shear zone, but in the flow zone are drawn out to many times their original length, and to a thickness as small as (0.1).Lm. The deformed inclusions in the flow zone lie parallel to the chip

underside, and their interfacial area with the steel matrix is many times greater when they are in this form. Hence they may function as internal lubricants; forming easy shear bands and so lower the total shear stress on the rake face which in tom, increase the shear plane angle and reduces chip thickness. Using a scanning electron microscope Trent [83] has shown a very high concentration of thin ribbons of sulphide in the flow zone on the under surface of free cutting steel chips.

It has been confirmed by Trent [83] that the presence of the sulphides reduces the temperatures in high speed steel tools.

High sulphur content in the steel raises the machinability and very low sulphur content makes machining more difficult Hazra and co-workers [84] have cut low carbon free-cutting steel on a stage in the scanning electron microscope. De-cohesion and cavitations took place at the interface between the manganese sulphide inclusions and the ferrite matrix.

Keane [85] has shown that the wear rate of high speed steel cutting tools when machining low carbon free machining steels is strongly dependent on the volume fraction of manganese sulphide inclusions up to a volume fraction of 1 % (0.2%S) but that for volume fractions above this level, wear rates do not decrease further although the chip form and surface finish continue to improve (Fig 18).

2.7.2 Manganese sulphide inclusions:

Sulphur is soluble in molten steel and its solubility in solid steel is only slight. It is precipitated and appears as a form of metal sulphide during solidification of the steel with a strong segregation tendency.

The shape, composition and distribution of the sulphide inclusions is of great importance for free machining steels, and a major difference exists between the influence and behaviour of sulphide and oxide inclusions in those steels. ln modern steel making Mns has a lower free energy of formation than FeS86 and sulphur will therefore tend to form manganese sulphide in

preference to iron sulphide provided that the manganese content of the steel is sufficiently high.

Manganese is very widely used in steel production both for deoxidation and desulphurisation of the molten steel. It is generally added as ferromanganese and eliminates most of the oxygen and sulphur.

The MnS phase in the steel has always been found to have the stoichemetric composition.

It has cubic crystallattice with the parameter a = 5.226 A[71].

The physical properties are given by:

Melting point: 1610° C.

Density: 3.99*1*

Micro hardness: 170 *Mpa*

The conditions under which sulphides form in liquid steel as it is cooled can be predicted from knowledge of the thermo chemical data of the[20] reaction [87]

$$(Mn)Fe + (S)Fe = (Mn, Fe)s$$

Sulphur being rejected by the solidifying metal will increase in concentration in the liquid stress and sulphides will precipitate when the sulphur concentration has reached 1.0 to 1.5%88. The first sulphide to form will be mixed (Mn, Fe)S containing possibly as much at 50% FeS (30% Fe). This occurs for two reasons:

a) The equilibrium sulphide at a temperature of around 1530^0 C is rich in iron, but also, since manganese does'nt concentrate in the interdentric liquid as much as sulphur, there will not be sufficient manganese present to form MnS, so that sulphide rich in iron must form, (volatilises or joins the slag).

$$FsusbeS + Mn -> Fe + MnS$$

(Insoluble in iron so may join the slag)

In order that these reactions proceed as shown, an excess of manganese

must be added and the excess remains in the steel.

A condition conducive to the formation of globular sulphides is high oxygen content in the steel. This can be reached by keeping silicon to a level below 0.01 % and at a low carbon content of about 0.08% [89].

Three forms of manganese sulphide are generally found in steel.

Type 01:

These are large, globular inclusions of about 10-30 mum diameter and are associated sometimes with an oxide-sulphide, they occur at high levels of oxygen [90]. These elongate when the material is hot worked.

Type 02:

These are the eutectic sulphides - arrays of small spherical inclusions. They are Dot as beneficial to machining as type 1. They occur at intermediate levels of oxygen.

Type 03:

These are large angular inclusions occurring at low levels of oxygen. They are probably not as useful as type 1 in enhancing machining characteristics [78]. Figs (19,20 (a) (b)).

b) Other features being the same to obtain the type one sulphides, a high level of oxygen must be achieved in the molten bath of steel and the carbon level must be reduced. The relationship between carbon, oxygen and sulphide type is shown in (Fig 21) for plain carbon steels.

2.7.3 Inclusions Detrimental to Machinability:

The detrimental influence of non-metallic inclusions on steel properties has not yet been fully explained, but it is known that it depends on their amount, type, shape, size and distribution.

In free machining the distribution of the sulphide inclusions in the steel ingots depends on the steelmaking. In order to obtain a favourable distribution and

shape of sulphide inclusions, it is necessary to have relatively high liquid steel oxygen content The excess oxygen should be removed from the liquid steel to avoid the appearance of oxide inclusions. Also the accidental entrapment of non metallic inclusions, from slag or refractories during steelmaking needs to be avoided. The traditional steelmaking method of dealing with oxygen in solution is to de-oxidise with silicon or aluminium. The latter is generallyot used for free-cutting steels as hard AL_2O_3 inclusions can cause excessive tool wear. Silicate or other oxide inclusions so formed can also cause excessive tool wear [91] but this can be avoided by keeping silicon to a low level especially in the lower carbon steels.

The hard non deforming oxides, such as AL_2O_3 and silicate glasses are believed to limit shear and hinder plastic flow in the shear zone [92]. It can be observed that the deformation of this type of inclusion is much less than that of the other silicate-type inclusions. Thus raising the cutting temperatures and decreasing tool life. The large inclusions occasionally entrapped in steel from slag or refractories during solidification can be directly related to tool life, inclusions from such sources are usually very large and very abrasive. An individual inclusion, if sufficiently large can cause catastrophic tool failure.

Ekerot [93] found that most of the inclusions in the $Si0_2$-Al_2-Mno-caO systems were glassy and hard during hot working up to a well defined temperature where they changed behaviour and became very soft. It has been found [93] also that crystalline inclusions in the investigated systems were hard at all temperatures. This investigation has shown that it is possible to control the inclusion shape and behaviour during hot working by means of the composition and state of aggregate of the inclusions as well as by the working temperatures.

2.7 .4 Deformation of non-metallic Inclusions

The most important works reported which examined the distribution and

deformation of

inclusions are those of Maunder and Charles94, Kiesling9S, Baker and Charles[96], Waudly [97], Ekerot [98] and Klevebring [99].

In all of these workers papers use a deformation index of the inclusion which was first defined by Malkiewicz and Rudnik. The deformation index, (v), is defined as the ratio of the true strains for the inclusions and for the matrix.

$$v = \frac{E_i}{E_m}$$

Where:

Et is the true strain of the inclusion.

Em is the true strain of the steel matrix.

The work reported by Sundstrom [100] on the deformation of an inclusion embedded in steel matrix was as follows:

- That the flow stress-strain relationship is valid for both inclusions and matrix,

ie. $r = k.e^n$

Where:

r is the flow-stress,

k is a constant,

e is the true strain, and n is the strain hardening exponent.

- That the strain-hardening exponent is the same for both inclusions and steel matrix for a steel value of between 0.10 and 0.25 can be expected in most cases. For this range of values the analysis is graphically represented in (fig 21). The hardness of a phase is

approximately proportional to its flow-stress.

In order to estimate the deformation index using Sundstorm's model, the hardness data for the inclusion and the steel should be known.

Mann and Vlack [101] have also presented hot hardness data for MnS. This data can be used to predict the de formation index of MnS as a function of temperature. The plasticity of manganese sulphide inclusions in relation to the steel matrix at hot rolling temperatures decreases on raising the temperature (Fig 29), and depends on the type of inclusions [99]. The relative plasticity, (v),is given by [l02][23].

$$v = \frac{log\lambda}{z.\log H}$$

Where:

λ is the average aspect ratio of the inclusion population.

H is the rolling reduction.

MnS is frequently considered as a highly deformable inclusion but early investigations by Scheil and Schnell [103] indicated that it initially deforms to the same extent as the steel matrix during forging.

No effect of temperature was observed. Investigation by Moore [76] found that the sulphides deformed very much less than the matrix.

The deformability of MnS inclusions varies because they can be precipitated from the molten steel in three different morphologies (Type l, II and III). These different types and their formation have been described in the previous section.

The deformation behaviour of type II and type III MnS has received far less attention than type 1.

The three different morphologies have, however, been compared qualitatively, the deformability apparently increasing progressively from type 1 to III.

The type 1 MnS in the as cast state were globular and mostly in the size range 10-30μm.

The majority of the inclusions were single-phase MnS but some were associated with varying proportions of a duplex oxide sulphide eutectic.

The mean inclusion projection measurements vary consistently with temperature. With decreasing rolling temperature the plasticity initially increases to a maximum at 900^0C and then decreases. At most of the rolling temperatures the shapes of the curves (Le. the relative plasticity) decrease with increasing steel reduction.

This effect has been observed by many workerslO4. Because of the decrease in slope it is not possible to characterize the inclusion deformability by a single relative plasticity index.

Much of the observed variation in deformability is due to the presence of varying proportions of the oxide sulphide eutectic associated with some of the type 1 sulphide.

At below 1200^0 C the duplex inclusions deform far less than the single phase sulphides.

Baker and Charles [104] have reported that Type 1 MnS inclusions in a free-cutting steel deform less than the matrix during hot rolling. (Fig 22). The MnO-MnS constituent associated with type 1 MnS is fluid at 1200 ° C and brittle at lower temperatures.

Chao et al [105] have shown that pure manganese sulphide can dissolve up to 1.7% MnO at the eutectic temperature of 1232° C.

Furthermore, they have measured the hardness of MnS containing dissolved oxygen at temperatures up to 800° C and observe some increase in hardness [106].

Their curves indicate at least[24] a 20% increase at 800° C in hardness.

2.7.5 The relation between machining and manufacturing:

The main action of the sulphide is to provide a film on the rake face of the tool to reduce forces in the cutting area.

The existence of such a film has been very clearly established by microprobe analysis by Opitz and Koing [77] and subsequently by others [76]. The sulphide is extruded onto the tool face by the compressive stress developed in the chip between the primary shear zone and the limit of contact area after the inclusion is cut.

Flow of the sulphide from the inclusion will depend on the applied stress and on the orifice available for flow. The bonding of the sulphide to the rake face will then depend on the reactivity between the sulphide and the tool material. For a given stress developed during cutting, small diameter inclusions will contribute far less to film formation than larger diameter inclusions.

Thus machining performance is related to the diameter of inclusion and not to their length or aspect ratio. It has also been suggested that inclusions change shape very much less than the bulk change in the steel.

Therefore since the diameter of inclusions is the major factor in promoting machinability, and the change in inclusion shape during rolling is relatively small, the production of large diameter inclusions in the ingot is, of primary importance.

As cast inclusion size and shape is influenced by chemical and physical phenomena,

Type 2

Sulphides are not as beneficial to machinability a type 1 or type III because of their small diameters. Steelmakers can avoid formation of steel sulphides by careful chemical control and promote formation of the required type 1 sulphides.

Type 1

sulphides are detrimental to static tensile properties and in order to ensure optimum machinability in the part product, the steel maker must carefully control ingot solidification to produce large type 1 sulphides [107] uniformly distributed.

Plasticity ratios> 1 have been reported by Banks and Gladman [108] after the addition of Ti and Ca to high sulphur steel, which were then hot rolled at 900° and 1200° C. Baker and Charles reported values of v for type 1 MnS inclusions (sulphide and oxide) which increased from 0.4 to 0.64 as the temperature increased up to 1200° C.

C. Moore [76] observed the plasticity ratio of the sulphides is considerably greater than 1, much of the imposed strain is accommodated within the sulphides or even at the sulphide/matrix interface.

The present results clearly show values of v > lover a limited strain range, pointed out by Baker and Charles. Relative plasticity values greater than 1 for MnS in steel can be inferred from the observations of Iwata and Veda109 who carried out dynamic machining experiments in the S.E.M.. R.L. Aghan and J. Nutting reported that the MnS particles were more plastic than the matrix ie: plasticity ratio greater than 1.

Most of the experimental investigations do not directly apply to the conditions under which material deforms in metal cutting. ln machining strain rates of 1()4 - l06/sec and temperatures of 400 - 800° C are common along with strains of 10^2 - 10^5. The table [A] shows a summary of the experimental conditions used by various workers.

Author	Av	Test	'Pe	strain	strain rate
C.Moore	v<l	Rolling	800°C,900°		
	v=l	Rolled	1000,1200		
Scheil & Schnell	v=l		900,1200		
Banks & Gladman	v>l				
Iwater & Ueda	v>l	Machining S.E.M.			
Aghan & Nutting	v>l	Rolling	R.T.	100%,200	
Kleveloning,Ekerot	v>1	hot hardness	RT---- 1200°C		
Baker & Charles	v=O.4		1200		
	v=O.64		900		
	v=l		800		

Table A

CHAPTER III

EXPERIMENTAL TECHNIQUES

3.0 EXPERIMENTAL TECHNIQUES:

3.1 Machining Process:

Machining was carried out under non orthogonal cutting and without the use of coolants for most of test. A Boehringer DM640 lathe with a constantly variable speed ranging 5 to 2500 rpm and feeds of 0.05 to 1.8 mm/rev was used for the experiments. Machining was carried out under various cutting speed; but the feed and depth of cut kept constant throughout the experiments at 0.25 mm/rev and .05 mm. The surface speed was set using a Tachometer. After a series of preliminary tests, five different surface speeds ranging from 100 to 350 m/min were chosen. All the tests were carried out without the use of any chip breaker or deflector as these may influence the surface finish. The tangential and feed forces were measured by means of a kistler dynamometer type 9263, the first 30 seconds of cutting was part of the bar over which the surface finish was recorded.

3.2 Work piece materials:

The workpiece materials were all stainless steels having carbon contents varying from 0.03 to 0.054%. the chemical composition of each material is given in table 1.

All the steels contained a small volume fraction of non metallic inclusions (Fig 20A), one steel also showed a higher volume fraction of manganese sulphide inclusions. (Fig 20B), All the test bars were from commercial casts and originated from the middle part of an ingot, one of them being supplied as cold drawn and the other as annealed bar. Sections of all bars across their diameters revealed reasonably uniform microstructures typical examples beig shown in figs A and B.

Initial bar diameters varied from 51.35 to 48.95 but at least 2.0 mm depth of cut was turned off each surface before experimental machining was undertaken. The room temperature hardness of the work material is show in table (2). Hardness traverses across the bar diameter were also carried out this can be seen in table (2a).

3.3 Tool selection and geometry preparation:

Workpiece surfaces generated in any from of metal cutting are likely to be sensitive to the geometry and finish of the tool producing them. It is therefore necessary to have a standardized tool geometry and method production.

The inserts used for the tests were of the designation SNMA 12 04 16. This can be better understood with reference to appendix 1.

The tool holder used was designated CSSNR 25 32 12. The tool holder used in this experiment has the following geometries:

Side rake angle 0°
Top rake angle 4°
Approach angle 45°
Side clearance angle 0°
front clearance angle 0°

The tool material was GC 015 from sandvik (a TiC, AL_2O_3 coated cemented carbide).

3.4 Tool preparation:

All tools unless otherwise specified used the standard tool geometry; with short times of cutting no significant amount of wear was observed. Where necessary tool geometry was produced by grinding. These tools will have the same surface as those produced commercially and used for the majority of tests.

3.5 Polishing and etching:

To examine the variation in microstructure of these materials a scanning electron microscope (S.E.M).

These samples were mounted in moulds using a mounting press. One marked for later identification, they were ground and then polished on diamond wheels. The samples were then etched in methanolic aqua regia, this is used with austenitic steels to reveal the grain structure 45 mL HCL, 15 mL HNO_3, 20 mL methanol. The approximate time of tching was between 1.5 and2 minutes.

3.6 surface finish measurements and statistical techniques:

The surface roughness of the machined surface was measured after each test. A talysurf 5 was used to measure the surface roughness of the nowly formed surface. This machine uses a processor to provide a selection of roughness parameters, together with profile graphs. Measurements are obtained from a single traverse over the surface with a stylus, the parameter values then being directly obtainable from the stored information. A talysurf 5 enables the roughness and waviness of components to be assessed separately or in combination. Graphs of the roughness waviness and unfiltered profile can be obtained. However, in the present work the talysurf 5 was used largely to measure the surface roughness value (R_A) versus the cutting speed from 100 – 350 m/min.

In order to obtain a clear picture of the pattern of variability, statistical techniques have been used. Surface finish measurements on the stainless steel have been grouped into discrete classes such as in table. Form these sets of values the mean size, the range and standard deviation have been calculated.

A test for difference between two means has been carried out using the formula.

[110]

$$x_1 - x_2 + tx \frac{n_1 s_1 + n_2 s_2^2}{n_1 n_2} \times \frac{N_1 \times N_2}{N_1 N_2^{1/2}}$$

CHAPTER IV
EXPERIMENTAL RESULTS

4. EXPERIMENTAL RESULTS

4.1 Material characterisation:

The microstructure and the hardness of the workpiece material used in this investigation are shown in [table 1, 2] and (figures 24 A, and B).

[Table 1] shows the chemical composition and the condition of the materials.

4.2 Initial trials:

4.2.1 Parameters selection:

A wide selection of roughness parameters has been measured and the range of their values for any one surface has been calculated. This figure divided by the mean value is presented in [tables 3 to 9, 11, 12, 20 and 21]. This shows greatest scatter on the following parameters.

Rq, Rmax, Rt , Rtm, Rp, Rpm, Rsk, Hsc, Sm, Δa and Δq and least on

Ra and ***R3TM.***

4.2.2 Surface finishes measurements:

Tests were carried out at 150,200,250 and 300m/min with feed and depth of cut of 0.25mm/rev and 0.5 mm respectively on the 247165 cold drawn bars. The parameters obtained from the talysurf are tabulated in [table 3].

The same tests at the same cutting conditions were carried out on the 247165 annealed material and the parameters obtained are tabulated in [table 4 and 5].The cold drawn material was also machined at 200 and 250m/min under lubricated condition, the parameters recorded are tabulated in [table 6] and (figures 26-38).It was noticed that an improvement of the new surface was generated at the lower cutting speed and no improvement was seen at 250m/min when lubricated. (Figs 28-31).

The free machining steel was machined under the full range of cutting condition, results are tabulated in [table 7].The stainless 304SC and 303S21 were also machined under these conditions and these results are tabulated in [table 8].

All the stainless steel bars were machined again at 200m/mn,0.25mm/rev and 0.5mm depth of cut to check the reproducibility of the test parameters obtained from the talysurf and is tabulated in [table 9].

4.2.3 Statistical based experiments:

In order to reveal any difference or any dominant influences on the surface finish, statistical have been used using the Ra value obtained previously from the talysurf and using the formula mentioned in the experimental procedure. This can be better understood by references to [table 10].

4.2.4 Forces:

In order to identify the influence of the cutting forces on the surface roughness values, the forces were recorded and tabulated in [table 11].This also enabled the variation in surface finish on different parts of the bar to be examined.

The surface roughness values of all materials are tabulated in [table 12].

[Table 13 and 14] which are summaries of [table 14] indicate the relations between the forces acting on the tool and the surfaces generated. These are also plotted as Ra as cutting speed in (figure 25).In this test the free machining material gave a better finish than all materials used in this project(figure 25).

At250m/min the surface roughness values of all materials to be similar.

(Figure 25) shows that when using the lubricant the surface roughness values obtained under lubricated conditions was not as good as that under dry conditions at high cutting speeds.

[Table 13] shows thlation between the surface roughness values and the cutting forces. With high forces a poor surface roughness value was obtained. It was noticed that the annealed material gave a better finish than the cold drawn.

4.3 Forces shear plane angle and chip thickness relationships

For purposes of simple analysis the chip is assumed to form by shear along the shear plane angle is determined from experimental values of $t1$ and $t2$ using the relationship $\cos\Psi = \frac{(t_2/t_1 - \sin\alpha)}{\cos\alpha}$

Where:

$t1$ is the undeformed chip thickness .

$t2$ is the chip thickness.

The chip thickness $t2$ is equal to (0.25mm) the feed with a tolerance of +0.01mm.As a 45° approach angle was used the deformed chip thickness was not equal to the feed.t_1=f$\sin 45^0$therefore

$$\cos\Psi=\frac{(t_2/\sin 45)-\sin 4}{\cos 45}$$

The chip thichness $t2$ has been measured using a micrometer and is tabulated in [table 15].The mean chip thickness is a most important parameter.

The force on the tool has been tabulated using:

- Compressive force on the shear plane

$$Fc=T\cos\Psi - F_f \sin\Psi$$

- Shear force on the shear plane

$$Fs=F_f \cos\Psi + T \sin\Psi$$

- Normal force at the chip tool interface

$$N=F_f \cos\alpha + T \sin\alpha$$

These are tabulated with the chip thickness in [table 15]. [Table 16] shows the relation between the shear plane, forces and surface roughness values. From this, it has been found that the forces vary only slightly over a wide range of cutting speed and work materials. Cutting speed (v) has a relatively small influence on cutting ratio also and hence on tc for constant feed, this can be seen in [table 15-19].

The forces were recorded under the following conditions:

a) For different position in the bar

b) With the tool and workpiece degreased

c) Just the tool tip degreased

Parameters obtained from the talysurf and the dynamometers are tabulated in [tables 20-21].

4.4 Experiments with non standard geometries:

Tools with non standard geometries given in table with figure 40 have been produced. The stainless steel was machined at 200,250,300 and 350m/min. The parameters obtained from the talysurf are tabulated in [table 22, 23 24 and 25]. (Figures 39-60) show **S.E.M.** images of the surfaces developed. (Figures 42, 44, 45, 46) show cross sections through these surfaces. It can be seen that the cross section of the feed mark is not entirely consistent with the ground tool geometry shown in (fig 50, 51, 55).At the top of the feed mark metal has been extruded.

CHAPTER V
DISCUSSION

5. DISCUSSION:

5.1. Selected Parameters:

The parameter values selected from the stored information of talysurf 5 are tabulated in [tables 3, 9, 11 to 14] for all the experiments carried out under different cutting conditions and on different materials. These are twelve parameters all together some of which are more universally recognised, and most used.

To provide a selection of the roughness parameters, a study has been carried out considering which parameters varies most significantly and which one gave consistency from result i.e. least variations.

The range has been calculated from the series of measurements taken on the work piece material. Dividing this by mean value gives the variation of the parameter which has been used to make the selection of the roughness parameters. With reference to the tables of these derived parameters this can be better understood i.e. [tables 3 to 9,11,12,20 and 21]. The several different parameters used in measuring surface finish which relate to certain characteristics of the finish (see tables) can be classified in three groups, according to the type of characteristic that they measure.

Amplitude parameters: Is measure of the profile height. These are generally good indicators of chatter (periodic tool/work piece deflection), feed marks (produced by the nose radius of the tool on each revolution) and fine scale surface damage to these feed marks. These are:

$$Ra, Rq, Rmax, Rt, Rtm, Rz, R3TM, Rp, Rpm, RSK$$

Spacing parameters: are measures of irregularity of spacing along the surface, irrespective of the amplitude of these irregularities, these are Hsc and Sm.

Hybrid parameters: relate to both the amplitude and spacing of the surface irregularities$(\Delta a, \Delta q, \lambda a, \lambda q, tp)$. From all the parameters (refer to a derived tables) we have five particular variables, which show least scatter off a piece of turned surface and consequently can be described as characterising the surface.

(1)The "HSC" high spot counts [i.e. the number of peaks on the surface] count the top of the feed marks within the assessment length. Within a given sampling length there will be approximately l/f marks. However some variation will occur the sampling

length may start and finishes in different positions relative to the first feed mark: (see figures).

(2)Sm. This is the mean spacing between profile peaks at the mean line within a given sampling length. It measures in continuous chip formation the number of feed marks, it could also measure the number of scales in the presence of the built up edge

(3)$R3TM$: This is the height difference between the third highest peak and the third lowest valley within a given sampling length. In other words it is a measure of the height of feed marks when a continuous chip is formed. In this condition it could measure the sponzipfel as well.

(4) Ra. This is defined as the root mean square of the arithmetic mean of the departures of the profile from the mean line within a sampling length. In continuous chip formation, it measures compromise geometry as sponzipfel, nose radius; feed mark height...etc. will all affect the parameter.

(5) Rq. is the parameter most universally used as the international parameter of roughness.

It is normally determined as average height from a mean line of all the ordinates of the surface regardless of sign. As Ra it measures compromise geometry i.e. sponzipfel, nose radius and the height of feed mark. Squeezing caused by forces on primary shear plane, these have origin in forces on secondary shear plane via the two force equations. The force on the secondary shear plane comes area x strength therefore increasing either (assuming other constant) would give increased forces on prime planes. Usually increase area comes from increased ductility and increased strength ductility. Therefore these tend to be traded off. It can usually be seen that soft ductile materials can have high forces (see EMT Comp force for pureFe) and in these cases because the Fe will have low yield strength it will squeeze badly. With very hard (which from a continuous chip) can again have high forces but the metal is stronger therefore expect less squeezing. The link between ductility strength, contact length, forces and surface finish is thus established. We know that in turning operation the spacing parameters are controlled by the feed. These will not change for a given value of that parameter even if the surface finish is affected. Consequently the use of Hsc and Sm while giving very reproducible results should not be used with turned surfaces when a continuous chip is present as they will not measure aspects of geometry of primary importance.

Out of five parameter we have got there parameters left which exhibit low scatter of those three Ra has been used because it shows a lower scatter than R_{3TM} and is more widely used than the Rq. Ra therefore characterises these surfaces most consistently but in examining a surface for variability R_{3TM} would be a better guide. R_{3TM} should be used when it is desirable to see how varied a surface is.

5.2. Surface Finish Measurements:

The surface finish as measured by the Ra value does not correspond to that determined from nose radius and tool geometry as shown in the literature survey. From examination of the surface only two defects from the perfect shape can be observed. The ridges of the feed marks show some material apparently extruded above the feed mark height (fig 30) while the grove bottom shows a series of small ridges running parallel to the feed marks (figures 32, 33, 34, 35, 36). If we consider these latter features first we can make an estimation of the effect on the theoretical roughness by assuming them to be hemispherical in cross section resulting in possibly an apparent change in nose radius (as far as the stylus is concerned). The height of these ridges would be equal to half their width and this height would therefore lead to a corresponding reduction in nose radius. The calculation for the effect on surface finish is as follows. We can ignore the areas a picture taken on the samples of 247165 cold drawn machined under dry condition at 250 m/min we can count 27 lines which occupy the 0.25mm of feed. The width of 1 line is therefore equal to:

$$\frac{0.25}{27} = 0.00925 \text{ mm}$$

The lines can assure semicircular in cross section. Therefore the height of a line above the profile is equal to:

$$\frac{0.000925}{2} = 0.004625 \text{ mm}$$

These lines give an apparent reduction in Nose Radius. A change in surface roughness value could occur due to the apparent change in nose radius. The estimated difference between actual nose radius and effective one is given by:

$$NRnew = 1.6 - 0.004625 = 1.595375mm$$

Thus the effective surface roughness value is:

$$R_a = 1.253\mu m^5$$

Instead of a theoretical value of 1.25µm.

Similarly for machining at 250m/min lubricated we can count 32 lines which occupy 0.25mm of feed. The width of 1 line is therefore equal to:

$$\frac{0.25}{32} = 0.0078725 \text{ mm}$$

The height of a line is equal to

$$\frac{0.0078125}{2} = 0.00390625 \text{ mm}$$

The actual nose radius is:

$$1.6 - 0.00390625 = 1.5960mm$$

Effective surface roughness value is therefore :

$$Ra = 1.2531\mu m$$

Actual R_a=1.781µm

At 200m/min Lubricated:

We count 24 lines which occupy 0.25mm of feed. The width of 1 line is equal to:

$$\frac{0.25}{24} = 0.0104 \text{ mm}^6$$

The height of a line is equal to:

$$\frac{0.0104}{2} = 0.005208 \text{ mm}$$

The actual nose radius is:

$$1.6 - 0.002508 = 1.59479166mm$$

Effective surface roughness value is:

$$Ra = 1.2540$$

Actual R_a = 1.4330µm

Under dry conditions machined at 200m/min 25 lines occupy 0.25mm of feed. The width of 1 line is equal to:

$$\frac{0.25}{25} = 0.01 \text{ mm}$$

Therefore the actual nose radius is NR change = 1.6 – 0.005 = 1.595mm. effective surface roughness value is:

$$Ra = 1.253\mu m$$

Actual R_a = 1.739

Under dry condition machined at 150m/mm 28 lines occupy 0.25mm of feed. The width of 1 line is equal to:

$$\frac{0.25}{28} = 0.00892$$

The height of a line is equal to:

$$\frac{0.00892}{2} = 0.0044642$$

The actual nose radius is: NR change 1.6-0,0044642 = 1.5955 .

Effective surface roughness value is

R_a = 12535 µm

$$\frac{0.25}{28} = 0.00892$$

Actual R_a =1.739

Under dry condition machined at 150m/mm 28 lines occupy 0.25mm of feed. The width of line is equal to

$$\frac{0.25}{28} = 0.00892$$

The height of a line is equal to:

$$\frac{0.00892}{2} = 0.0044642$$

The actual nose radius is: NR CHANGE 1.6-0.0044642 = 1.5955. Effective surface roughness value is

$$Ra = 12535\,\mu m$$

The annealed material machined at 300 m/min under dry conditions shows 24 lines occupies 0.25mn of feed. The width of line is given by:

$$\frac{0.25}{28} = 0.00892 \text{ mm}$$

The height of a line is equal to:

$$\frac{0.0104}{2} = 0.005208 \text{ mm}$$

The actual nose radius is:

NR change = 1.6-0.005208

NR change =1.59479166 mm

Effective surface roughness value is:

$$Ra = 1.254\ \mu m^{7}$$

Actual R_a = cold drawn machined at 200 m/min using a specially ground tool r =1.27 mm and 17 lines are present. Therefore the width is: $\frac{0.2}{17} = 0.0147$ mm

The height of a line is equal to:

The actual nose radius is: NR: $1.27 - 0.00735294 = 1.26264\ mm.$

effective surface roughness value is: $Ra = 1.583\ mm$

The annealed material machined at 250 m/mm using ground tools r = 1.27 mm. 25 lines are present. The width is: $\frac{0.25}{25} = 0.1\ mm$mm

The height of a line is equal to

$\frac{0.01}{2} = 0.005$ mm[8]

The actual nose radius is: NR: 1K.27 – 0.005 = 1.265 mm

$Ra = 1.581 \mu m$

Theoretical value: $1.5748\ \mu m$

Summarising these results gives:

Speed m/min	Material	Condition	Theoretical Ideal Ra	Calculated Ra	Actual Ra
250	247165CD	Dry	1.25	1.253	1.74
250	247165CD	Lubricated	1.25	1.2531	1.781
200	247165CD	Lubricated	1.25	1.2540	1.433
200	247165A	Dry	1.25	1.253	1.739
150	247165CD	Dry	1.25	1.2535	1.739
300	247165A	Dry	1.25	1.2540	1.519
200	247165CD	Dry	1.5748	1.283	2.106
250	247165A	Dry	1.5748	1.281	1.905

From these simple calculations it is easy to appreciate that the deviations from the theoretical surface finish must be associated with the defect seen at the top of the feed mark. These defects have in the past bracketed as sponzipfel and often only thought of occurring when notch war is present. The present trials show that:

(a) Some change to the feed mark edge occurs in a system tool wear. (Figures 37, 38 and 61, 62) For the tool with non standard geometries.

(b) This results in a surface with a variable character.

(c) A single trace by a stylus instrument is not sufficient to act as even a quality control parameter and certainly not as a research tool.

The change in surface finish by alternations to the feed mark usually results in a worse surface finish but can lead to an improvement. It is therefore necessary to understand what happens in this region where the crest of the feed mark is formed. The SEM micrographs do not appear to give sufficient amounts of sponzipfel to account for the large variations in Surface Roughness.

5.3 Variation of surface finish:

The variation of arithmetic roughness R_a as measured with the talysurf 5 system, is shown in (figure 22). Versus the cutting speed for speeds from 150 to 300 m/mn.

It can be seen that there is large difference between the 304sc stainless steel and the free machining (303S21).

On cutting the 303S21 steel the presence of manganese sulphides inclusions did not prevent a continuous straight chip with a relatively smooth underside being formed. The

large volume of MnS inclusions in the steel would tend to prevent a strong bond between the chip underside and the squeezing can be expected resulting in a better surface finish. The 304 stainless steel would be expected to give poorer finish in a better surface finish than the ones recorded for the 303S21 at all speeds. Thus the sulphide inclusion in the secondary shear zone under compressive stress act as internal lubricants probably reducing stresses and minimising binding. As the interface stresses with the 303s21 will be governed by the behaviour of the MnS inclusions the improved surface finish seen at high speeds with the 3041SD stainless steel is not as apparent.

A small effect could be noticed on the 247165 by cold drawing from the annealed condition op to 200m/min with the annealed producing a better surface finish. As the ductility of the material decreases by cold to a decrease in stresses and so the squeezing effect should decrease. The result was indeed a better finish obtained by the cold drawn material. Cold drawing also increases the strength of the material which is thus able to produce higher stresses which would encourage squeezing to occur. The balance between strength and lower ductility could result in better or worse finish depending on the exact drawing conditions. In this case little difference in hardness was seen on these two conditions and probably minimal changes in properties had occurred by cold drawing. The forces associated with the 304SC and 303S21 are shown in [tables 11, 13, 14 and 20,21] and reflect the changes in stress discussed above while for the 247165 annealed and cold drawn also shown in these tables little difference can be seen[11].

5.4 Forces:

The calculation of the shear force on the primary shear plane has shown it to vary only slightly over wide range of cutting speeds and work materials.

When cutting the free cutting steels generally a lower cutting force is required than when cutting the non free machining stainless steel, particularly at 200m/min (see table 20).

The cold drawn material had an initially higher hardness which would lead to a higher shear stress. Machined at 200 m/min higher forces were recorded table 14 and a worse finish was observed. This is unlikely to be due to a larger contact length and this thus is associated with higher strength of the material on the primary shear plane.

Machining the 247165 annealed materials at 200 m/min under the same cutting conditions lower and the relative squeezing force may be correspondingly lower.

Machining the cold drawn material at 200 m/min using cutting lubricants a better finish was recorded at low speed than when machining dry and worse finish was obtained at high speed. As the name implies, A cutting lubricant, if effective reduces friction on the face of the tool in areas of low contact stress which should result in a decrease in the cutting forces. It is difficult to introduce a cutting lubricant to the area of contact between the tool and the chip; hence the lubricating action is limited.

Machining at 200 m/min and 250m/min a similar surface finish could be seen under dry and lubricated condition was not as good as that under dry conditions. This may be due to lubricants which tend to lose their effectiveness when machining at high cutting speed and the cooling action which could effectively result in machining a stronger material (figure 40).

The net result being more squeezing.

Tests of significance have been used to reveal any difference between the surface roughness value obtained on the new surface generated surfaces machined under different condition or using different bars of work material (annealed cold drawn). The discrepancy between those observations reported previously, is therefore not significant at the 5% level and it can be inferred and cold drawing) that can be definitely proved. [Table 10].

5.5 Forces shear plane angle and chip thickness:

It may be inferred from the preceding discussion that the contact length affects both the squeezing action and primary shear plane. Therefore it may be expected that a relationship between chip thickness (from shear plane angle) and surface finish when machining without a built-up-edge exists. This would be useful in diagnosing the cause of poor surface finish in case where sophisticated microscopes were not present.

The measurement of chip thickness however varies by up to 0.02mm in 0.25mm i.e. about 8 %. This will give a variation in shear plane angle of between 45° and 43° i.e. 4 %. The surface finish variation for any one cutting operation has been shown to give up to 10% whish is exceeded if different parts of the bar etc are used. As the two measurements (chip thickness and surface finish) are taken independently an expected total variation would be closer to 15%.

With the range of cutting conditions used the variations in forces was of the same order. Consequently there is little correlation between these parameters and unless gross changes are seen, the inference that poor surface finish and thick chip cross sections are connected cannot be made. However where gross changes are seen (i.e. with the machining stainless steel) low forces, low chip thickness and good surface finishes result, [table 15].

5.6 Experiment with non standard geometries:

Machining stainless steel with standard tool geometries small amounts of squeezing have been observed using the scanning electron microscope. The talysurf 5 and study of the variation of the ideal surface roughness values confirms these showing surfaces with values greater than the feed. It has been seen that there is no difference or any significant variation on the bottom of the feed marks and as the surface roughness is greatly increased, the conclusion must be that the amount of ‘sponzipfel’ at the top of the feed marks is responsible.

Pekelharing [27] suggested that the defect which leads to sponzipfel is groove formation but, this was not observed in the tools used during these experiments.

Pekelharing reported that the amount of squeezing and the surface roughness is greatly increased when the first groove has developed to its full depth. The surfaces produced in value.

Pekelharing observed that a newly sharpened tool squeezed only slightly and a worn tool squeezed badly. The squeezing was thought to occur mainly below the rake face. However it was also suggested that the squeezing occurred just above the rake face. However it was also suggested that the squeezing just above the rake face in the lower part of the shear zone. It has been found that squeezing occurs on primary shear plane due to compression [27] which are constrained from release and if the clearance angles are very small the effect is magnified. These observations lead to experiments with geometry and large feed marks which enhanced the squeezing effect to observe the defects of squeezing in more detail (figure 39).

S.E.M. pictures, (figures 41-60) were taken of the new surfaces generated under the condition above which lead automatically to the formation of sponzipfel due to the geometry of the tool. (Figures 42, 44, 45, 46) are cross sections of these surfaces. It can

be seen that the feed marks produced were visible and large enough with squeezing of the type described previously.

Machined at 200 m/min, the sponzipfel has been observed on the new surface generated when machining the 247165 annealed and cold drawn[13].

As the speed is further increased the sponzipfel appears to decrease (figure 55) and an improvement in surface finish is observed but the sponzipfel is still present. Examination on the **S.E.M.** of the tool used at this stage shows that no groove formation has taken place.

From the **S.E.M.** picture (figure 55, a) measurement of the included angle of the feed mark has been taken. The real profile of the tool has been drawn and it has been found that the two included angles at the nose do not coincide. This phenomenon has been observed particularly at 250m/min. The volume of the material enclosed by the surface tool profiles appears to have been displaced in the opposite direction to the feed producing the squeezing action. (Figs 24 and 25) show that the effect is not localised to the top of the feed mark but extends to the part of the flank of the feed mark.

From the discussion above and the **S.E.M.** photographs observation have shown typical squeezing similar to pekelharing's work and a new phenomena a bulging behind the feed mark which could occur during the formation of the next feed mark.

This distortion of the previous feed mark by the forces necessary to plastically deform material[14] into a chip alters the shape of the feed marks in a manner which may be difficult to observe directly when using a scanning electron microscope on surface produced by conventional tool geometries. The feed mark shape distortion can be modelled as in (fig 67).

The effect of this would be to raise the height of the feed mark possibly with little observable sponzipfel present and to change the profile into one with an approximate oval shape. The effect is also likely to be variable along the length of the feed mark as shown in (fig 67) resulting in variable readings from the talysurf on an apparently uniform surface. It is phenomena that are probably the major cause of surfaces created by single point turning not being of the theoretical Ra or Rz value[15].

CONCLUSION

CONCLUSION

The effect on chip formation, surface finish tool forces of sulphur, annealing and cold drawing when machining austenitic stainless steel has been investigated. The following conclusions are based on calculation of tools and work pieces using scanning electron microscopy and talysurf 5.

1. It has been found that the parameter Ra characterises a specific surface with a lowest scattered figure but yet is capable of distinguishing between relevant criteria.
2. It has been concluded that a single trace by a stylus instrument is not sufficient to characterise a surface finish with even least scattered parameter showing ±10% of the mean on a particular surface.
3. The free machining steel 303S21 shows a much improved surface finish and low forces under the test conditions.
4. The forces on the primary shear plane. Have been found they vary only slightly over a wide range of cutting speeds and work materials.
5. It has been found that there is no statistical difference in surface finish produced on annealed or cold drawn material.
6. some defects have been observed on the surface which do not replicate the tool perfectly.

   (1) The ridges of the feed mark show material apparently extruded above the feed mark height. (2) The groove bottom shows a series of small ridges running parallel to the feed height. (3) The side wall of the feed mark shows evidence of bulging. These effects have all been observed on tools with no visible wear.
7. It can be concluded that although sponzipfel was not formed to extent previously seen, it was still the major cause of surfaces not being “ideally smooth”. Unless the tool geometry was such as to cause large amounts of squeezing formed to the extent previously seen, it was such as to cause large amounts of squeezing force the diagnosis of sponzipfel being present may not be possible using the S.E.M.[2]

REFERENCES

References:

[1] E.M. Trent Metal Cutting second edition Butterworths 1984 p1.

[2] E.M. Trent Metal Cutting second edition Butterworths p 2.

[3] E.M. Trent Metal Cutting second edition Butterworths p 3.

[4] E.M. Trent Metal Cutting second edition Butterworths p 5.

[5] Wright, P.K., PhD Thesis, University of Brinningham, 1971.

[6]Takeyma and ono, T. Trans. ASME (B), 1968, May p 335.

[7] Williams, J.E., Smart, E.F. and Milner, D.R., Metallurgia 1970.

[8] Ashby, M.E., phil. mag. 8 ser, 1966 vol 14, p 1157.

[9] Williams and Rollason, E.C., J.I.M., 1970 vol 98 p 114.

[10] Hovinga, H.J. Annals EIRP, 1973, vol 21, p 31.

[11] Dynes, B.W., PhD Thesis, Binningham, 1975.

[12] Shaw, M.C., Cook, N.H. and Smith P.A., Trans. ASME (B) 1961 May p 134.

[13]T. Wallbank PhD Thesis University of Binningham, 1978.

[14] J. Wallbank, J. Metals Technology, 1979 April, 1978.

[15] E.M. Trent, J. Iron and Steel Inst, 1963,201,(11), p 923.

[16] Shelboume, PhD Thesis Birmingham University, 1983.

[17] E.M. Trent, J. Iron and Steel Inst. 1963,201, Il p 923.

[18] Forev, N.N., Metal Cutting Mechanics, Pergamon, 1966.

[19] Nadai, A. and Majoine, *Ml.* Trans. ASME, 1941, p 77.

[20] Wright, P.K. and Trent E.M., Metal Techu, 1974, l,p 3.

[21] Campbell and Ferguson, W.G. Phil Mag, 1970,21,169 p 63.

[22] De Salvo, DJ. and Shaw, M.C. MTDR Conf., 1968 part 2, p 921.

[23] Stume, H.P. ISI report No.94 Machinability p 179.

[24] E.M. Trent, Iron and steel institution special report 94, 1965, p.11

[25] Machinability of Engineering Materials B. Mills and A.H. Redford, 1983 p.22

[26] Surfaces generated by single point turning, Msc Thesis J Wallbank 1979

[27] A.J. Pekelharing and C.A. Gieszen, Deft University of technology, Netherlands, vol.20p.21, 1971

[28] Shaw, M.C., Trans. ASME/B/ 1961, p.163

[29] Bailey, J.A. and Azangoou, G.A., SME Tech.pap. 10 75, 126, 1975

[30]Iawata, K. and Ueda, K., Proc 3 North Amer.Met.Work. Conf.1975,p.603

[31] Bailey, J.A.wear, 1977, vol.42, p.277

[32] Williams, J.E. and Rollason, E.C., JIM, 1970, vol.98 p.144

[33] Landhere, D. and Zaat, J.H. wear, 1974 vol 27, p.129

[34] Black, J.T. and Romalingham, S. International Journal of Mechanical. Tools Des. RES, 1970, vol.10, p.439

[35] Bailey, J.A. and G.A. Azangou , SME technology paper No 1075-126 1975

[36] Bailey, J.A. and Becker, S.E. Trans ASME (B), 1974, p.163.

[37] Nishina, k. Bull. Japanese Society Proc. Engineers1974, vol8, No.4 p.159

[38] Fundamentals of metal Machining and machine tools Geoffrey Boothroyd ISE 1985 p.113

[39] E.M. Trent, Metal Cutting 2nd edition Butterworth's, p.1984

[40] E.M.Trent.Metal Cutting 2nd edition Butterworths.p110

[41] Ranko Milovic, MSc Thesis, Birmingham University 1980

[42] Optiz H. and Konig, W., ISI publication, 126, 6 (1970)

[43]. E.M. Trent. Tool wear and machinability. The production engineer (London) vol. 38, no.3, p.105, 1959.

[44] E.M. Trent. Metal Cutting Second Edition Butterworth's 1984 p.99-108

[45] Wright, P.k. and Trent, E.M. Metals Technology journal 1974 p 13.

[46] E .M. Trent, Metal Cutting 2nd edition. Butterworth 1984 p.99 1974 p.13

[47] Effect of temperature on formality. Open University course Material, Manufacture, material Design pt. 600 Unit 4 Forming p.28 1985.

[48] Wright, P.K. and Trent E.M.1974

[49] Trent, E.M., J. Inst. Prod Eng. Eng. 1979, 38(3), p.105

[50] Trent, E.M. proc. 8th MTDR Conf. 1967 Manchester p.629

[51] Trent, E.M. Metal Cutting 2nd edition, Butterworth's 1984 p.26

[52] Trent, E.M. Wear of metal cutting tools.

[53] Venkatesk, P.A. and Trent, E.M. Metals Technology, 1974, 1, p.3

[54] E.M. Trent, J. inst. Prod. Eng. 1959, 38 (3) p.105

[55] Bhattacharyya S.K. A. Jawaid, M.H. Lewis, J. Wallbank. Metals Technology December 1983 vol 10 p.482

[56] Trent, E.M. Metal cutting 1977 London, Butterworths

[57] Bhattacharyya S.K. Jawaid A. and Wallbank J. in press. Metals technology 1983.

[58] E.M. Trent, wear of Metal Cutting Tools Material science and technology. 13, 1979

[59] E.M. Trent, Wear of Metal Cutting Tools Butterworth 1st edition1977

[60] E.M.Trent.Wear of cutting Tool.

[61] Heydari.F.Msc.Thesis, University of Warwick.1985

[62] Ezugwu E.O.and Wallbank j. Material Science and technology vol .3 881(1987)

[63] Ezugwu E.O. PhD thesis, University of Warwick, 1986.

[64]E.M.Trent Wear of Metal Cutting Tool.

[65]E.M.Trent Wear of Metal Cutting 2nd edition 1984.

[66]A.Jawaid, PhD Thesis University of Warwick,1982.

[67] Trent, E.M.Wear of Metal Cutting Tools, Treatise on material science and technology vol 13.

[68] Opitz H.and W.Lehwald,1963 Kolm and opladeu,West Deutscher Verlag.

[69] Braiden, P.M.Thermal Conditions in Metal Cutting.

[70] Lewis Lay,Bsc.Corrosion Resistance of technical ceramics 1983 p.5.

[71] Riessling R.ISI Publication 115,1968,London.

[72] Joseph, R.A.and Tipris,V.A.Influence of Metallurgy on Machinability,1975.

[73] Wicker

[74] Joseph, R.A.and Tipris,V.A.Influence of Metallurgy on machinability,1975.

[75] Manston, G.J.and Murray,J.D,S.Iron and Steel Inst.1970 p.568

[76] Moore C, Proc.9th Int.MTDR Conf.1968 p.929 Publication 94p.35

[77]Konig.W. Industry an Zeiger,1965,87,61,131,165.

[78] Trent, E.M.ISI Publication 94, 1967, p.77.

[79] Zalwali, Z. Wear, 1976,38 p, 1.

[80] Williams, J.E.Smart E.F.and Milner,D.R.Metallurgia. 81, 6(1970)

[81] Shaw, M.C.Usui E.and Smith,P.A.Trans(B) 1961,May p.181.

[82] Trent, E.M.Metal Cutting 2nd ed. Butterworth 1984 p.191.

[83]Azra J.Caffernelli,D.and Romalingram S.Trans.ASME1974 96B(4),p.1230.

[84] Keane, D.M.ISI Leeds, 1974.

[85] Brown.T.J.and Charles,J,A.J.Iron and steel Ins.1972,240,p.702.

[86] Hilty, D.C.and Crafts,W.,Trans AIME,1964,233p.210.

[87] Clayton, D.B. and Brown J.R.J Iron and Steel Aug 1969 215.

[88] Baker, T.J and Charles,J.A. Iron and Steel Inst.1972,240,p.702.

[89] Moore, C.Proc 9th Int. MTDR Conf.1968p.929.

[90] Brown G.G. and Watsosn,J.d. Metals Austilisia April 1978p.10.

[91] Joseph, R.A.and tipris,V.A.Influence of Metalurgy.

[92] Ekerot, S.The behavior of silicate inclusions in steel during hot working sand.J Metallurgy 3.1974,21-27.

[93] Mander, P.H.J.and Charles,J.A.J.Iron and steel Inst.1968,206,p.705.

[94] Kiesling, R.Journal of Metal,Oct.1969,p.48.

[95] Baker, J.J.and Charles,J.A.J.Iron and steel inst.1972,210,p.680.

[96] Vaubly P.E.Steel times Annual Review 1972,200,p.147.

[97] Ekerot S.Stand J. Metallurgy 1974,3,p.102.

[98]Klevebruig B.Scand.J. Metallurgy 1974,3,p.102.

[99] Sundstrom B., J.Comp, Mater, 1971, 5p.277.

[100] Mann, G.S.Van Vlack,L.H.Metallurgy Trans.1972,3,p.2005.

[101] Gove, K.B.and Charles,J.A.Metals Technology 1974(a)p.425.E Sheinel and R.Schell:Stehl Eiseu, 1952, 72,683.

[102] BakerT.J.and J.A.Charles, 1972 680 J.Iron and steel Institute.

[103] H.C.Chas et al Trans.AIME1963,227,796.

[104] H.C.Chas et al Trans.ASM 1964.

[106]Reane D.M.(1974) The influence of inclusions on machinability.Proc.Conf.on inclusions And their effect on steel properties, ISI Leeds. Publication 94, p.35.

[107] T.M.Banks and T Gladman. Met Technology 1979. , 6, 81.

[108] L.E.Wood and L.M.Van Vlack.ASM Trans. A 1963,56,770.

[109] Iwata and Veda Proc .Int.Conf. Prod.Eng.part 1, 516, 1974.

[110] (1)y.k.Chou,Evans M.M. barash, Experimental investigation on CBN turning of AISI 52100 steel, Journals of Materials Technology 134(2003)pp.1-9.

[111]Z.W. Zhong,L.P Khon, S.T.Han. Prediction of surface roughness of turned surfaces using neural network,International Journal of advanced Manufacture Technology 28 (2006),pp688-693.

[112].Agapio J.S.,G.W. DeVries M.F.,On the machinability of powder metallurgy austenitic stainless.Journal of engineering for industry.Transactions of the ASME 110(1988)11,pp.339-343.

[113].Belejechak P.,Machining Stainless steel,Advanced materials & processes,December 97,vol.152,Issue 6,pp.23-25.

[114]K.Ibsan,K.Mustafa,C.Ibrahim,S.Ulvi, Determination of optimum cutting parameters during machining of AISI 304 austenitic stainless ,Materials and Design 25(2004),pp.303-305.

[115]E.C.Bordinassi,M.F.Stipkovic,G.F Bastalha,S.Delijaicoy,Superficial integrity analysis in a super duplex Stainless , after turning,journal of achievements in materials and manufacturing Engineering 18(2006),pp.335-338.

[116]N.H.Elmagrahi,Shuaeih,C.h.C.Haron,an overview on the cutting tool factors in machinability assessment,Journal of Achievements in Materials and Manufacturing Engineering 23/2(2007).pp87-90.

[117]G.P.Petropoulos,Multi-parameter analysis and modeling of engineering surface,texture,Journal of achievements in Materials 24/2(2007),pp.91-100.

[118]K.Chou,H.Song,Tool nose radius effects on finish hard turning,texture,Journal of Materials Processing Technology 148(2004).pp.259-268.

[119] T.S.Wang, J.yang, Sliding friction surface macrostructure and wear.Journal surface and coating Technology 202(2008).4036-4040.

[120]Christopher C.Statistics for technology, 1975, p.140.

APPENDICE

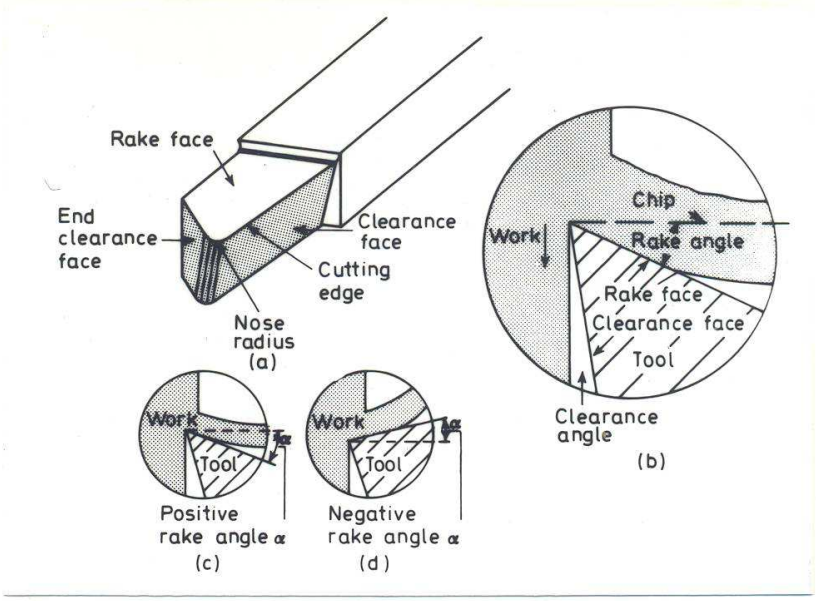

Fig 1A. Cutting Tool terminology (after Trent)

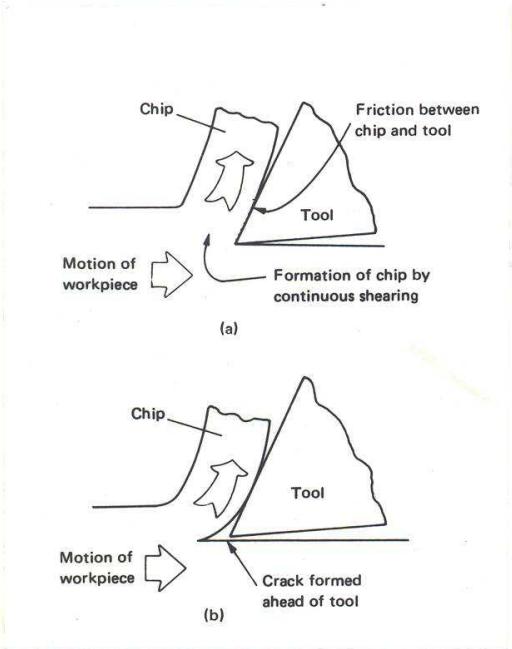

Fig 1B.Models of the cutting process. a) present day model: b) earlier misconception

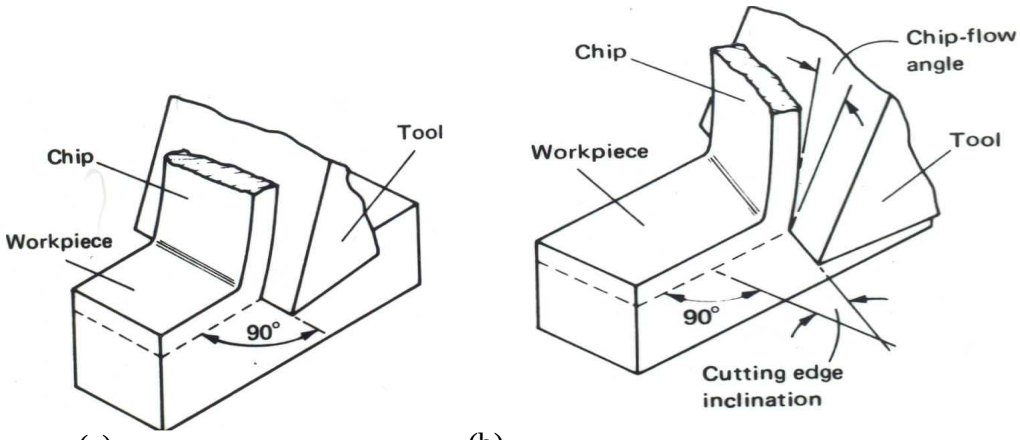

(a) (b)

Fig. 2: Orthogonal and oblique cutting.

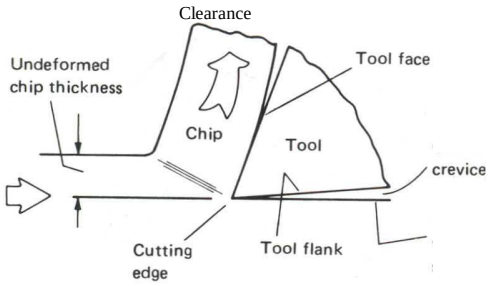

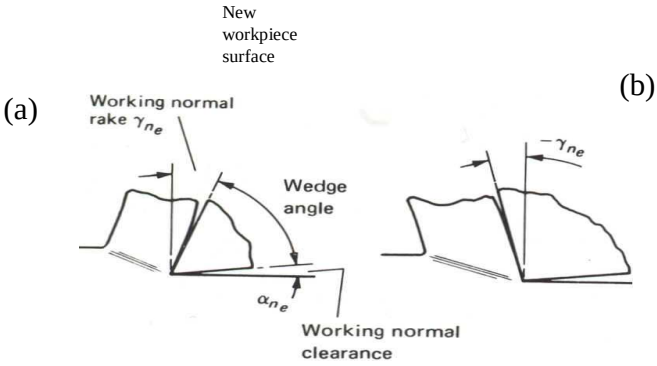

Fig.3: Terms used in metal cutting

f

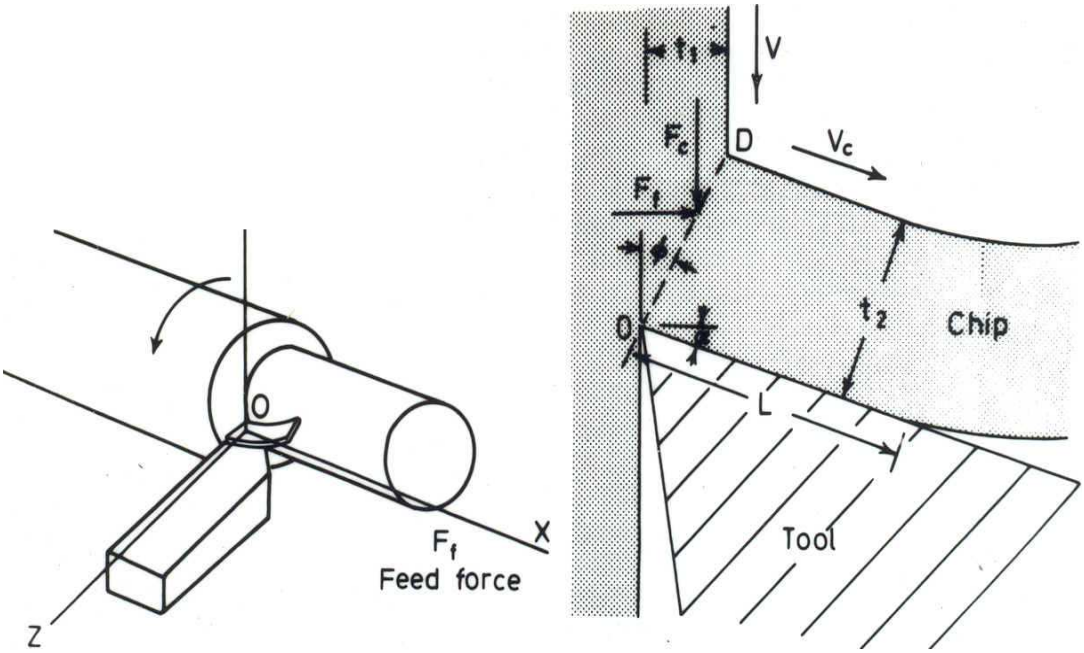

Fig.4 : Forces acting on cutting tool

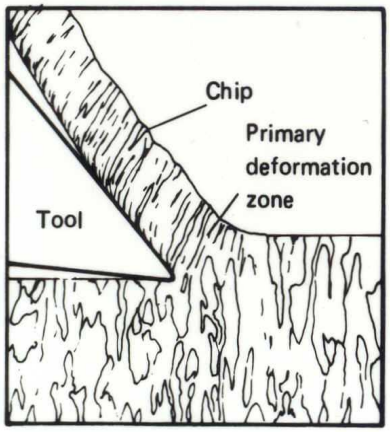

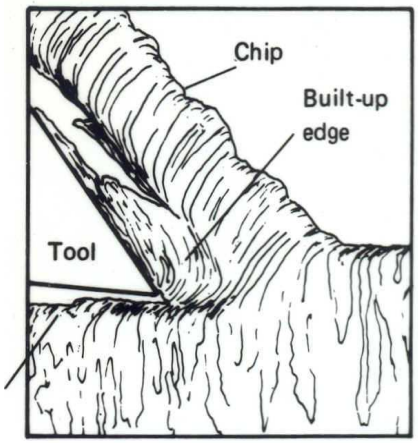

Rough workpiece surface

a) Continuous chip **b) Continuous chip with built up edge**

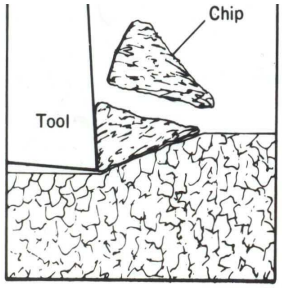

C) Discontinuous chip.

Fig 5. Chip formation

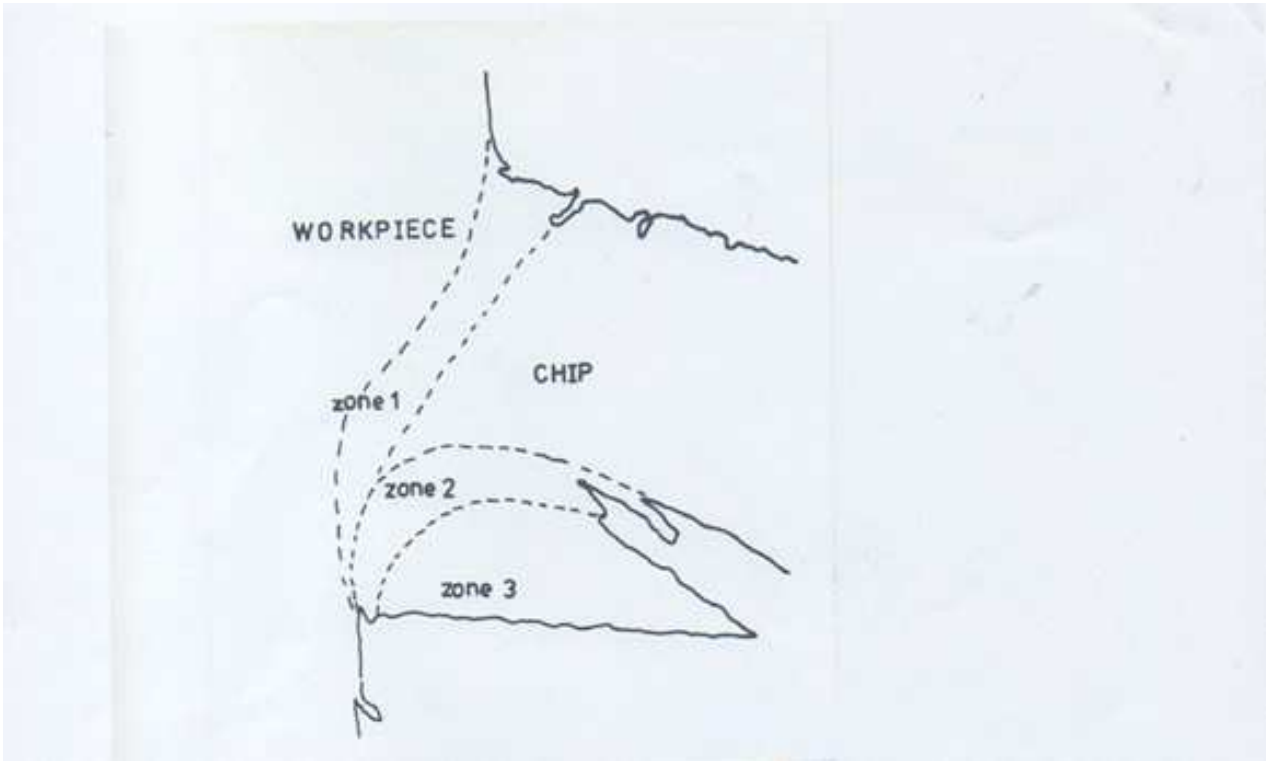

Fig. 6: a) Diagram of built up – edge showing the three zones of deformation (after Wallbank)

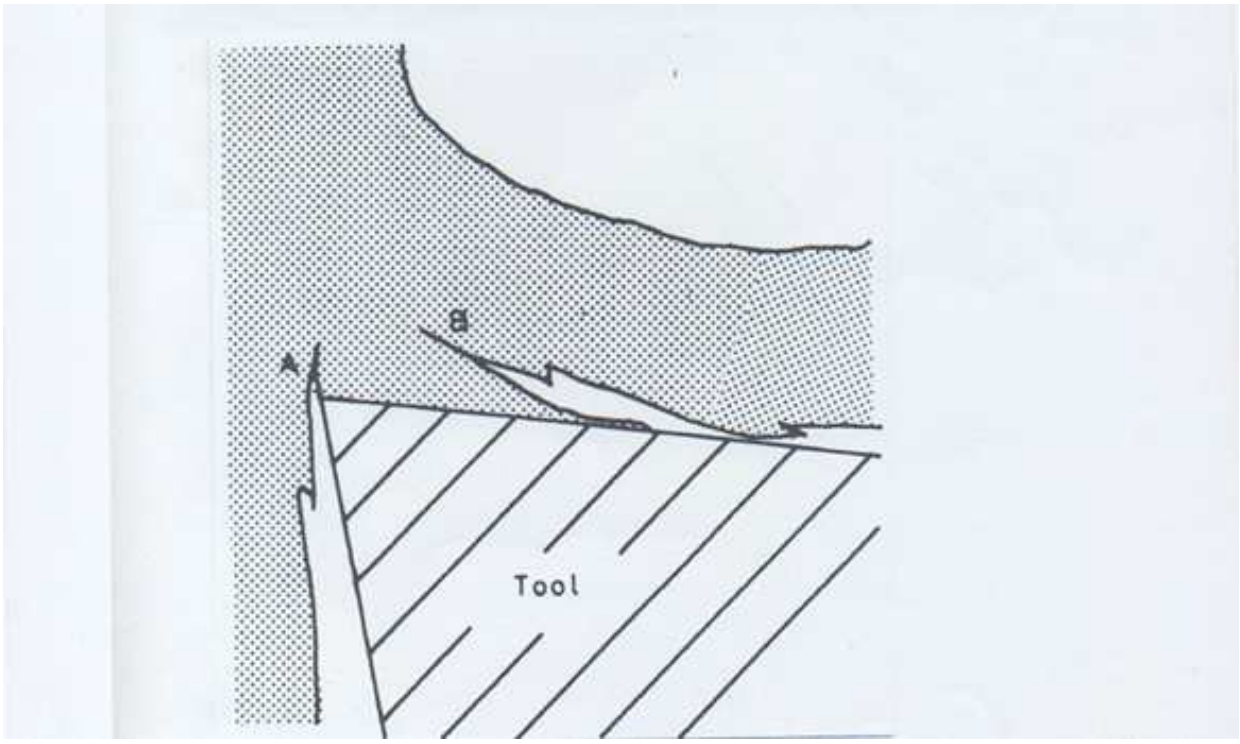

Fig. 6: b) Form of built – up edge (Trent)

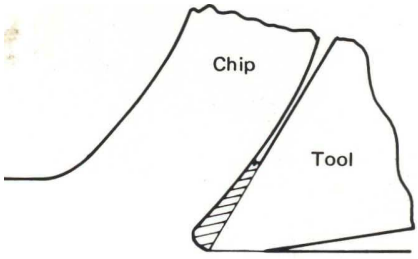

(a)Built-up-edge protecting tool face

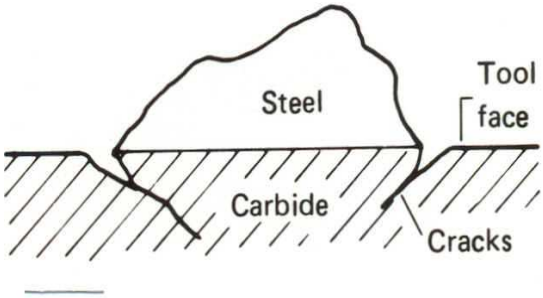

Built up edge fragment
(b) Cracks formed (After Trent)

Fig. 7

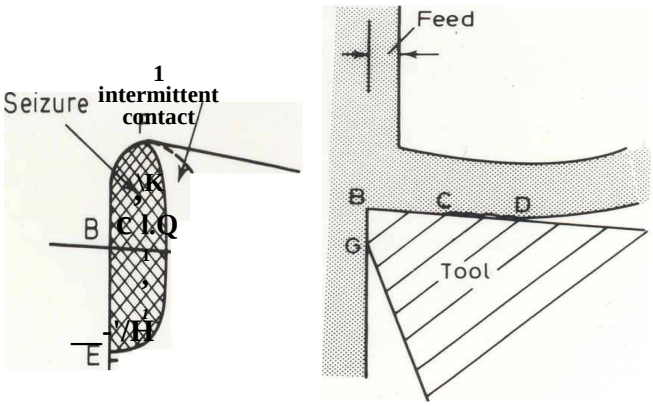

Fig. 8: Areas of seizure on cutting tool.

Works material	Cutting force Fc (N)	(lbf)	Contact area (mm^2)	(in^2)	Mean compressive stress ($N\ mm^{-2}$)	($tonf/in^2$)
Iron.	1070	240	3.1	0.004 8	340	22
Copper	4150	930	13.5	0.021	310	20
Titanium	4.55	102	0.77	0.001 2	570	37
Steel						
medium carbon)	490	110	0.65	0.001	770	50
70/30 brass	500	111.5	12.2	0.019	420	27
Lead	323	72.5	22.5	0.035	14	0.9

Fig 9. Estimated values for the mean compressive stress.

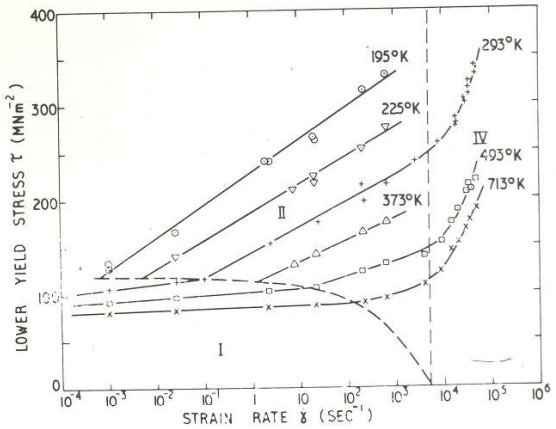

Variation of lower yield stress with strain rate, at constant temperature.

(a)

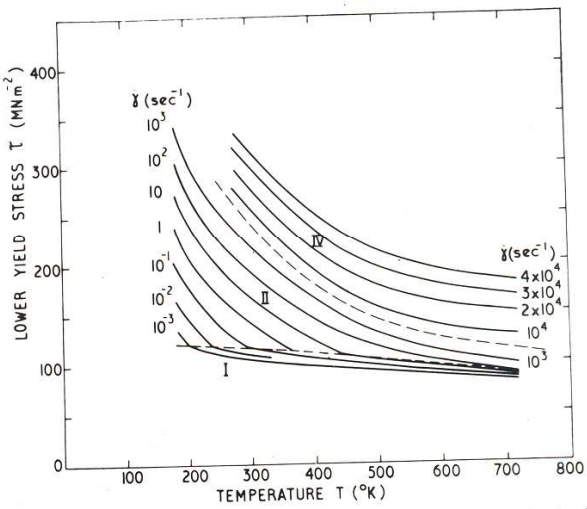

Variation of lower yield stress with temperature, at constant strain rate.

(b)

Fig 10. (After Campbell and Ferguson)

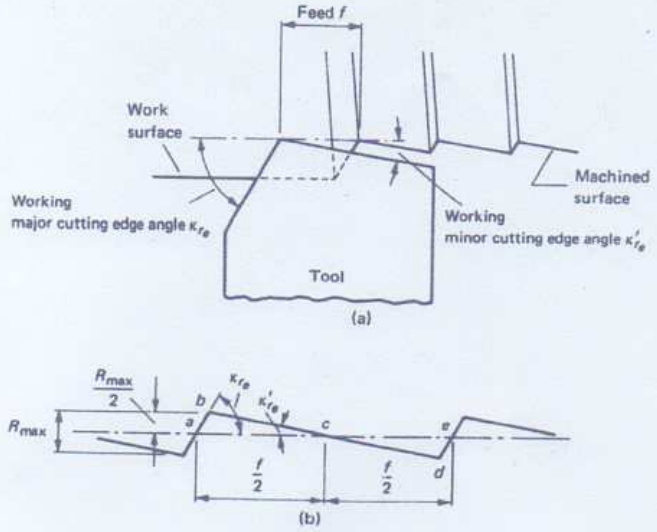

(a) Idealized model of surface roughness for a cutting tool with a sharp corner (after Boothroyd)

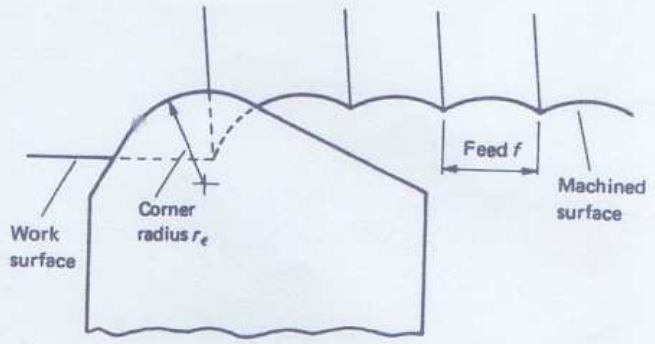

(b) Idealized model of surface roughness for a tool with a rounded corner (after Boothroyd)

- Fig 11. -

$$C.L.A = \frac{A_1+A_2+A_3+\cdots+A_n}{L}$$

$$= \frac{\sum_n^1 A}{L}$$

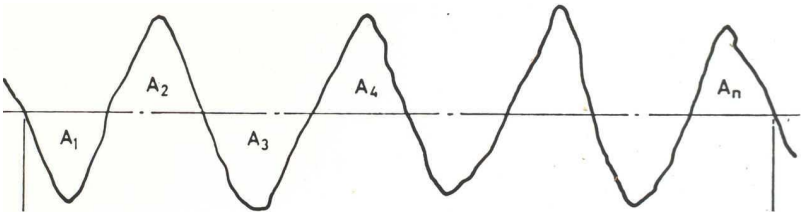

a) Graphical representation of R_a.

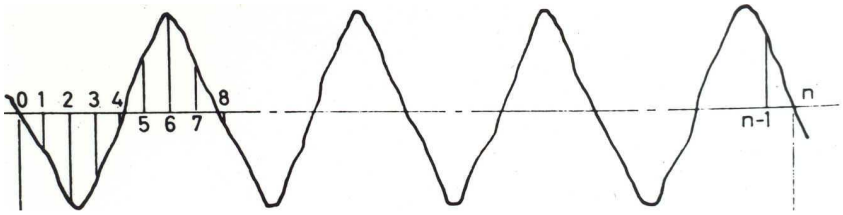

b) Graphical representation of R_q.

Fig. 12

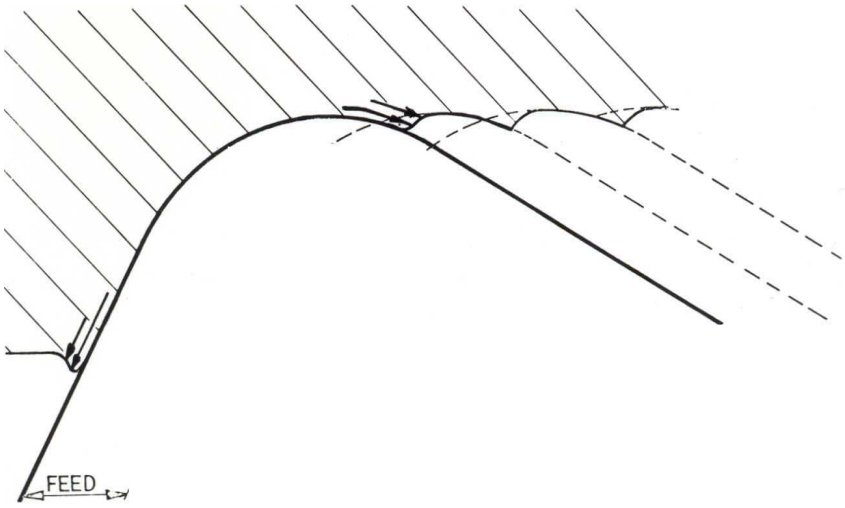

- **Schematic diagram Showing cracks which form at tool tip at low cutting speed (50 rpm) and their consequence with regard to surface fracture.**

Fig. 13: Showing how squeezing may affect surface finish in turning after Pekelharing.

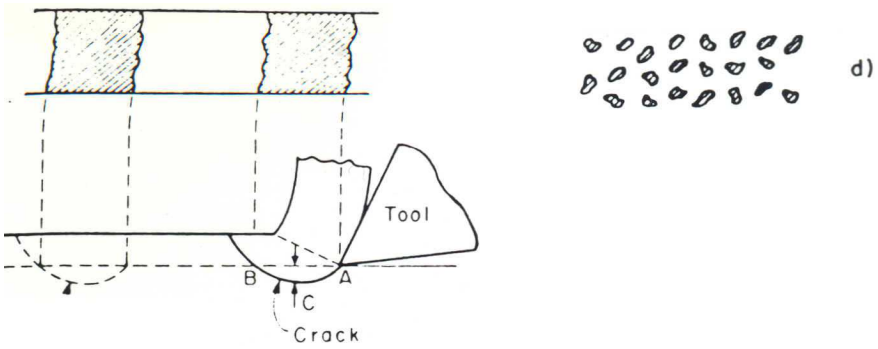

Fig. 14 (a): Formation of the surface in discontinuous chip formation range, after Shaw.

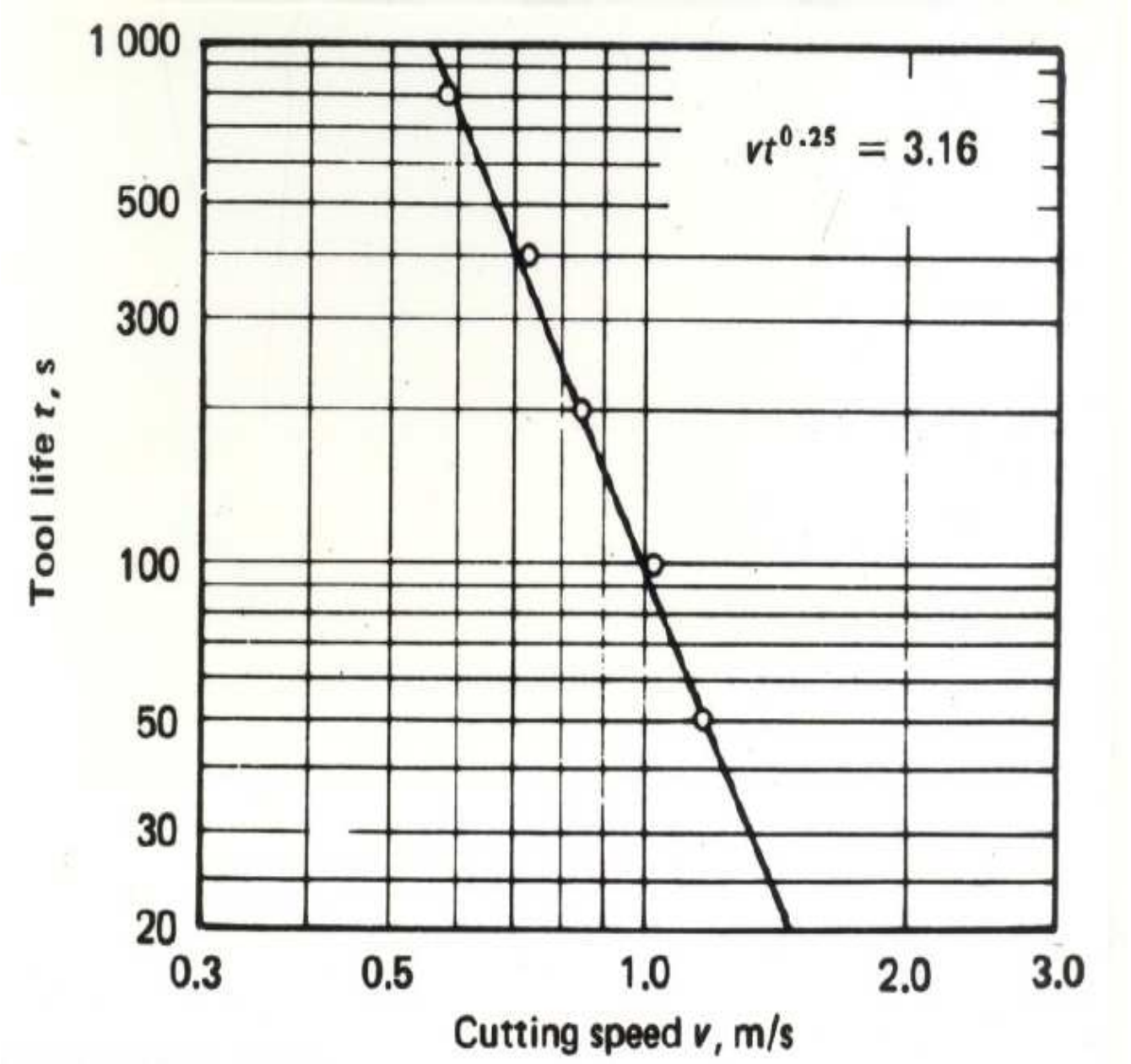

Fig 15. Relationship between tool life and cutting speed (after Geoffrey Boothroyd)

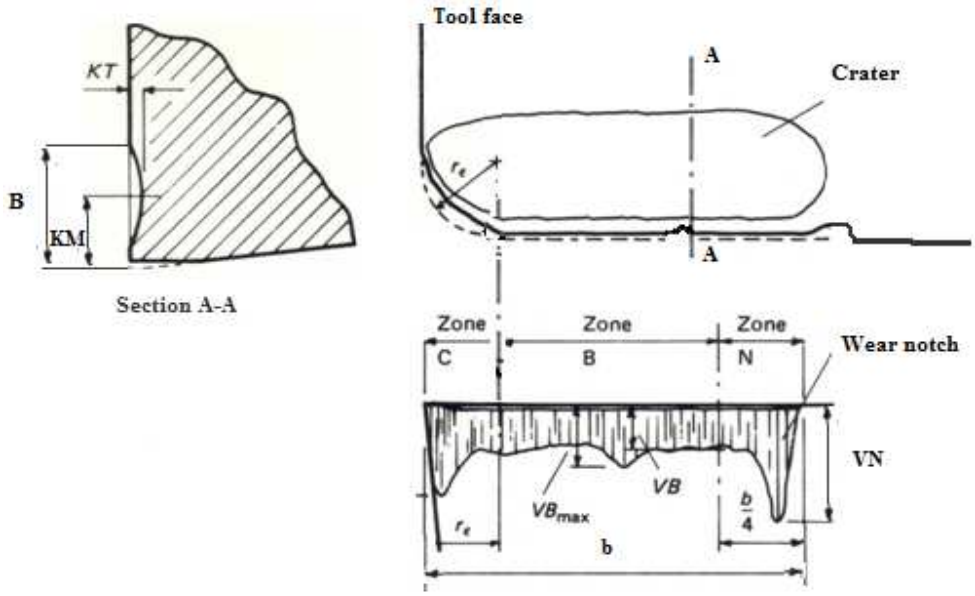

a) Some features of single pt tool wear in turning operations (after ISO/TC29/WG).

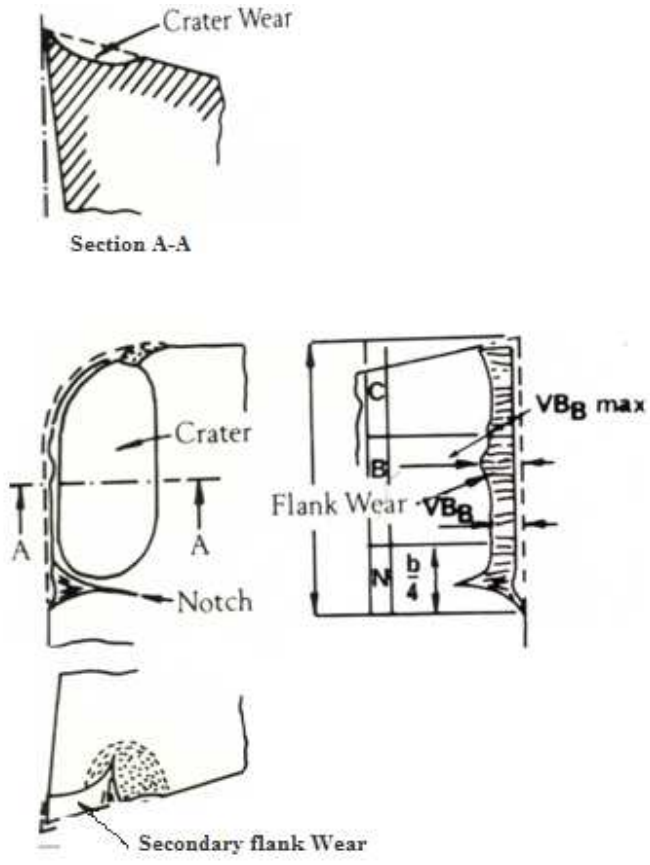

b) Types of Wear in turning tools

Fig. 16

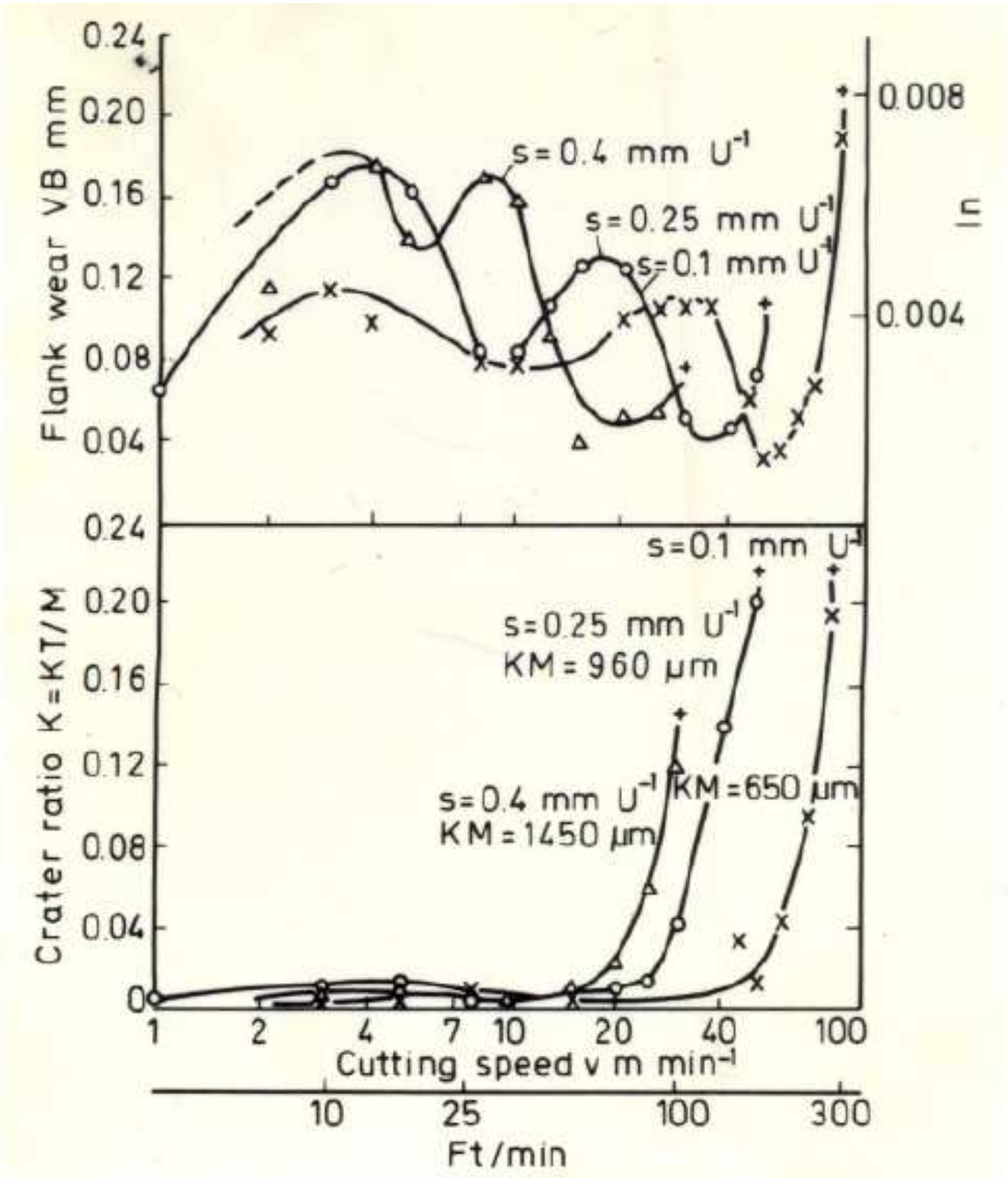

Fig. 17: Influence of cutting speed and feed on flank and crater wear of high speed steel tools after cutting steel (after Opitz and Konig).

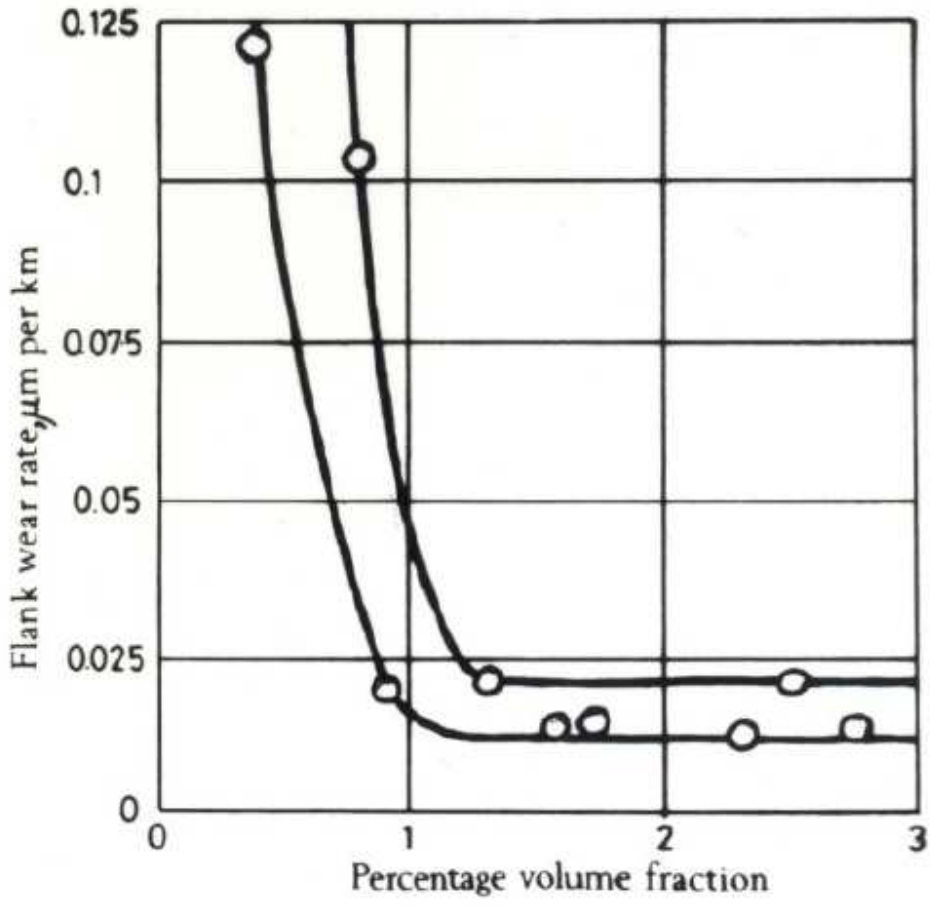

Fig. 18: The effect of volume fraction of manganese sulphide inclusions on the wear rate of a high speed steeltool (after Keane).

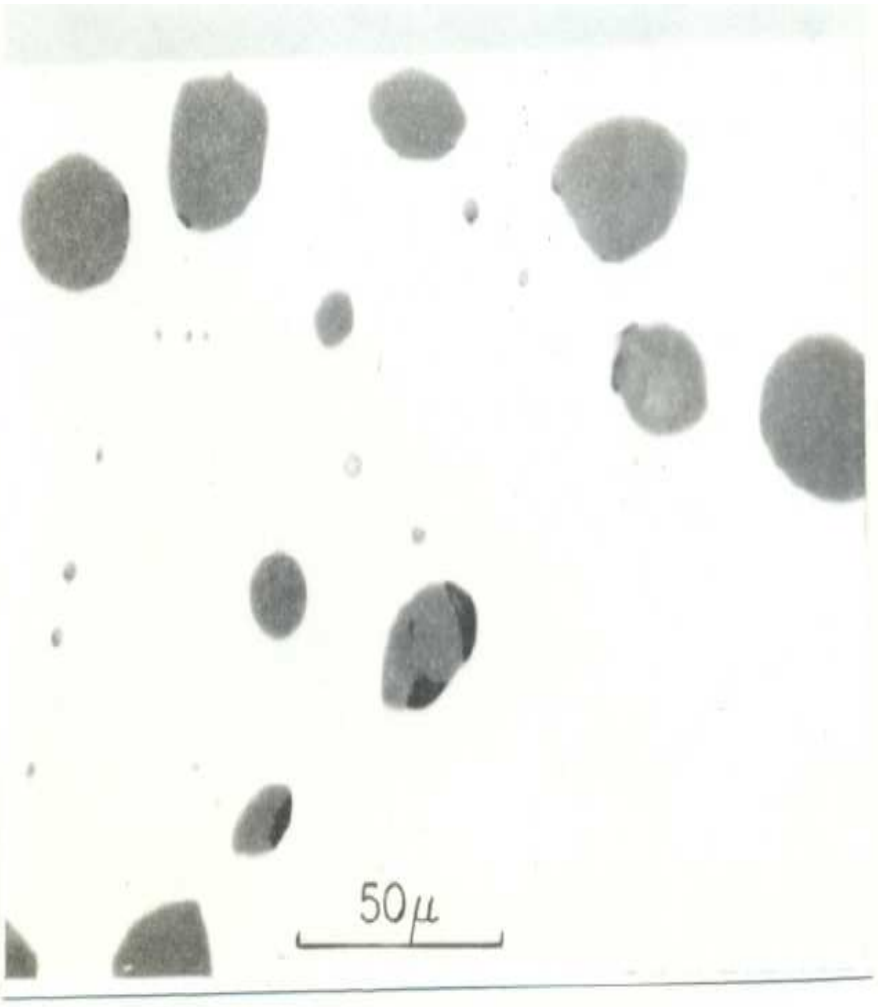

Fig. 19: Type I Sulphides.

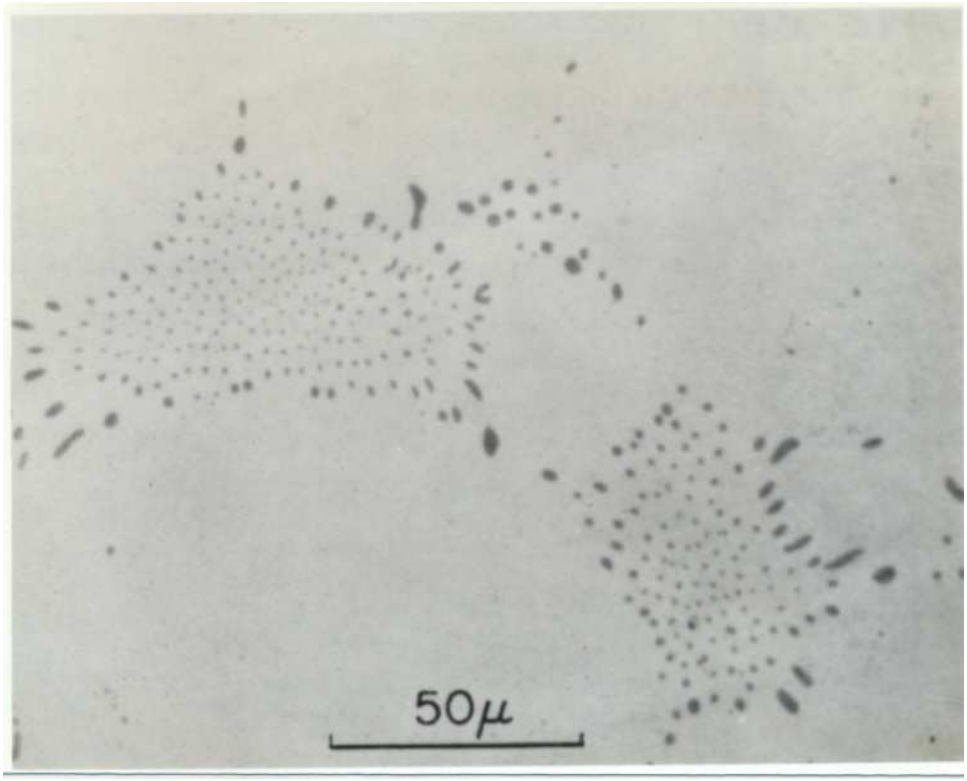

(a) Type 2 Sulphides.

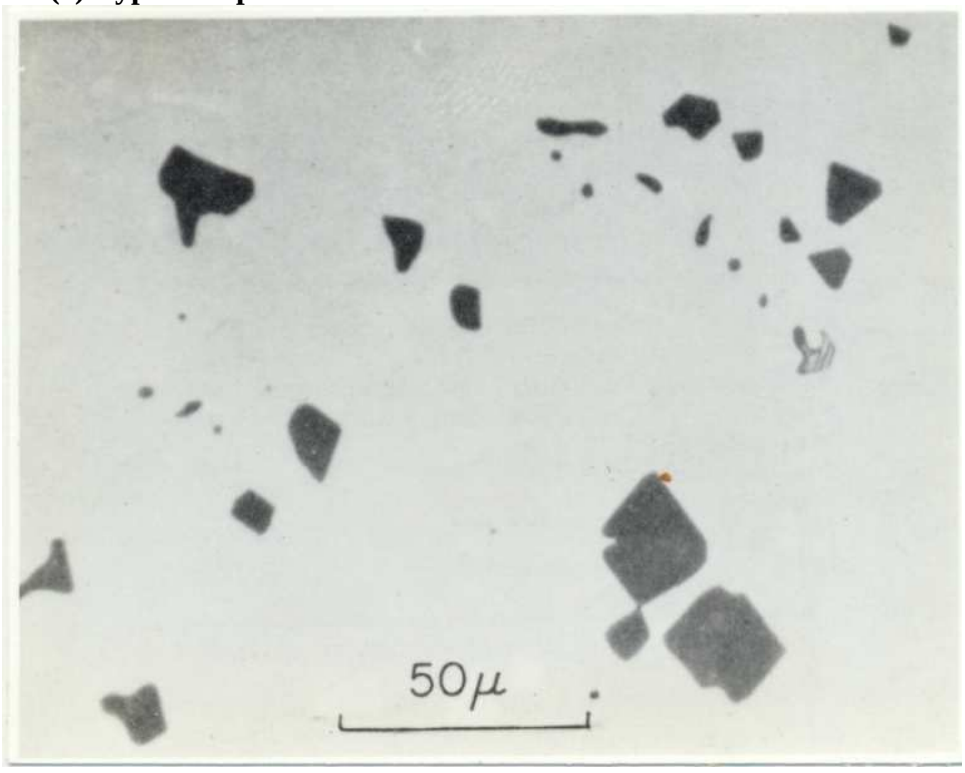

(b) Type 3 Sulphides.

Fig. 20

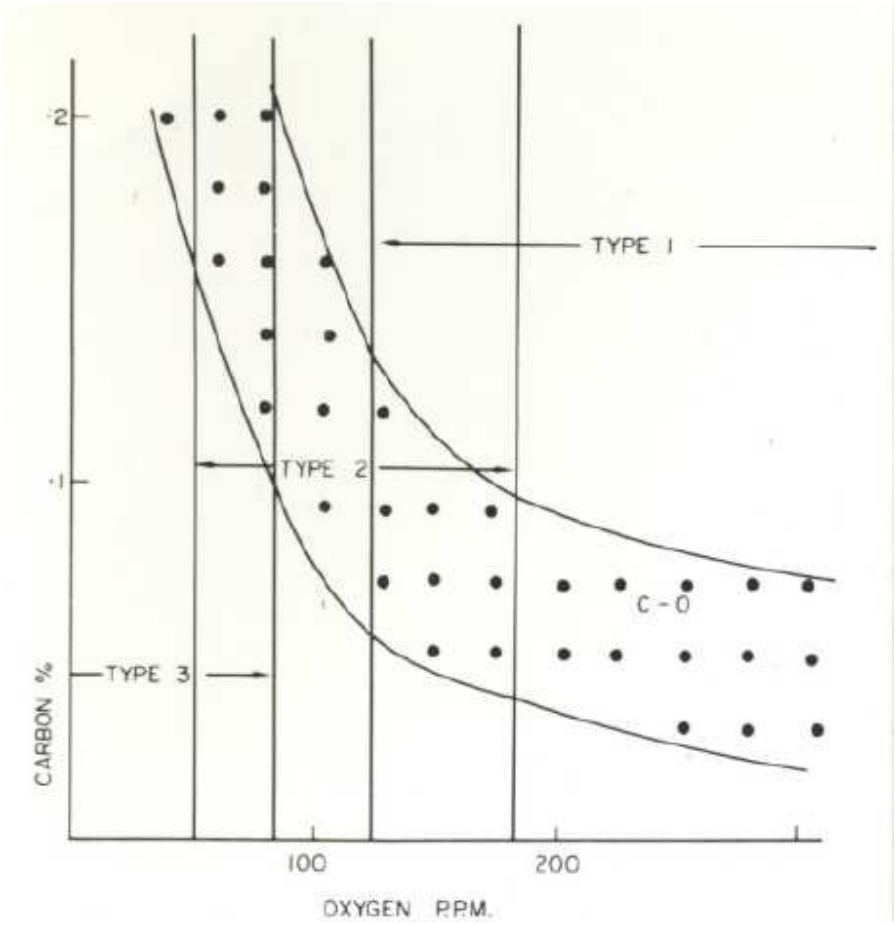

Fig. 21: Carbon, Oxygen and sulphide type diagram

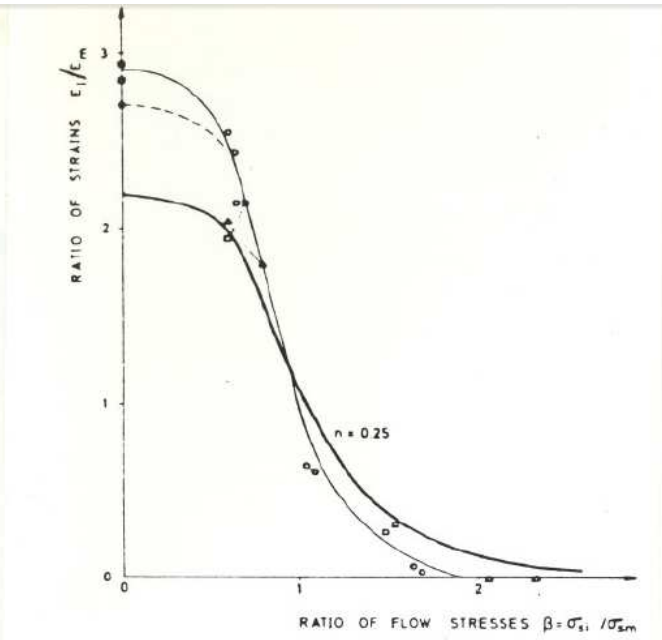

Fig 22. Deformation index as a function of the flow stress ratio of inclusion and steel matrix for two values of the strain-hardening parameter after Sundstrom[70]

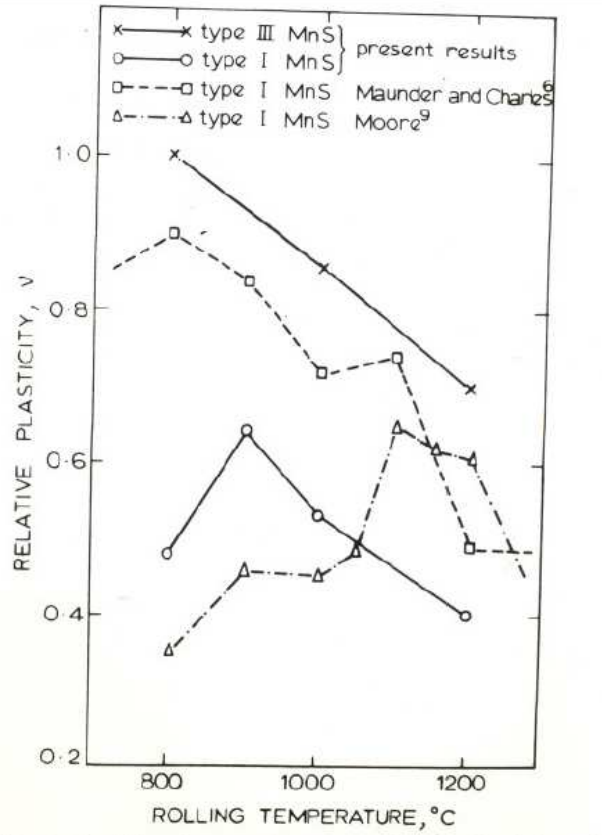

Effect of rolling temperature on relative plasticity of MnS

. After Baker and Ferguson[65]

Fig. 23

a) Microstructure of the workpiece material

b) Microstructure of the workpiece material

Fig. 24

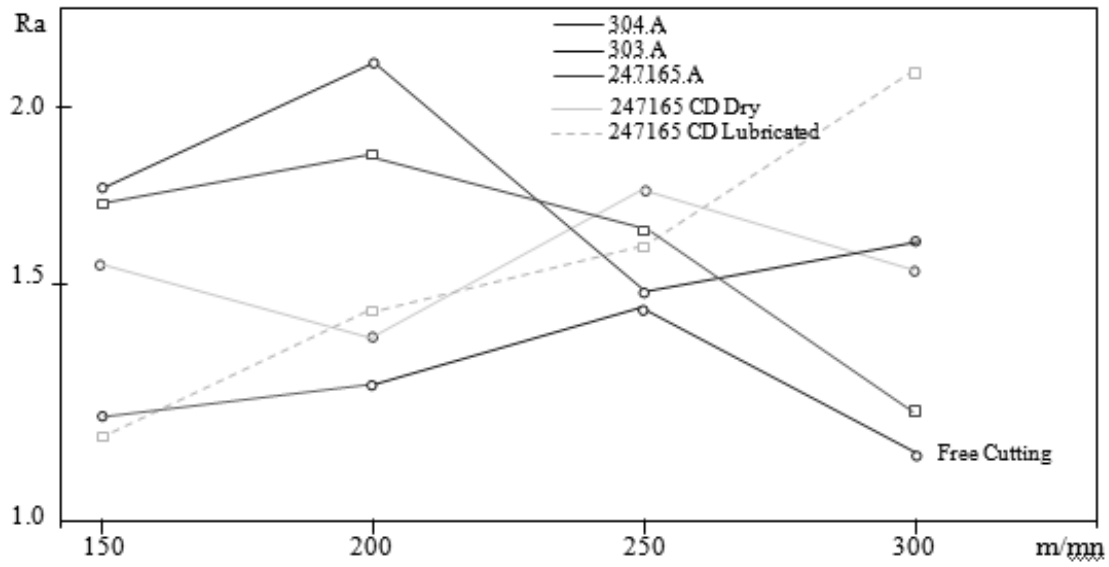

Fig.25: Variation of surface roughness value against cutting speed

Fig. 26: Surface finish of 247165 cold drawn at a speed of 150m/min. Dry condition.

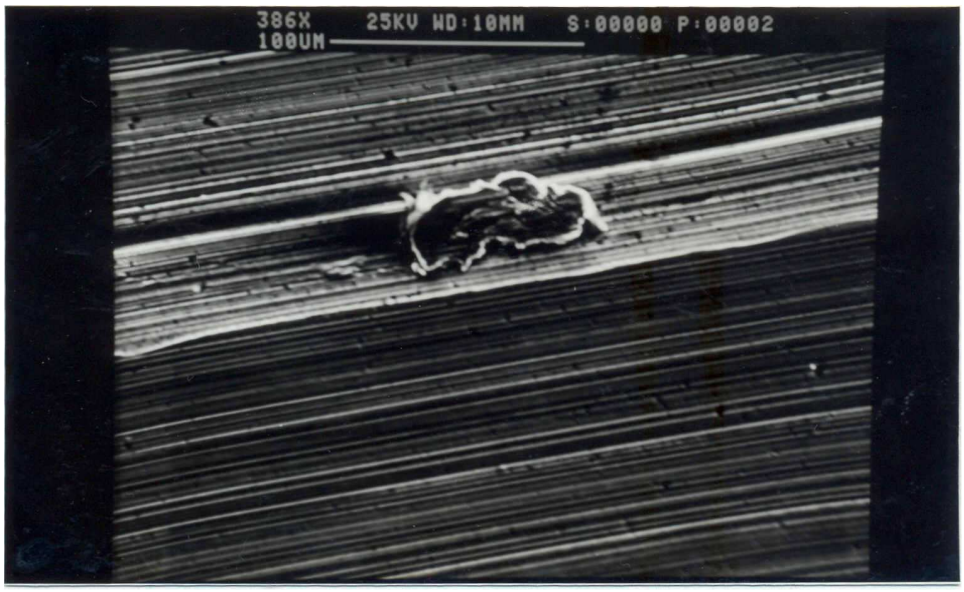

Fig. 27: Surface finish of cold drawn at a speed of 15Om/min Dry condition

Fig. 28: Surface finish of cold drawn at a speed of 200m/min. Lubricated condition.

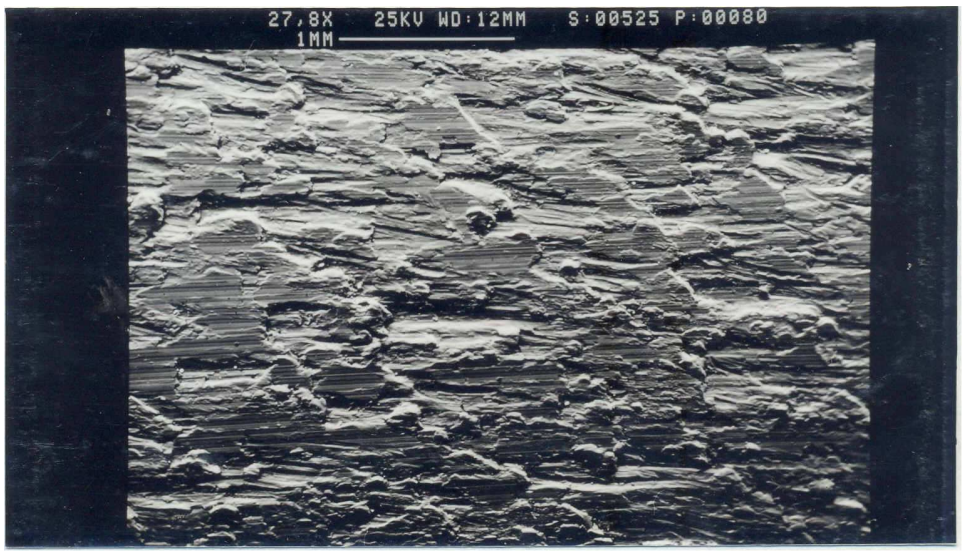

Fig. 29: Surface finish of Annealed at 200m/min Dry condition.

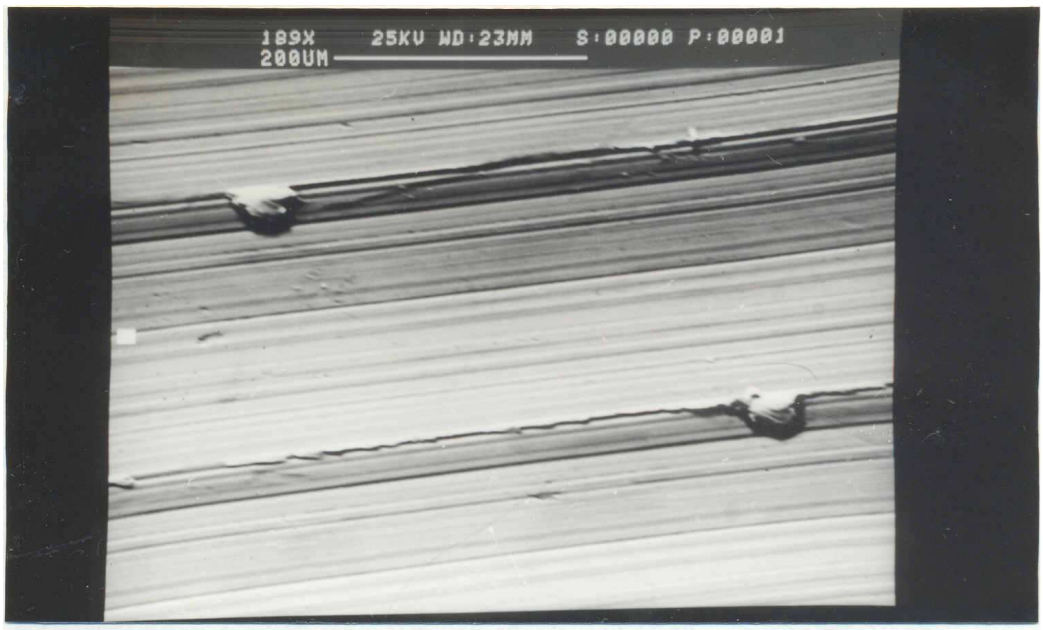

Fig. 30: Surface finish of Annealed at a speed of 250m/mn. Dry condition.

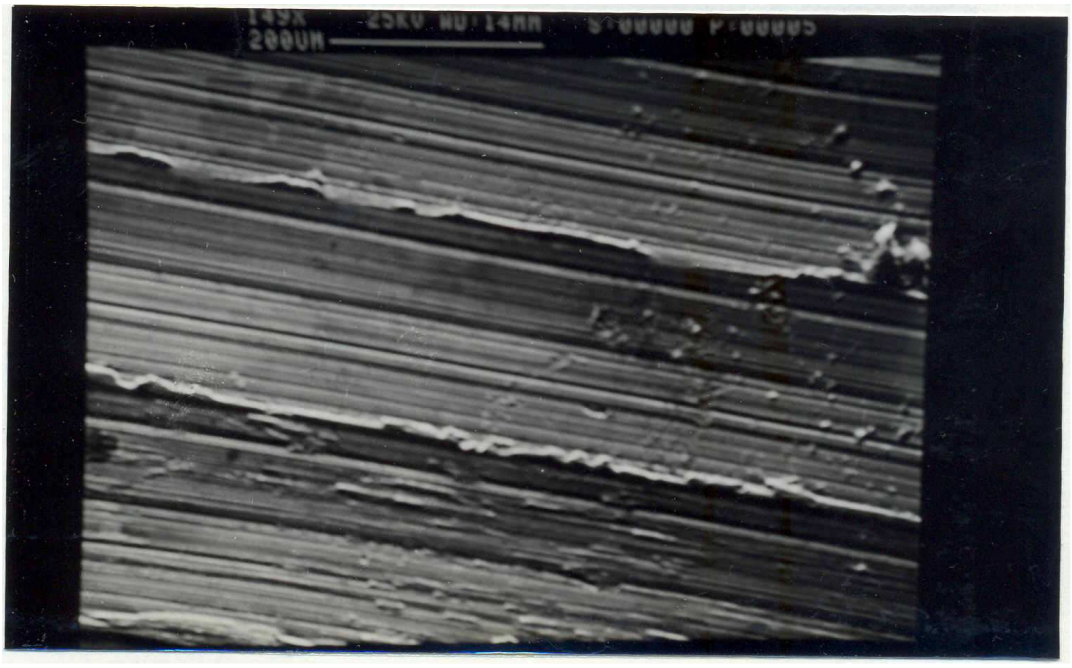

Fig. 31: Surface finish of cold drawn at a speed of 250m/min. Lubricated condition.

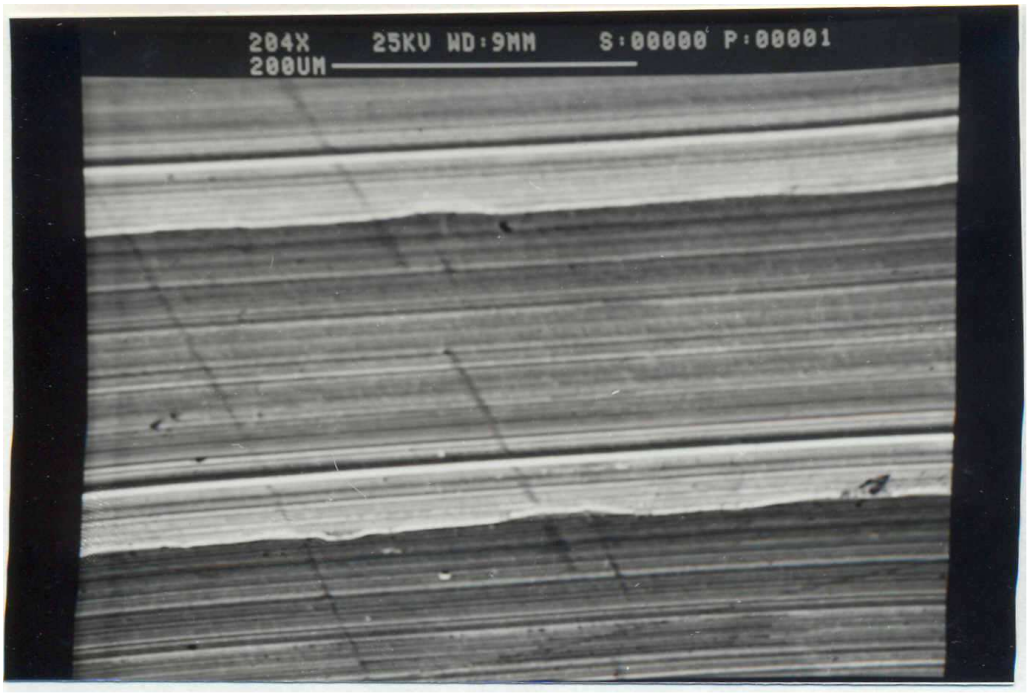

Fig.32: Surface finish of Annealed at at speed of 150m/mn. Dry condition.

Fig. 33: Surface finish of Annealed at a speed of 150m/mn. Dry condition.

Fig. 34: Surface finish of Annealed at speed of 200 m/min. Dry condition.

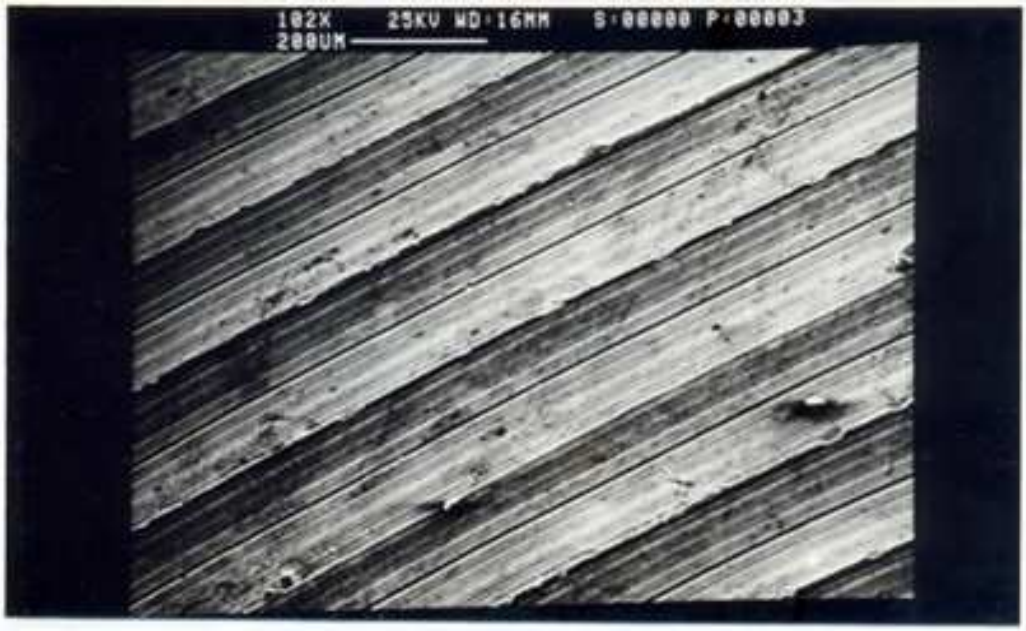

Fig. 35: Surface finish of Annealed at speed of 200 m/min. Dry condition.

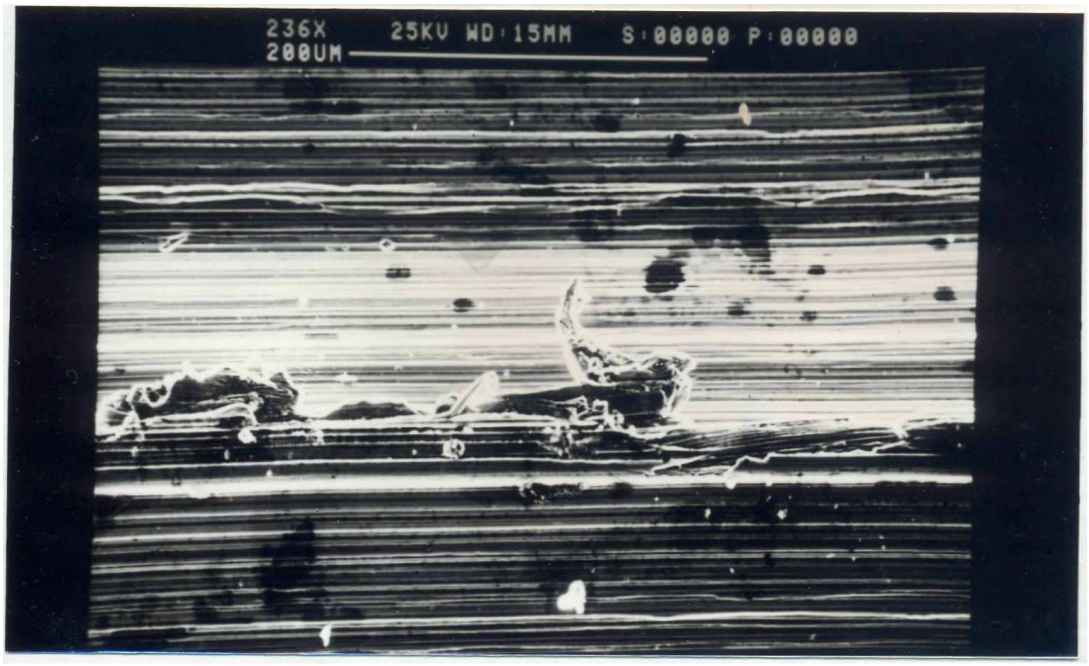

Fig. 36: Surface finish of Annealed at speed of 200 m/min. Dry condition.

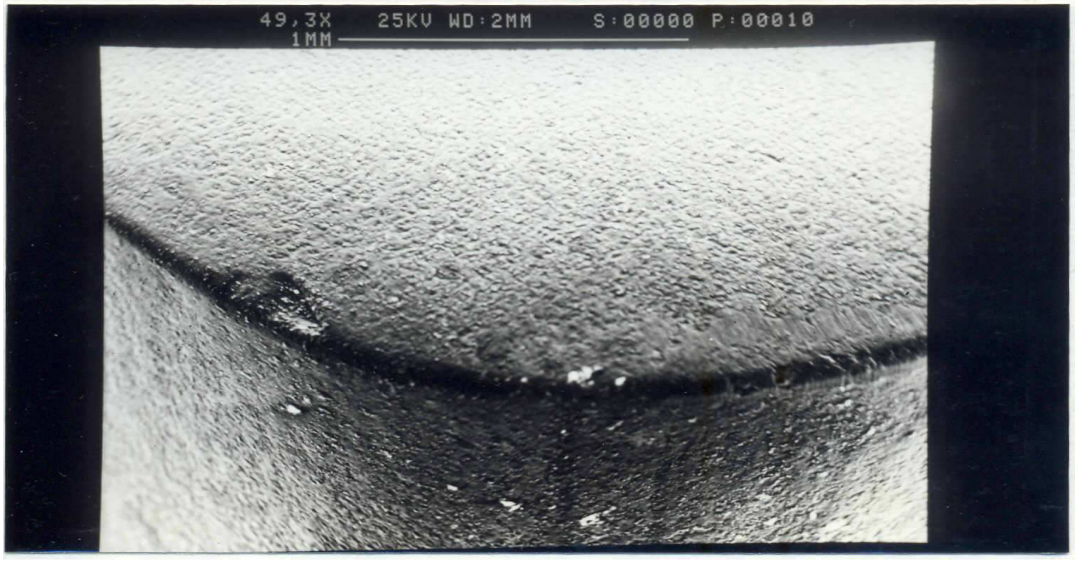

Fig. 37: GC 015 after 30 seconds of cutting time at a speed of 200 /min.

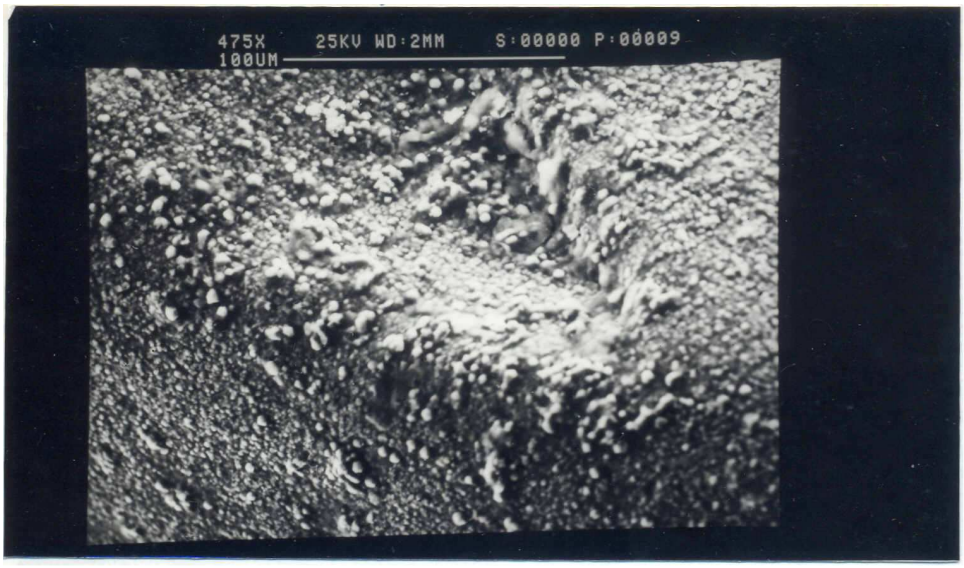

Fig. 38: GC 015 after 30 seconds of cutting at of 200 m/min.

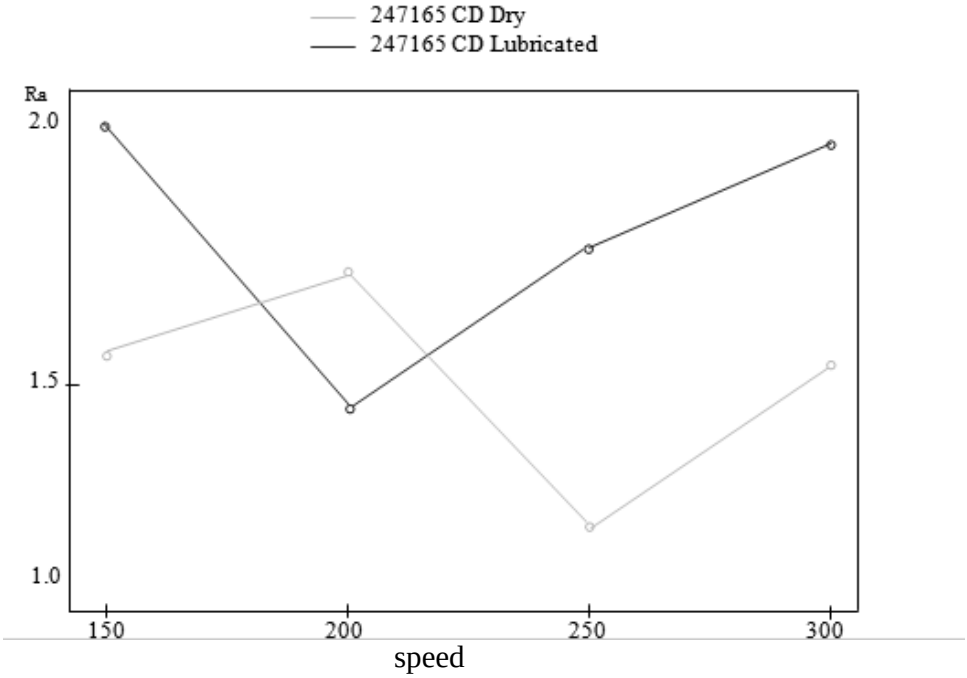

Fig.39: Variation of surface finish of cold drawn material Dry and lubricated condition

Fig.40: General view of a ground tool.
Negative rake angle α=6.11°
Clearance angle α=4.76°
Flank clearance 2
End clearance 1
0.2*[6] 25

Fig. 41: Surface finish at cold drawn at a speed of 200 m/min.
Using ground tool. r=1.27 mm

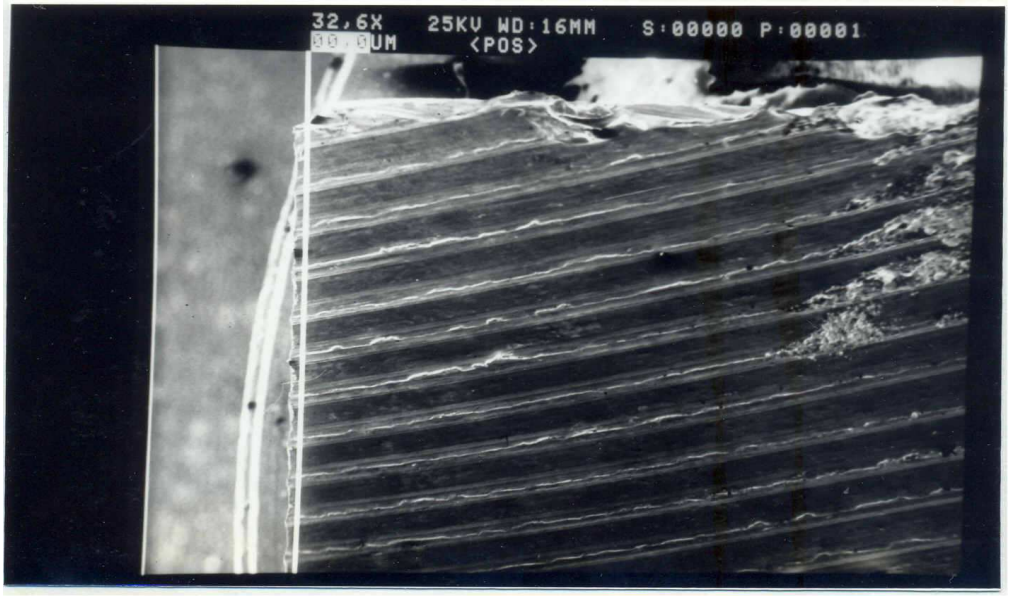

Fig. 42: Cross section of cold drawn at a speed of 200 m/min. Using ground tool. r=1.27 mm

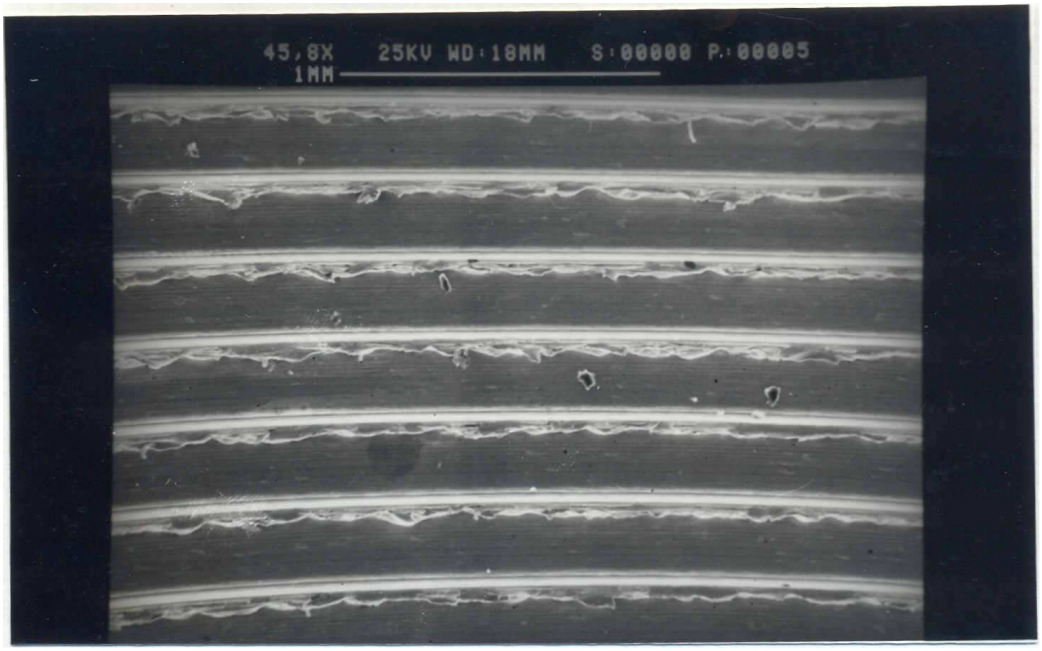

Fig43: Surface finish of cold drawn at a speed of *200m/min.* Using ground tool showing feed marks distortion.

Fig 44: Surface finish of cold drawn at a speed of 200m/min. Cross section, showing real profile of the surface.

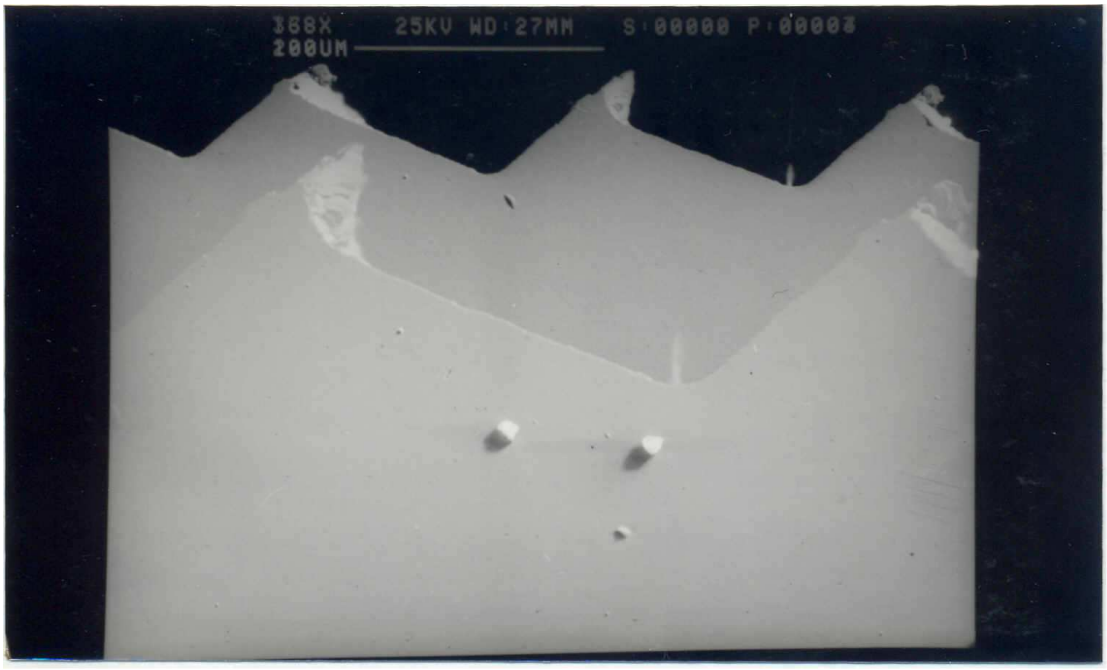

Fig 45: Surface finish of Annealed at a speed of 200m/min. Cross section showing extruded material.

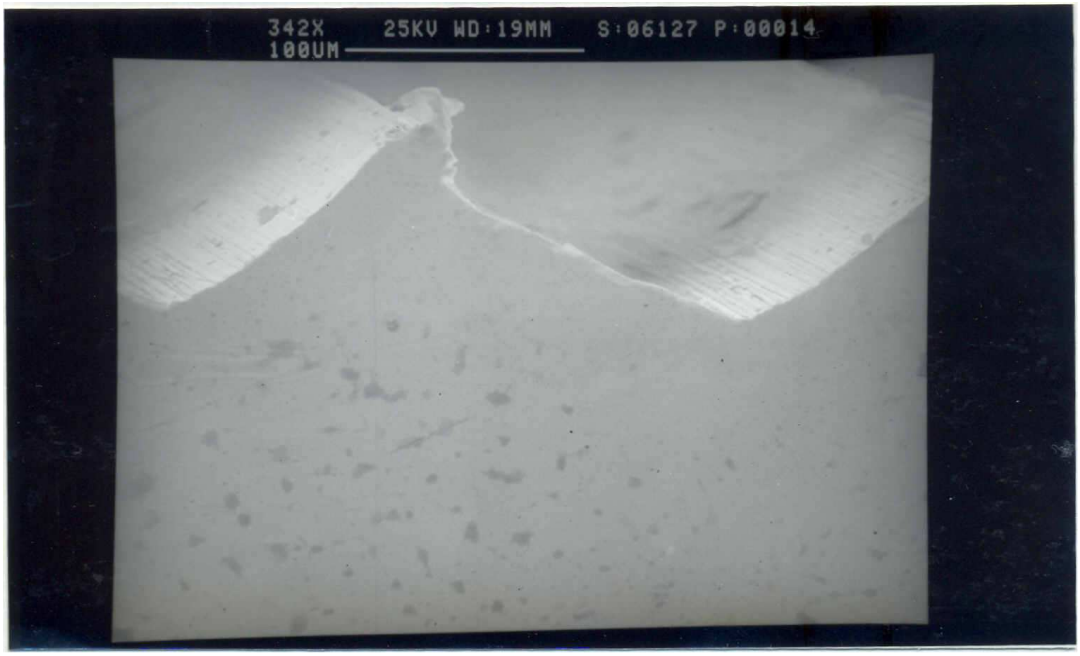

Fig 46: Surface finish of Annealed at a speed of 200m/min. Top of the feed marks.

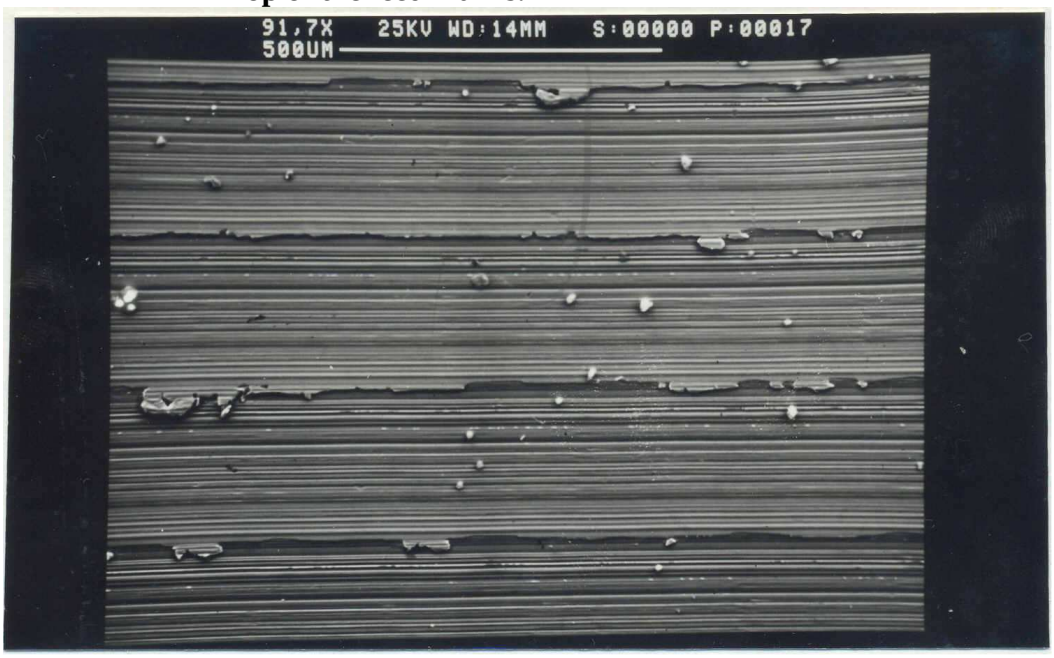

Fig47: Surface finish of Annealed at a speed of 250m/min.

Fig.48: Surface finish of cold drawn at 200m/min. Showing the feed marks.

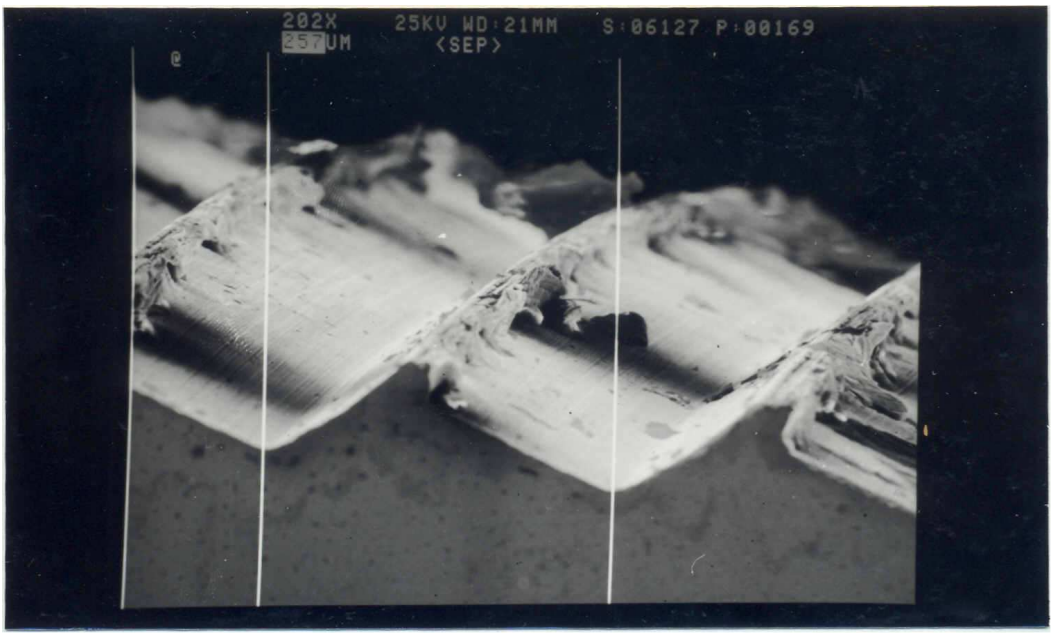

Fig.49: Cross section of surface finish of annealed at a speed of 250 m/min. Showing sponzipfel.

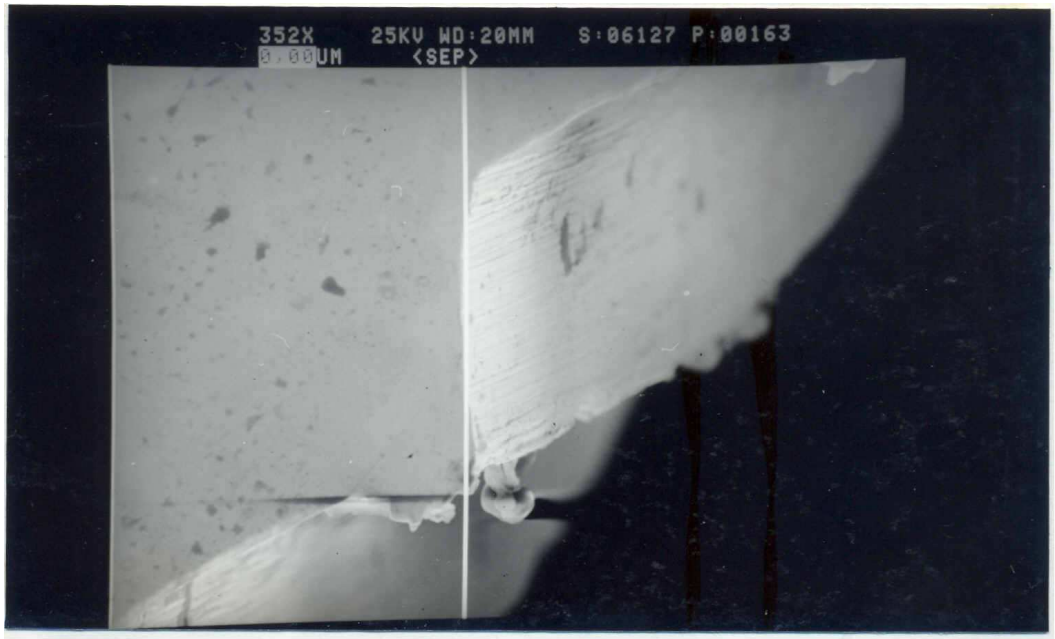

Fig.50: Cross sections of Annealed finish at 25Om/min. Showing the angle of the surface finish profile.

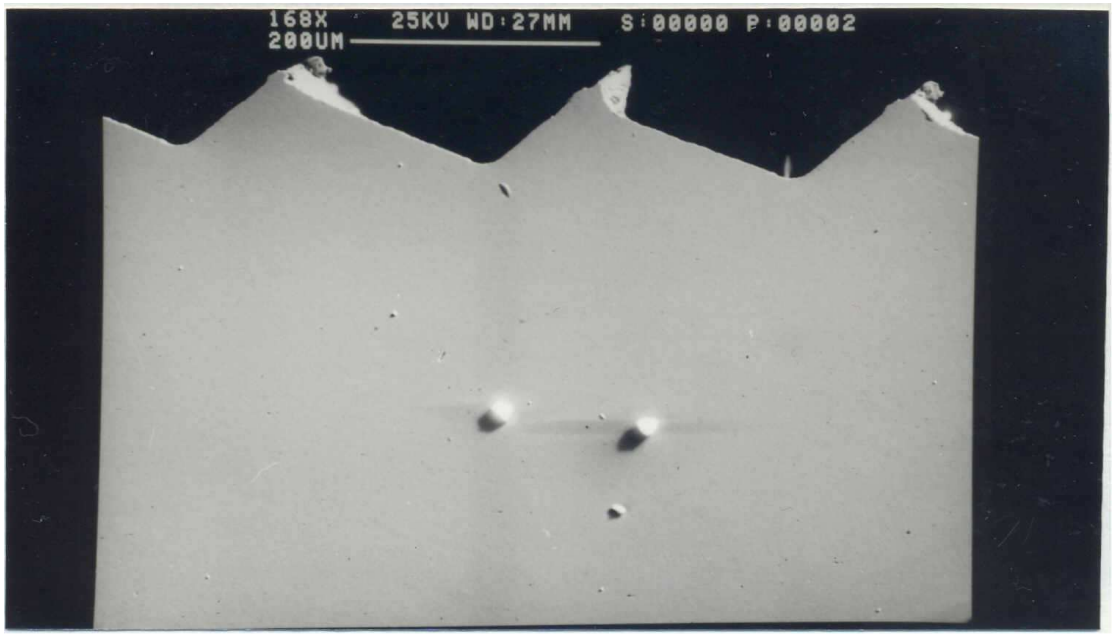

Fig. 51: Surface finish of Annealed at a speed of 200m/min. Cross section showing the top of the feed marks.

Fig. 52: Cross section of Annealed finish at a speed of 200m/min. Showing new shape of the feed marks.

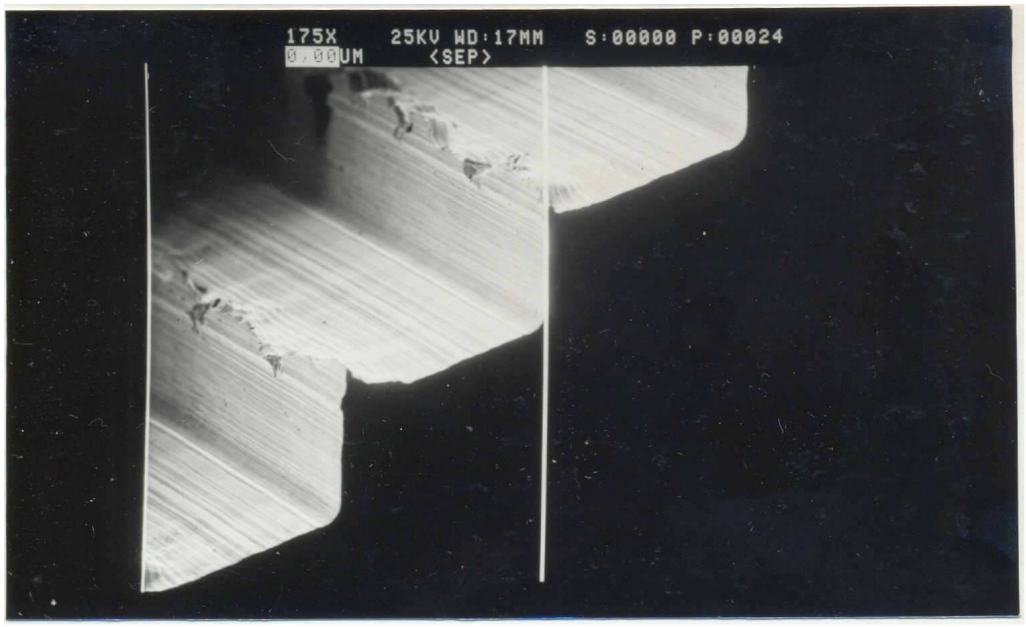

Fig. 53: Cross section showing squeezed material (247165 AD2) v = 200m/min.

Fig. 54: Cross section showing distortion of the feed marks (247165 AD2) v = 200m/min.

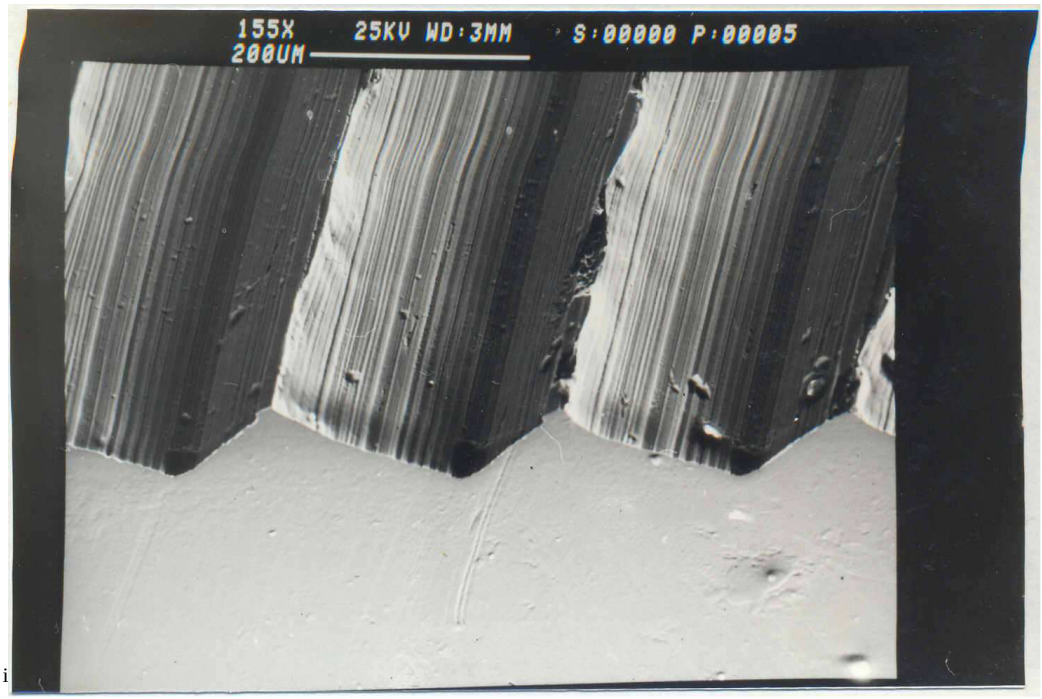

Fig. 55: Cross section showing real profile of the surface (247165A) 250m/min

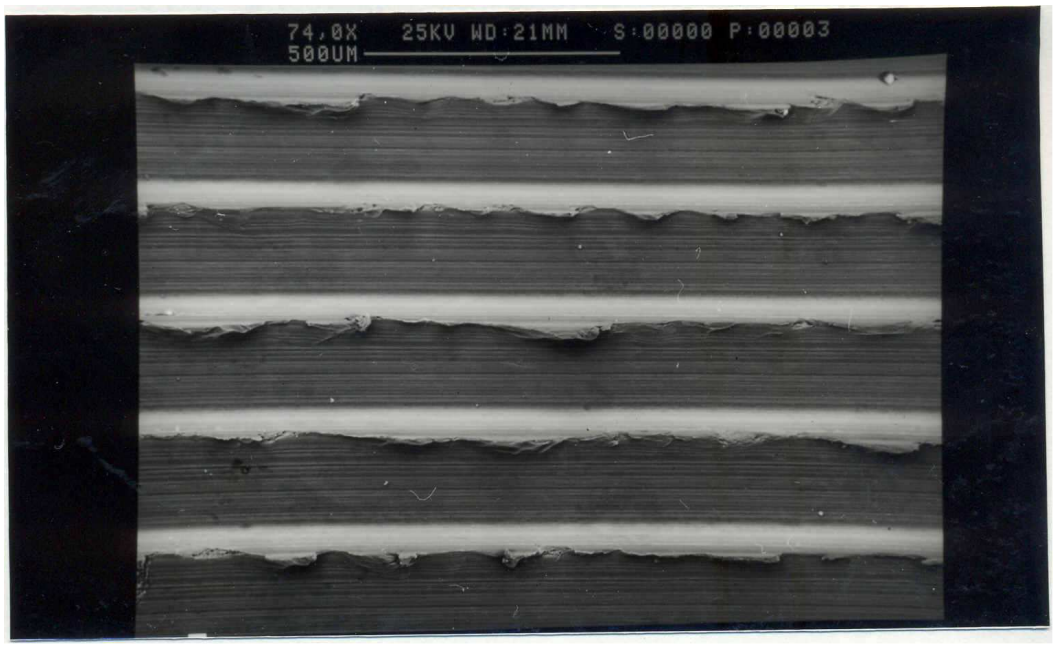

Fig. 56: Surface finish of cold drawn at a speed of 250m/min.

Showing feed marks.

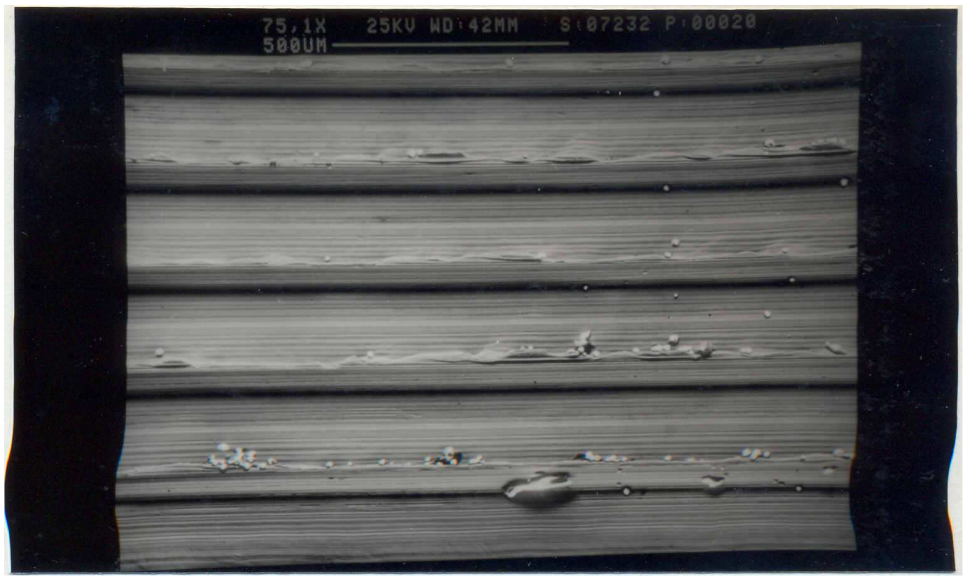

Fig. 57: Surface finish of Cold drawn at a speed of 300 m/min. Showing improved finish.

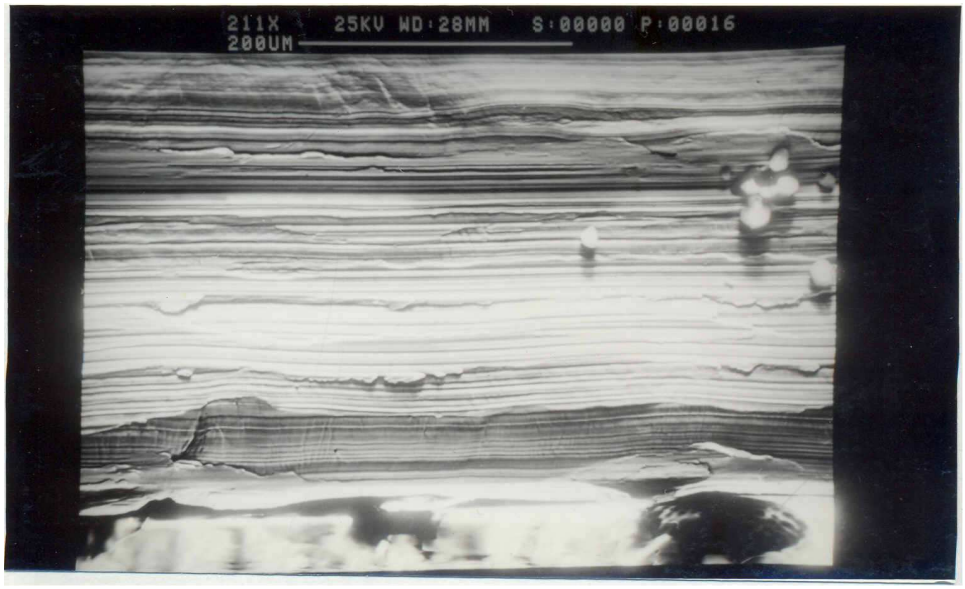

Fig58. Feed mark at the end of cut. Cold drawn machined at300m/min.

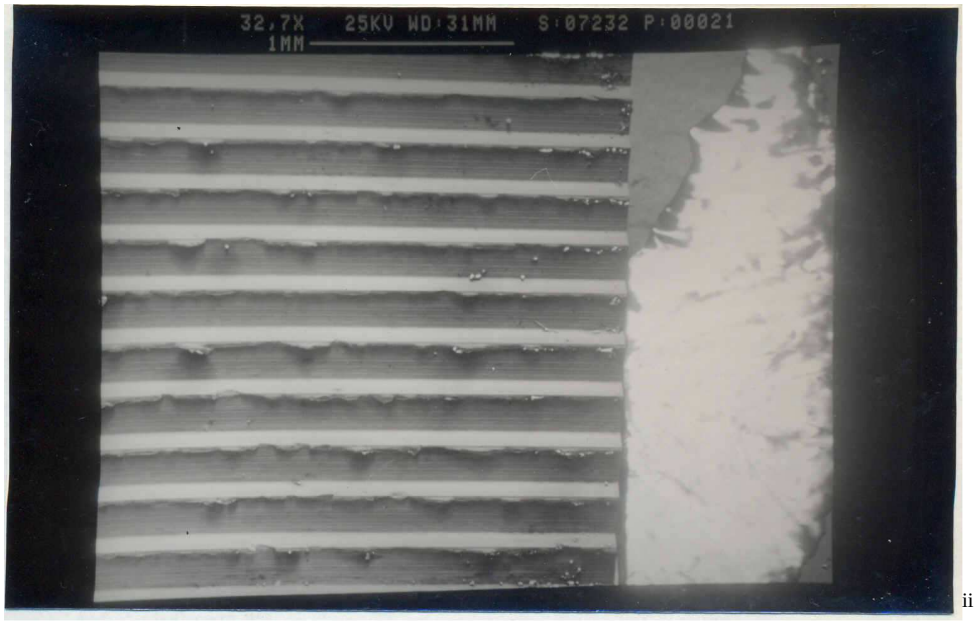

ii

Fig. 59: Surface finish of cold drawn, machined at 350m/min. showing feed marks parallelisms.

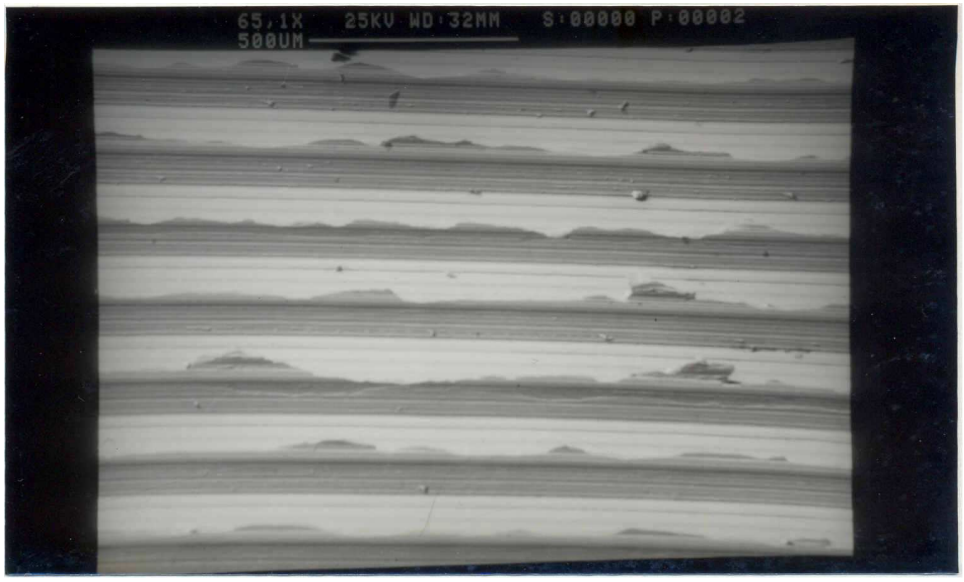

Fig. 60: Surface finish of cold drawn machined at a speed of 350m/min. Showing feed marks damage.

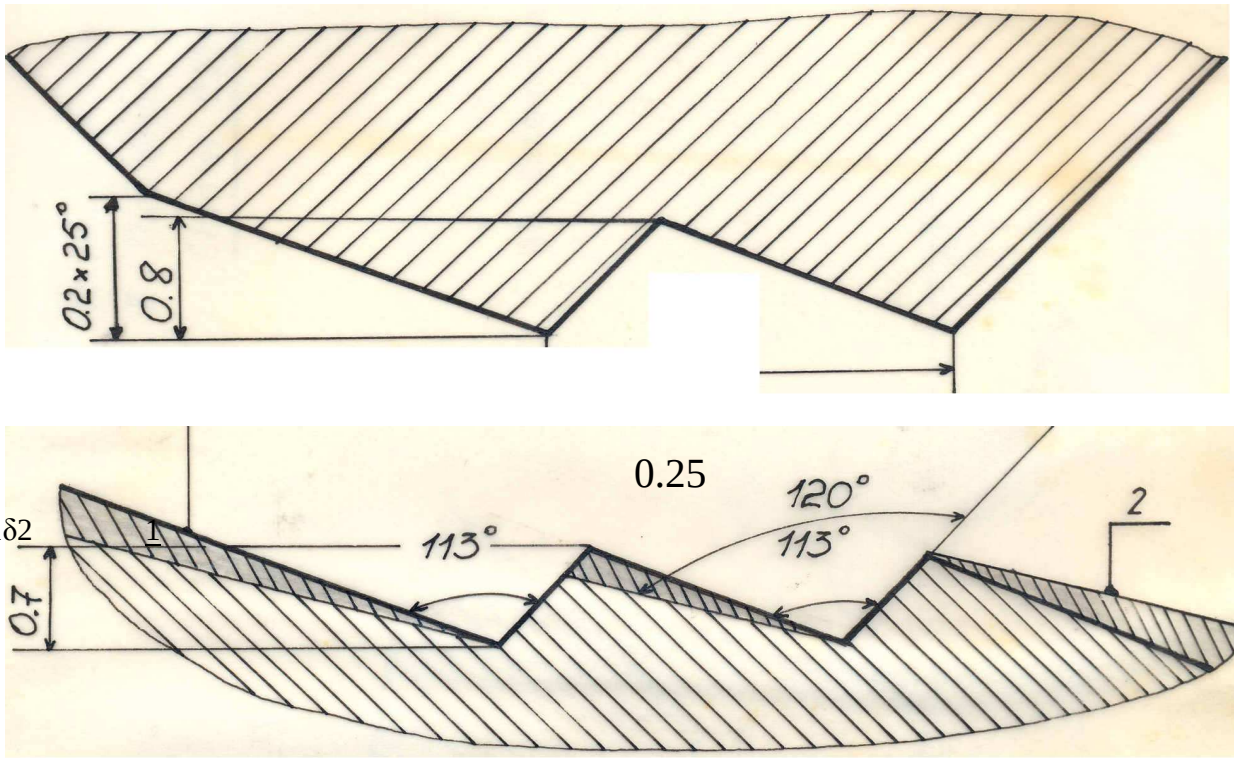

1. Real profile.

2. Theoretical profile

Speed	Angle
200	113^0
250	120^0

All dimensions in mm.

Fig. 61:

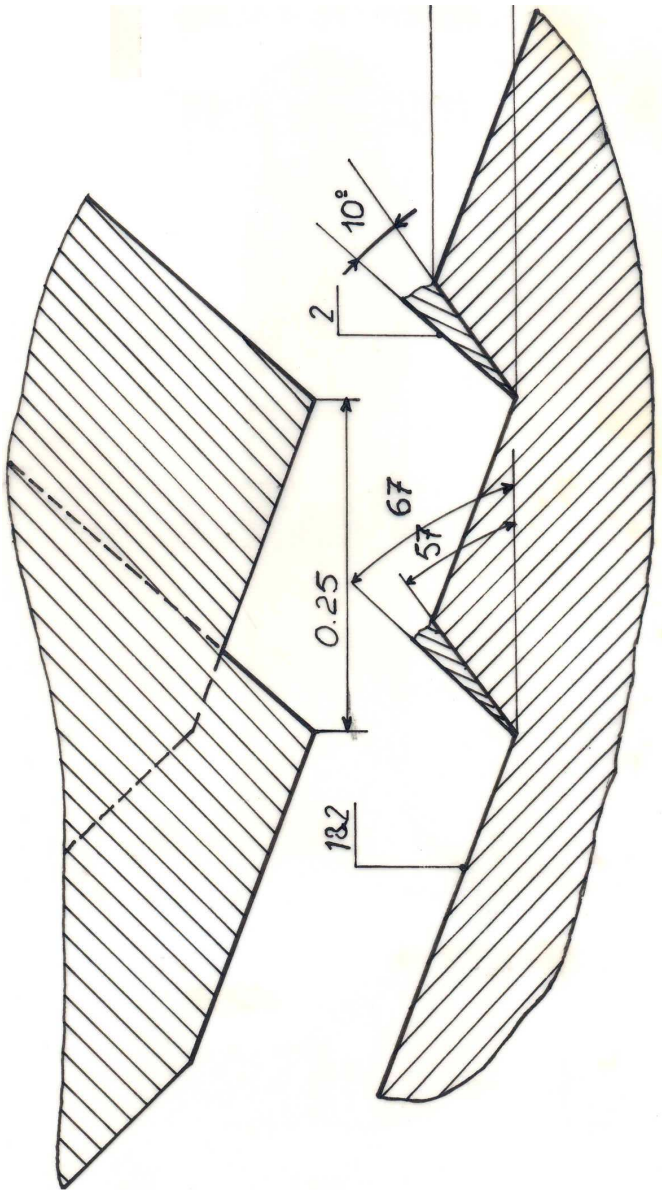

Fig. 62:

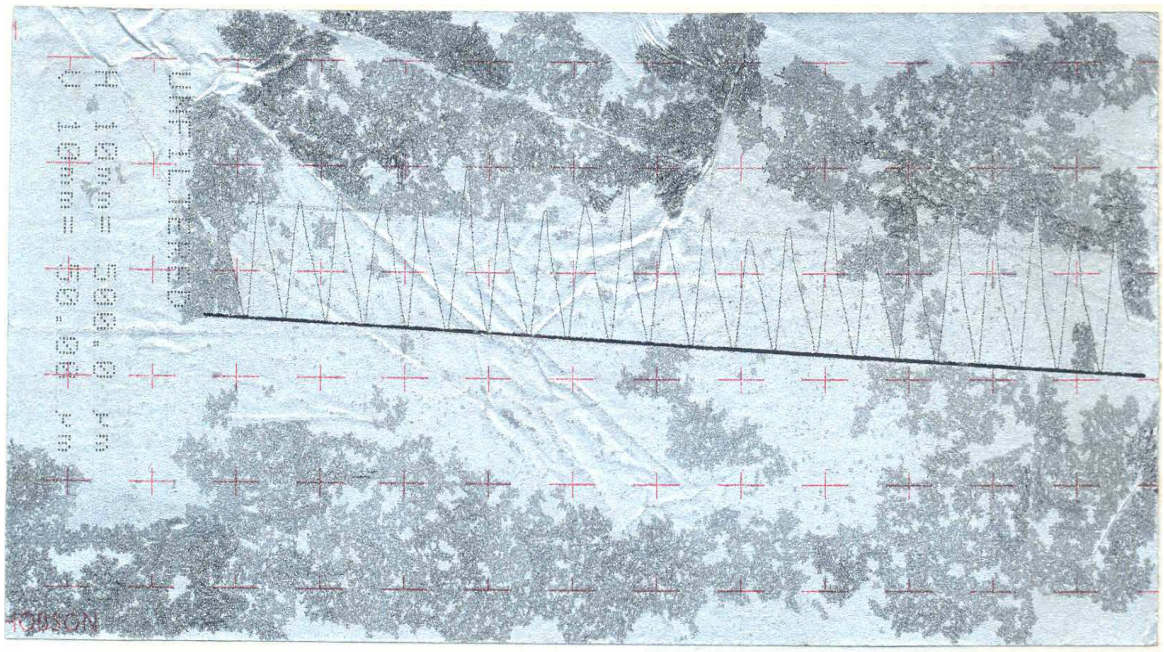

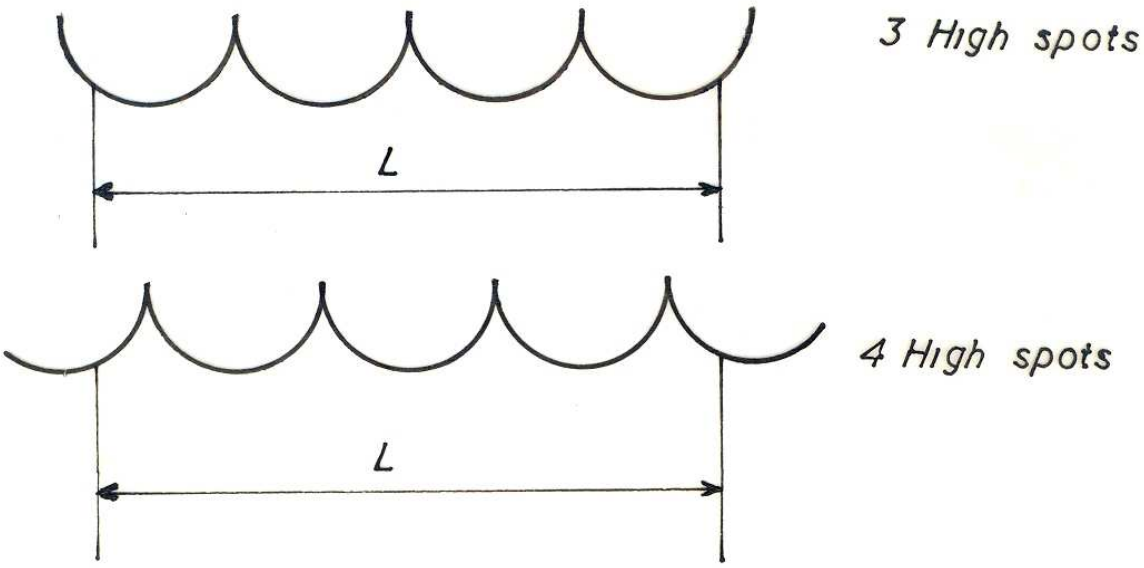

Fig. 63: Variation of High Spots

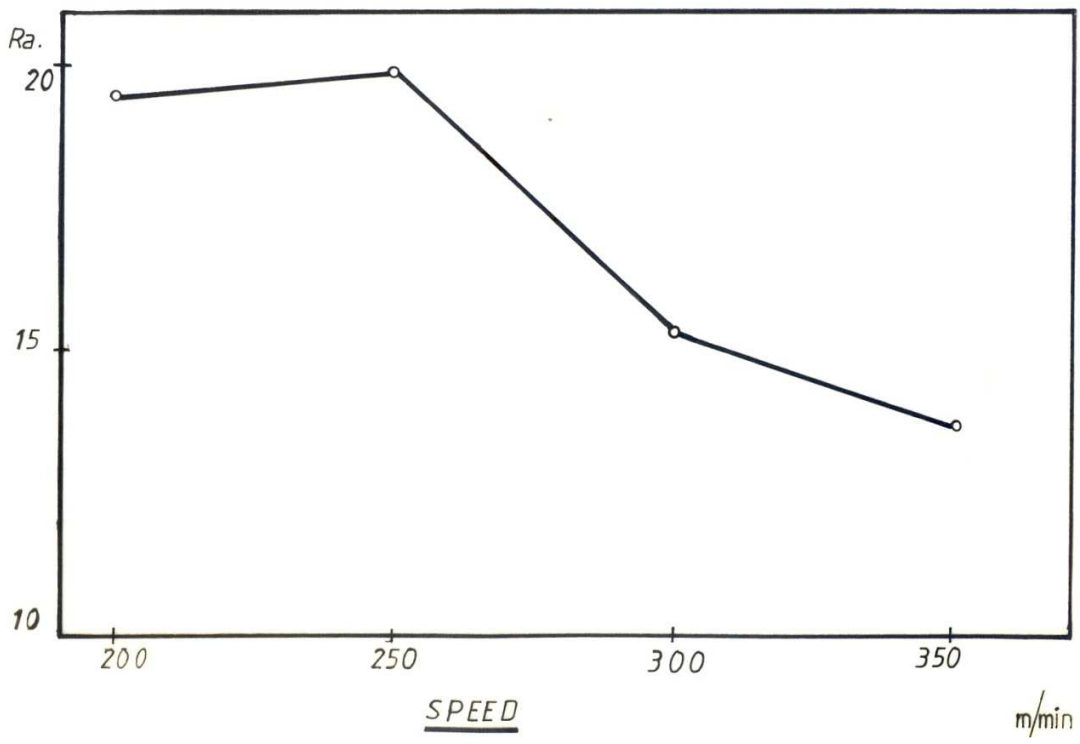

Fig. 64: Variation of surface roughness vs cutting speed

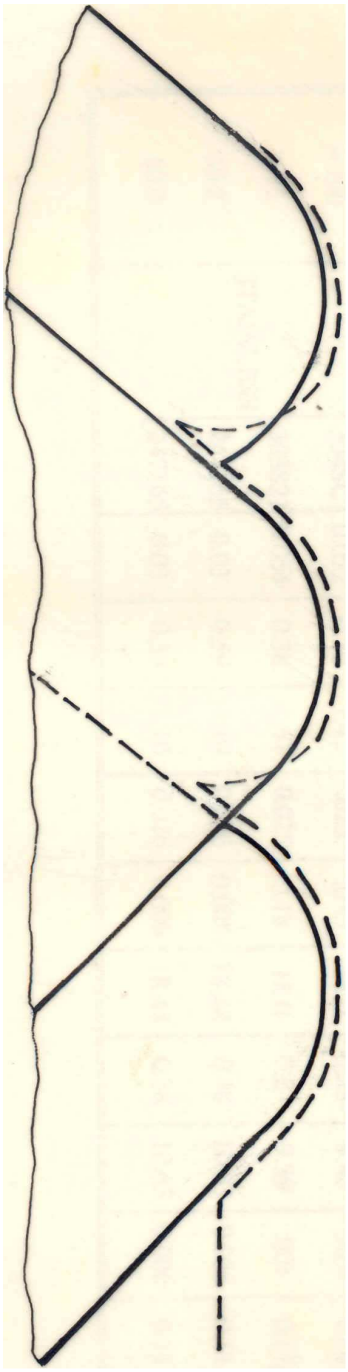

------ Tool nose radius

- - - -true shape of the surface

Fig. 65: Feed mark shape distortion

Table 1: Composition of the material- EX BSC

Nominal Dia. (mm)	Identité	C	Si	Mn	P	S	Cr	Mo	Ni	Al	Cu	N	Pb	Condition
100	304SC	0.052	0.36	1.42	.025	.010	18.0	0.23	9.48	.015	0.18	0.054	-	Recuit
75	303S21	0.054	0.38	1.67	0.025	0.18	18.0	0.27	9.39	.001	0.17	.073	-	Recuit
	Acier inoxydable													
50.8	247165	0.03	0.59	1.10	0.026	0.006	18.44	0.38	10.63	0.006	0.11	0.012	-	Recuit
50.0	247165	0.03	0.59	1.10	0.026	0.006	18.44	0.38	10.63	0.006	0.11	0.12	-	Etire à froid

Table 2: Hardness of the material

ISCI	157.45	149	156.6	**Dl**	159.55	159.65	164.8
ISC2	84.5	90.95	90.95	**D2**	95.95	92.25	85.05
ISC3	156.65	164.85	170.9	**D3**	135.65	135.6	132.5
ISC4	98.65	94.3	98.5	**D4**	179	178.7	176.9
ISC5	174.7	172.7	177.7	**D5**	188.4	189.05	179.95
ISC6	84.35	83	83.45	**D6**	116.55	102.8	106.9
7S1	140.55	141.75	154.5	**Al**	181.6	173.35	
7S2	81.15	73.25	72.9	**A2**	109.75	106.6	105.85
7S3	154.3	139.55	152.75	**A3**	163.1	159.1	164.25
7S4	82.5	84.3	79.6	**A4**	78.1	91.65	81.8
7S5	156.2	156.1	1522.05	**A5**	175.55	181.9	179.05
7S6	84.25	78.6	77.1	**A6**	78.85	65.6	79.9

Table 3 : 247165 cold drawn Material

Speed 150 m/min							Speed 200 m/min					
HSC	21	21	21	22	22	21.4	21	21	21	22	21	21.2
SM	9.955	10.08	10.01	9.899	9.731	9.935	9.999	9.985	10.03	9.949	9.936	9.979
ΛQ	3.910	4.200	3.822	3.797	3.702	3.886	3.943	3.996	3.875	3.793	3.869	3.895
ΔQ	0.131	0.119	0.134	0.135	0.136	0.131	0.133	0.134	0.138	0.147	0.147	0.139
RMAX	0.357	0.373	0.411	0.367	0.360	0.373	0.524	0.499	0.467	0.526	0.540	0.511
R3TM	0.282	0.271	0.278	0.288	0.286	0.281	0.286	0.271	0.287	0.266	0.285	0.279
RTM	0.329	0.329	0.348	0.330	0.331	0.333	0.407	0.433	0.424	0.441	0.445	0.430
RP	0.333	0.216	0.255	0.289	0.213	0.231	0.362	0.347	0.312	0.369	0.372	0.352
RT	0.382	0.373	0.411	0.390	0.361	0.383	0.539	0.541	0.473	0.557	0.596	0.541
RSK	0.715	0.653	0.637	0.608	0.644	0.651	0.019	0.655	0.866	0.983	0.649	0.634
RQ	0.081	0.080	0.082	0.081	0.080	0.080	0.083	0.085	0.085	0.088	0.090	0.086
RA	0.066	0.067	0.069	0.068	0.067	0.067	0.069	0.071	0.070	0.071	0.073	0.070
Speed 250 m/min							**Speed 300 m/min**					
HSC	22	21	21	22	22	21.6	21	21	22	22	22	21.6
SM	9.627	9.891	9.988	9.889	9.939	9.866	9.988	9.891	9.627	9.889	9.939	9.866
ΛQ	3.021	3.961	3.699	3.873	3.866	3.668	3.679	3.961	3.821	3.873	3.866	3.828
ΔQ	0.130	0.119	0.127	0.121	0.119	0.123	0.127	0.119	0.130	0.121	0.110	0.121
RMAX	0.561	0363	0.372	0.362	0.348	0.401	0.372	0.363	0.561	0.362	0.348	0.401
R3TM	0.240	0.242	0.242	0.246	0.238	0.241	0.242	0.242	0.240	0.246	0.238	0.241
RTM	0.357	0.338	0.337	0.324	0.314	0.334	0.337	0.338	0.357	0.324	0.314	0.334
RP	0.431	0.248	0.241	0.246	0.238	0.280	0.241	0.248	0.431	0.246	0.328	0.280
RT	0.569	0.379	0.373	0.385	0.362	0.413	0.373	0.379	0.569	0.385	0.362	0.413
RSK	1.115	0.637	0.676	0.687	0.644	0.751	0.676	0.637	1.115	0.687	0.644	0.751
RQ	0.079	0.075	0.074	0.073	0.073	0.074	0.074	0.075	0.079	0.073	0.073	0.073
RA	0.064	0.062	0.062	0.061	0.061	0.062	0.062	0.062	0.064	0061	0.061	0.062

Table 4 : 247165 Annealed Material

Speed 150 m/min							Speed 200 m/min					
HSC	22	22	21	22	22	21.8	23	22	22	22	22	22.2
SM	9.76	9.785	9.850	9.774	9.799	9.793	9.216	9.584	9.398	9.828	9.398	9.478
ΛQ	4.206	4.177	4.038	4.029	4.211	4.143	3.829	3.849	3.976	4.011	3.594	3.851
ΔQ	0.106	0.108	0.112	0.116	0.106	0.109	0.109	0.104	0.148	0.102	0.119	0.116
RMAX	0.309	0.309	0.304	0.396	0.309	0.325	0.369	0.286	0.540	0.339	0.371	0.380
R3TM	0.242	0.246	0.238	0.252	0.244	0.244	0.190	0.201	0.200	0.181	0.190	0.192
RTM	0.287	0.287	0.290	0.302	0.288	0.290	0.285	0.272	0.398	0.286	0.302	0.308
RP	0.178	0.178	0.177	0.266	0.173	0.194	0.254	0.194	0.348	0.216	0.238	0.25
RT	0.309	0.309	0.316	0.397	0.312	0.329	0.369	0.328	0.573	0.347	0.377	0.398
RSK	0.496	0.508	0.733	0.552	0.461	0.55	0.414	0.285	0.577	0.590	0.607	0.494
RQ	0.072	0.072	0.072	0.074	0.071	0.072	0.066	0.064	0.093	0.065	0.063	0.071
RA	0.061	0.061	0.060	0.063	0.061	0.061	0.055	0.054	0.071	0.054	0.055	0.057
Speed 250 m/min							**Speed 300 m/min**					
HSC	24	22	21	21	22	22	22	22	22	22	22	22
SM	9.101	9.887	9.966	9.876	9.864	9.373	9.821	9.753	9.974	9.713	9.742	9.800
ΛQ	3.168	4.603	4.715	4.518	4.398	4.280	3.832	3.840	4.065	4.433	3.914	4.016
ΔQ	0.158	0.105	0.100	0.113	0.115	0.118	0.119	0.115	0.109	0.117	0.128	0.117
RMAX	0.573	0.403	0.363	0.470	0.493	0.460	0.467	0.394	0.392	0.671	0.525	0.489
R3TM	0.245	0.224	0.223	0.220	0.223	0.227	0.175	0.192	0.174	0.149	0.177	0.173
RTM	0.356	0.320	0.295	0.359	0.360	0.338	0.352	0.337	0.320	0.365	0.338	0.352
RP	0.389	0.279	0.238	0.334	0.331	0.314	0.313	0.286	0.238	0.355	0.417	0.321
RT	0.573	0.417	0.363	0.472	0.493	0.463	0.467	0.433	0.392	0.671	0.609	0.514
RSK	0.488	0.438	0.436	0.652	0.554	0.513	0.533	0.584	0.464	0.669	0.628	0.575
RQ	0.080	0.077	0.075	0.081	0.080	0.078	0.073	0.070	0.071	0.083	0.080	0.075
RA	0.067	0.066	0.065	0.068	0.068	0.066	0.059	0.057	0.058	0.064	0.063	0.070

Table 5 : 247165 Cold-Drawn material

Speed= 150m/min					Speed= 200m/min				Speed=250m/min			
HSC	21	21	22	21.33	21	23	23	22.33	22	22	22	22
SM	253.4	252.5	251.4	252.43	251.9	233.3	234.1	239.7	238.9	249.6	250.2	246.73
ΛQ	70.40	71.89	73.15	71.81	74.15	85.20	76.50	78.61	112.6	111.3	101.3	108.4
ΔQ	0.128	0.124	0.123	0.125	0.140	0.121	0.138	0.133	0.111	0.112	0.132	0.118
RMAX	7.292	7.362	7.355	7.336	9.383	7.046	8.020	8.149	11.10	11.54	12.05	11.56
R3TM	5.748	5.748	5.664	5.720	4.897	5.120	5.455	5.157	5.399	5.399	6.230	5.676
RTM	6.995	7.056	7.033	7.028	7.615	6.770	7.092	7.159	8.676	8.963	9.699	9.112
RP	3.833	3.910	3.812	3.851	5.576	5.002	4.785	5.118	7.752	7.003	7.736	7.507
RT	7.610	7.654	7.452	7.565	9.838	0.213	8.420	6.005	11.41	12.92	12.05	12.12
RSK	0.448	0.471	0.511	0.476	0.708	0.673	0.713	0.698	0.705	0.651	0.833	0.729
RQ	1.429	1.424	1.431	1.428	1.652	1.645	1.678	1.658	1.980	1.991	2.134	2.035
RA	1.164	1.158	1.164	1.162	1.391	1.396	1.421	1.402	1.646	1.639	1.745	1.676

Table 6 & 7 : Dry condition

Speed 200 m/min							Speed 250 m/min					
HSC	21	21	21	22	21	21.2	21	21	21	21	21	21
SM	251.0	254.6	252.2	252.0	252.5	252.4	254.7	254.2	256.1	252.6	255.0	254.5
ΛQ	94.16	103.9	102.8	95.08	93.32	97.85	104.6	102.6		104.1	105.2	105.1
ΔQ	0.139	0.129	0.130	0.144	0.162	0.140	0.120	0.121		0.137	0.118	0.124
RMAX	12.12	12.38	12.18	12.93	12.70	12.46	11.72	9.989	11.72	14.14	11.60	11.83
R3TM	6.864	7.115	6.529	6.752	7.757	5.396	5.525	5.501		5.566	5.720	5.578
RTM	10.78	10.30	10.74	11.41	11.52	10.96	9.099	9.023		10.44	9.009	9.392
RP	8.804	8.209	8.276	8.624	8.599	8.502	7.617	7.056	8.008	10.40	7.886	8.193
RT	12.71	12.73	12.74	12.93	17.07	13.03	11.72	10.77	11.73	14.70	11.81	12.14
RSK	1.011	0.638	0.622	0.888	0.764	0.784	0.554	0.708	0.705	0.990	0.694	0.730
RQ	2.089	2.135	2.122	2.186	2.404	2.187	2.001	1.969	2.115	2.275	1.981	2.068
RA	1.7	1.77	1.763	1.778	1.936	1.789	1.64	1.629	1.72	1.801	1.627	1.683
Speed 150 m/min							**Speed 300 m/min**					
HSC	22	21	21	22	21	1.4	19	16	16	17	18	17.2
SM	250.7		249.2	245.5	253	249.6	201.6	239.2	242.2	219.6	211.3	222.7
ΛQ	107.8		108.5	100.2	107	105.78	50.76	51.44	59.32	54.9	52.79	53.84
ΔQ	0.122		0.117	0.133	0.128	0.125	0.169	0.180	0.169	0.180	0.175	0.140
RMAX	9.772		9.081	11.75	13.94	11.13	8.057	10.82	11.40	12.60	8.347	10.24
R3TM	7.031		6.920	6.948	6.892	6.947	6.172	5.937	5.859	5.937	5.703	5.921
RTM	8.332		8.255	8.946	8.695	8.557	7.627	7.974	8.809	8.667	7.773	8.17
RP	5.86		6.128	7.836	8.252	7.019	23.735	6.25	6.909	7.714	4.102	5.742
RT	9.791		9.708	11.75	13.94	11.29	8.435	10.94	11.41	12.6	9.006	10.47
RSK	0.585	0.667	0.614	0.768	0.583	0.643	0.167	0.448	0.559	0.532	0.134	0.368
RQ	2.084	2.004	2.019	2.119	2.187	2.082	1.365	1.469	1.593	1.753	1.473	1.494
RA	1.749	1.686	1.703	1.759	1.799	1.739	1.144	1.187	1.286	1.272	1.213	1.22

Table 6 & 7 : Lubricated condition

Speed 200 m/min							Speed 250 m/min					
HSC	21	21	21	22	21	21.2	21	21	21	21	21	21
SM	254.3	252.7	249.6	251.2	240.9	249.5	250	248.1	248.2	250.8	252.7	250.06
ΔQ	68.96	76.15	74.02	74.35	74.54	73.6	11.9	110.05	111.2	108.8	105.2	109.43
ΔQ	0.150	0.154	0.142	0.153	0.144	0.148	0.105	0.137	0.111	0.109	0.137	0.119
RMAX	8.664	12.40	99.229	12.24	9.204	10.34	11.40	11.91	11.40	11.45	13.72	11.97
R3TM	5.358	4.883	4.715	5.245	5.273	5.100	5.312	5.957	5.608	5.703	5.195	5.555
RTM	7.495	8.747	7.912	8.573	7.935	8.134	8.577	9.940	8.880	9.152	10.45	9.387
RP	4.907	7.714	6.275	8.228	5.127	6.45	7.861	7.813	7.495	8.814	8.643	8.125
RT	8.664	12.40	9.876	12.36	9.253	10.51	11.58	12.70	11.41	12.16	14.50	12.47
RSK	0.873	1.030	0.626	0.758	0.714	0.800	0.525	0.931	0.800	0.694	0.957	0.781
RQ	1.648	1.870	1.667	1.807	1.705	1.739	1.862	2.168	1.973	1.880	2.294	2.035
RA	1.367	1.508	1.401	1.484	1.407	1.433	1.559	1.729	1.606	1.564	1.781	1.647
Speed 150 m/min							**Speed 300 m/min**					
HSC	22	22	22	21	21	21.6	15	15	15	15	15	15
SM	249.4	251.3	252.1	251.5	253.5	251.5	251.1	250.1	252.7	252.4	245.3	250.3
ΔQ	69.58	69.68	68.07	63.69	68.35	69.87	95.76	89.78	100.2	92.94	97.93	95.32
ΔQ	0.130	0.127	0.130	0.139	0.135	0.132	0.161	0.172	0.158	0.158	0.152	0.160
RMAX	7.471	6.909	6.989	7.230	7.929	7.305	10.45	9.973	10.45	10.84	10.05	10.35
R3TM	5.776	5.971	5.804	5.776	5.887	5.842	6.211	6.992	7.187	5.908	5.055	6.47
RTM	6.989	6.787	6.787	6.948	7.146	6.931	9.717	9.473	9.761	9.531	9.180	9.53
RP	4.346	3.754	3.717	3.391	4.346	4.018	6.104	6.256	6.104	6.275	5.554	6.05
RT	7.891	7.098	7.092	7.449	8.088	7.523	10.45	10.55	10.45	10.84	10.05	10.46
RSK	0.695	0.655	0.596	0.599	0.645	0.638	0.244	0.284	0.239	0.249	0.143	0.231
RQ	1.434	1.410	1.405	1.407	1.466	1.424	2.451	2.462	2.511	2.334	2.375	2.426
RA	1.1150	1.137	1.136	1.131	1.181	1.147	2.123	2.152	2.174	1.057	2.097	2.12

Table 7: 303S21 Annealed condition

	Speed 150 m/min						Speed 200 m/min					
HSC	15	15	15	15	20	16	20	16	17	16	18	15.8
SM	252.4	251.5	252.7	254.9	184.3	239.16	190.3	231.5	227.1	234.1	206.9	218.7
ΛQ	79.46	77.31	75.75	74.75	80.14	77.44	49.76	48.57	49.79	50.79	49.11	49.60
ΔQ	0.111	0.114	0.114	0.117	0.112	0.113	0.195	0.195	0.187	0.188	0.202	0.193
RMAX	5.695	5.704	5.689	5.866	5.917	5.810	7.160	7.086	6.671	7.038	7.935	7.178
R3TM	5.000	5.000	5.078	4.344	5.088	4.901	5.820	5.820	5.859	5.664	6.016	5.835
RTM	5.57	5.561	5.596	5.664	5.735	5.622	6.787	6.655	6.470	6.631	7.270	6.762
RP	3.125	3.131	3.525	3.174	3.298	3.25	3.223	3.223	3.326	3.516	4.346	3.526
RT	5.884	5.896	6.259	6.104	6.116	6.051	7.159	7.159	6.886	7.040	8.283	7.305
RSK	0.260	0.295	0.665	0.208	0.429	0.371	-0.128	-0.124	-0.041	0.228	-0.117	-0.036
RQ	1.399	1.399	1.377	1.386	1.426	1.397	1.544	1.507	1.483	1.507	1.582	1.524
RA	1.174	1.173	1.133	1.177	1.191	1.169	1.276	1.240	1.225	1.241	1.301	1.256
	Speed 150 m/min						**Speed 200 m/min**					
HSC	14	15	15	16	16	15.2	15	16	15	17	16	15.8
SM	268.6	263.8	249.5	241.4	249.4	254.54	251.5	236.1	252.5	228.9	243.1	242.42
ΛQ	91.83	98.33	88.10	93.42	92.49	92.83	70.16	70.18	76.15	67.90	72.41	71.56
ΔQ	0.096	0.090	0.092	0.092	0.092	0.092	0.152	0.149	0.137	0.156	0.147	0.148
RMAX	6.317	6.192	5.677	5.866	5.670	5.944	9.235	8.728	7.935	8.434	8.649	8.596
R3TM	4.97	3.867	4.023	4.062	4.18	4.085	5.742	5.977	5.664	5.937	6.016	5.867
RTM	5.708	5.557	5.405	5.449	5.264	5.476	8.130	7.066	7.402	7.788	8.047	7.686
RP	4.144	4.150	3.522	3.735	3.711	3.852	5.127	4.346	4.321	4.346	4.517	4.531
RT	6.903	6.500	6.067	5.908	6.079	6.291	9.235	8.840	8.032	8.673	9.012	8.758
RSK	0.733	0.825	0.528	0.695	0.669	0.690	0.539	0.537	0.620	0.403	0.439	0.507
RQ	1.400	1.407	1.289	1.363	1.348	1.361	1.701	1.690	1.661	1.690	1.697	1.687
RA	1.136	1.161	1.071	1.129	1.117	1.122	1.242	1.417	1.401	1.438	1.433	1.422

Table 8: 304SC Annealed condition

	Speed 150 m/min						Speed 200 m/min					
HSC	15	15	16	15	15	15.2	30	21	24	14	28	23.4
SM	250.0	249.1	229.6	263.0	250.0	246.34	128.0	177.5	157.4	230.4	133.2	165.3
ΛQ	117.8	111.6	110.9	114.5	121.6	115.28	80.57	82.42	85.32	70.66	80.61	79.916
ΔQ	0.138	0.140	0.147	0.140	0.124	0.1378	0.209	0.182	0.184	0.159	0.194	0.185
RMAX	12.16	11.76	12.55	12.59	9.033	11.618	13.68	11.04	12.19	11.16	13.39	12.09
R3TM	7.344	7.656	7.344	7.578	7.656	7.515	8.398	7.812	7.383	8.594	8.320	8.101
RTM	10.95	10.32	11.29	10.77	8.657	10.39	11.87	10.10	10.53	5.493	11.04	9.806
RP	7.836	7.465	7.324	7.898	4.883	7.081	8.203	6.641	8.405	7.819	8.032	7.82
RT	12.96	12.41	12.80	12.59	9.033	11.95	13.68	11.62	13.95	12.33	12.39	12.794
RSK	0.398	0.225	0.364	0.455	0.311	0.350	0.837	0.588	0.547	0.068	0.618	0.631
RQ	2.584	2.481	2.588	2.553	2.392	2.5192	2.676	2.383	2.498	1.786	2.495	2.367
RA	2.180	2.124	2.186	2.166	2.072	2.145	2.130	1.925	2.013	1.226	2.006	1.86
	Speed 150 m/min						**Speed 200 m/min**					
HSC	15	17	16	15	15	15.6	15	15	15	16	15	15.2
SM	254.8	231.4	243.5	252.7	244.4	245.36	250.5	242.9	249.6	242.5	250.4	247.18
ΛQ	88.84	95.41	90.59	88.85	93	91.33	74.62	76.38	76.04	78.41	77.28	76.54
ΔQ	0.140	0.122	0.133	0.132	0.131	0.131	0.183	0.183	0.182	0.170	0.178	0.179
RMAX	10.49	8.624	10.24	11.27	12.82	10.77	13.12	12.18	11.55	11.75	11.14	11.948
R3TM	6.406	5.977	6.289	5.469	6.299	6.088	9.492	9.473	9.336	8.437	9.062	9.16
RTM	0.002	0.002	0.002	0.002	0.002	0.002	0.002	0.002	10.70	10.81	10.75	6.45
RP	7.819	5.280	6.9	7.681	9.400	7.416	8.814	8.057	7.836	7.447	7.471	7.925
RT	11.92	8.625	11.01	11.40	12.82	11.15	13.12	12.18	11.55	11.75	11.18	11.95
RSK	0.88	0.81	0.74	0.72	0.93	0.816	1.28	1.32	1.403	1.184	1.238	1.285
RQ	1.981	1.859	1.917	1.867	1.939	1.912	2.171	2.220	2.202	2.126	2.187	2.181
RA	1.582	1.501	1.548	1.510	1.551	1.538	1.577	1.614	1.591	1.567	1.600	1.589

Table 9: 247165 Annealed A1

	Speed 150 m/min						Speed 200 m/min					
HSC	22	22	22	22	21	21.8	22	23	22	22	23	22.4
SM	249.7	243.4	245.2	250.0	251.8	248.02	248.8	235.6	250.3	250.4	232.6	243.54
ΔQ	106.2	109.2	104.1	104.3	103.6	105.48	95.80	57.43	96.29	98.41	97.24	95.03
ΔQ	0.108	0.106	0.110	0.109	0.110	0.108	0.111	0.126	0.108	0.108	0.122	0.115
RMAX	7.697	7.087	7.703	7.471	7.072	7.806	8.624	10.45	8.414	9.521	11.72	9.74
R3TM	6.194	5.859	6.389	6.250	6.083	6.155	5.022	5.469	5.636	5.050	5.273	5.29
RTM	7.321	7.460	7.356	7.241	7.544	7.385	7.893	8.423	7.502	8.200	8.447	8.093
RP	4.499	4.517	4.578	4.346	4.947	4.577	6.079	7.300	5.680	6.665	7.233	6.591
RT	7.843	8.301	7.904	7.477	8.146	7.934	9.644	10.45	8.414	10.43	11.73	10.13
RSK	0.431	0.515	0.508	0.486	0.717	0.531	0.663	0.829	0.842	0.827	0.725	0.777
RQ	1.822	1.850	1.830	1.811	1.818	1.826	1.698	1.749	1.657	1.689	1.882	1.735
RA	1.555	1.568	1.556	1.539	1.525	1.548	1.372	1.405	1.348	1.350	1.498	1.394
	Speed 150 m/min						**Speed 200 m/min**					
HSC	21	21	22	21	21	21.2	21	20	21	21	21	20.8
SM	253.0	253.8	247.0	256.1	256.5	253.28	251.1	265.0	258.8	252.3	253.8	256.2
ΔQ	116.8	126.1	122.8	124.6	123.6	122.78	106.5	111.3	105.7	101.2	101.2	105.18
ΔQ	0.111	0.108	0.105	0.103	0.104	0.106	0.107	0.108	0.128	0.107	0.111	0.112
RMAX	12.58	14.89	12.12	19.55	12.94	12.81	10.57	12.34	13.09	9.601	10.20	11.16
R3TM	5.371	4.720	4.883	4.818	4.980	4.954	4.727	4.185	3.071	4.590	4.269	4.348
RTM	8.437	9.406	8.897	8.904	8.674	8.863	8.297	8.486	10.31	7.767	7.997	8.571
RP	8.667	9.400	8.472	7.447	8.643	8.525	6.836	8.814	9.183	6.680	7.250	7.78
RT	12.58	14.89	12.19	11.55	12.94	12.83	11.14	12.72	13.48	10.77	11.21	11.86
RSK	0.263	0.398	0.461	0.330	0.349	0.360	0.514	0.695	0.844	0.347	0.415	0.563
RQ	2.059	2.174	2.056	2.046	2.047	2.076	1.815	1.919	2.147	1.726	1.783	1.878
RA	1.746	1.798	1.734	1.727	1.729	1.746	1.485	1.533	1.681	1.425	1.473	1.519

Table 10: Statistical technics

	B_Q	B	D_Q	D
AB2	1.107	1.522 (-)	1.755	1.35(-)
AA2	1.525	3.24 (-)	1.858	1.522 (-)
AC2	1.568	1.426 (-)	1.632	1.904 (+)
DA1	0.25	---	0.25	---
DA3	2.141	2.072 (-)	1.88	1.130 (-)
DB1	1.703	1.185 (-)	1.248	1.636 (+)
DC1	1.644	1.56 (-)	1.133	1.359 (+)

Test for difference between tow means:

$$B_Q \,\&\, B \quad t_\alpha = 2.57 \quad for\, v = 5 \quad P = 6$$

$$\overline{Ra}_{QB} = 1.614, \quad S_1 = 0.332, \quad S_1^{\,2} = 0.110 \quad N_1 = 6$$

$$\overline{Ra}_{QB} = 1.8 \quad S_2 = 0.766, \quad S2^{\,2} = 0.58 \quad N1 = 6$$

$$\bar{x}_1 - x_2 \pm t_2 \left[\frac{n_1 S_1^2 + \times\, n_2 S_2^2}{n_1 + n_2} \times \frac{N_1 + N_2}{N_1 N_2}\right]^{1/2}$$

$$1.614 - 1.8 \pm 2.57 \left[\frac{5 \times 0.110 + 5 \times 0.58}{5+5} \times \frac{6+6}{6 \times 6}\right]^{1/2}$$

$$1.614 - 1.8 \pm 2.57 \left[\frac{0.110 + 0.58}{2} \times \frac{1}{3}\right]^{1/2}$$

$$1.614 - 1.8 \pm 0.871$$

$$-0.186 \pm 0.871$$

$$]-1.057, 0.685[\ Contrains\ zero, there\ is\ no\ statistical\ difference$$

Test for difference between tow means:

$$B_Q \ \&\ D \quad t_\alpha = 2.57 \quad for\ v = 5 \quad P = 5$$

$$\overline{Ra}_{QD} = 1.585, \quad S_1 = 0.321, \quad S_1^{\ 2} = 0.103 \quad N_1 = 6$$

$$\overline{Ra_{QD}} = 1.483, \quad S_2 = 0.268, \quad S_2^{\ 2} = 0.071 \quad N_2 = 6$$

$$\overline{x}_1 - x_2 \pm t_2 \left[\frac{n_1 S_1^2 + n_2 S_2^2}{n_1 + n_2} \times \frac{N_1 + N_2}{N_1 N_2}\right]^{1/2}$$

$$1.587 - 1.483 \pm 2.57 \left[\frac{5 \times 0.103 + 5 \times 0.071}{5+5} \times \frac{6+6}{6 \times 6}\right]^{1/2}$$

$$1.583 - 1.483 \pm 0.437$$

$$1.104 \pm 0.437$$

$$]-0.333, 0.541[\ Contrains\ zero, there\ is\ no\ statistical\ difference$$

Test for difference between tow means:

$$B_Q \ \&\ D_Q$$

$$\overline{Ra}_{BQ} = 1.614, \quad S1 = 0.332, \quad S1^{\,2} = 0.110 \quad N1 = 6$$

$$\overline{Ra_{DQ}} = 1.587, \quad S2 = 0.268, \quad S2^{\,2} = 0.071 \quad N1 = 6$$

$$\bar{x}_1 - x_2 \pm t_2 \left[\frac{n_1 S_1^2 + \times n_2 S_2^2}{n_1 + n_2} \times \frac{N_1 + N_2}{N_1 N_2} \right]^{1/2}$$

$$1.614 - 1.587 \pm 2.57 \left[\frac{5 \times 0.110 + 5 \times 0.071}{5 + 5} \times \frac{6 + 6}{6 \times 6} \right]^{1/2}$$

$$]-0.419, 0.473[\ \textit{Contrains zero, there is no statistical difference}$$

Table 10 (Cont…):

Material						
AB2 B	1.110	1.127	1.063	1.130	1.107	1.522
AB2 D	1.8	1.709	1.709	1.8	1.775	1.351
AA2 B	1.562	1.563	1.516	1.459	1.525	3.24
AA2 D	1.981	1.764	1.926	1.763	1.858	1.522
DA1 B	1.978	1.832	1.921	1.840	1.892	1.760
DA1 D	1.698	1.689	1.767	1.725	1.719	1.602
AC2 B	1.552	1.587	1.616	1.519	1.568	1.426
AC2 D	1.651	1.741	1.620	1.517	1.632	1.904
DA3 B	2.133	2.151	2.146	2.135	2.141	2.072
DA2 D	1.719	1.722	1.967	2.130	1.88	1.130
DB1 B	1.713	1.670	1.649	1.783	1.703	1.185
DB1 D	1.273	1.264	1.228	1.227	1.248	1.636
DC1 B	1.674	1.623	1.635	1.646	1.644	1.356
DC1 D	1.116	1.145	1.153	1.121	1.133	1.359

$$(1)\ \Sigma x = 19.219$$

$$(2)\ \sum \frac{x}{n} = 1.60$$

$$(3)\quad \sigma_s^2 = \frac{(x-m)^2}{n-1}$$

$$(1.107 - 1.6)\,2 + (1.775 - 1.6)\,2 + (1.525 - 1.6)\,2 + (1.858 - 1.6)\,2 + (1.568 - 1.6)$$

$$+ (1.632 - 1.6)\,2 + (2.141 - 1.6)\,2 + (1.88 - 1.6)\,2 + (1.703 - 1.6)\,2 + (1.248 - 1.6)$$

$$+ (1.644 - 1.6)\,2 + (1.133 - 1.6)\,2 =$$

$$\frac{1.049}{n-1} = 0.095$$

« ***C*** »

Sample Standard Deviation : $x_{\sigma_{n-1}} = 73.41$

Population Standard Deviation : $x_{\sigma_n} = 68.67$

Arithmatic Mean: $\bar{x} = 403.62$

Number of Data: $n + 8$

Sum of Value: $\sum x = 3229$

Sum of Squared Value: $\sum x^2 = 1341031$

Calculate the unbiased variance and the deviation between each data item and the average.

« ***D*** »

Unbiased variance: 5389.4

$x_{\sigma_{n-1}} = 33.38$

$x\,\sigma_n = 31.22$

$\bar{x} = 315.37$

$n + 8$

$\sum x = 2523$

$\sum x^2 = 803491$

« ***A*** »

$$x\,\sigma_{n-1} = 93.42$$

$$x\,\sigma_{n} = 87.39$$

$$\bar{x} = 366.37$$

$$n + 8$$

$$\sum x = 2931$$

$$\sum x^2 = 1134949$$

« ***B*** »

$$x\,\sigma_{n-1} = 18.25$$

$$x\,\sigma_{n} = 17.08$$

$$\bar{x} = 326.62$$

$$n + 8$$

$$\sum x = 2613$$

$$\sum x^2 = 855805$$

Percentage points of the t distribution $t_{\alpha} = 2.36$, for $P = 5$ and $\nu = 7$

Test for difference between tow means, C & D:

$\bar{F}_C = 403.62, \quad S_1 = 73.4\dot{1} \quad S_1^2 = 5389.02 \quad N_1 = 8$

$\bar{F}_D = 315.37, \quad S_2 = 23.3\dot{8} \quad S_2^2 = 1114.22 \quad N_2 = 8$

$$\bar{x}_1 - x_2 \pm t_2 \left[\frac{n_1 S_1^2 + n_2 S_2^2}{n_1 + n_2} \times \frac{N_1 + N_2}{N_1 N_2} \right]^{1/2}$$

$$88.25 \pm 2.36 \ [1486.53]^{1/2}$$
$$88.25 \pm 2.36 \ [38.55]^{1/2}$$
$$88.25 \pm 90.99$$

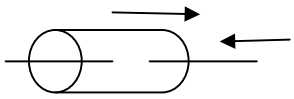

$]-2.74, 179.24[$ Contrains zero, there is no statistical difference.

Test for difference between tow means, A & B:

$\bar{F}_A = 366.37, \quad S_1 = 93.4\dot{2} \quad S_1^2 = 8727.29 \quad N_1 = 8$

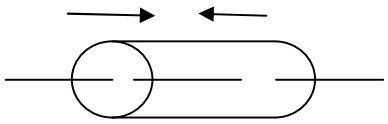

$\bar{F}_B = 326.62, \quad S_2 = 18.2\dot{5} \quad S_2^2 = 333.06 \quad N_2 = 8$

$$\bar{x}_1 - x_2 \pm t_2 \left[\frac{n_1 S_1^2 + n_2 S_2^2}{n_1 + n_2} \times \frac{N_1 + N_2}{N_1 N_2} \right]^{1/2}$$

$$39.75 \pm 2.36 \times 33.65$$

$$39.75 \pm 79.41.65$$

$]-39.66, 19.19[$ Contrains zero, there is no statistical difference.

Test for difference between tow means, A & C:

$\bar{F}_A = 366.37, \quad S_1 = 93.42\dot{} \quad S_1^2 = 8727.29 \quad N_1 = 8$

$\bar{F}_C = 403.62 \quad S_2 = 73.41\dot{}, \quad S_2^2 = 5389.02 \quad N_2 = 8$

$$\bar{x}_1 - x_2 \pm t_2 \left[\frac{n_1 S_1^2 + n_2 S_2^2}{n_1 + n_2} \times \frac{N_1 + N_2}{N_1 N_2} \right]^{1/2}$$

$$-37.25 \pm 2.36 \times 42.0$$

$$-37.25 \pm 99.12$$

$]-136.37, 61.87[$ Contrains zero, there is no statistical difference.

Test for difference between tow means, B & D:

$\bar{F}_B = 326.62, \quad S_1 = 18.25\dot{} \quad S_1^2 = 333.06 \quad N_1 = 8$

$\bar{F}_D = 315.37 \quad S_2 = 23.38\dot{}, \quad S_2^2 = 1114.22 \quad N_2 = 8$

$$\bar{x}_1 - x_2 \pm t_2 \left[\frac{n_1 S_1^2 + n_2 S_2^2}{n_1 + n_2} \times \frac{N_1 + N_2}{N_1 N_2} \right]^{1/2}$$

$$326.62 - 315.37 \pm 2.36\,[13.45]$$

$$326.62 - 315.37 \pm 31.74$$

$$11.25 \pm 31.74$$

$]-20.49, 42.99[$ Contrains zero, there is no statistical difference

Table 10 (Cont…): Statistical Technics.

Material	A	B	C	D
AB2	1.181	1.522	1.486	1.351
AC2	1.393	1.426	1.516	1.904
AD2	2.413	1.760	1.357	1.497
AA2	2.187	3.248	1.165	1.522
DA1	1.219	1.760	1.332	1.602
DB1	1.961	1.185	1.369	1.636
DC1	2.154	1.356	1.758	1.359
DA3	1.556	2.072	1.615	1.130
Sample Standard deviation X σ_{n-1}	0.479	0.650	0.172	0.23
Population Standard deviation X σ_n	0.448	0.60	0.184	0.21
Arithmetic Mean $\bar{x}$	1.758	1.79	1.444	1.5
Number of Data n	8	8	8	8
Sum of Value $\sum x$	14.06	14.32	11.59	12.00
Sum of Squared Value $\sum x^2$	26.33	28.63	17.05	18.37

Test for difference between tow means A & B:

Ra =1.758, $S_1 = 0.479$ $S_1^2 = 0.229$, $N_1 = 8$

$R_B = 1.79$, $S_2 = 0.650$, $S_2^2 = 0.4225$, $N_1 = 8$

$$\bar{x}_1 - x_2 \pm t_2 \left[\frac{n_1 S_1^2 + \times n_2 S_2^2}{n_1 + n_2} \times \frac{N_1 + N_2}{N_1 N_2} \right]^{1/2}$$

$$1.758 - 1.79 \pm 2.36 \left[\frac{7 \times 0.229 + 7 \times 0.422}{7 + 7} \times \frac{8 + 8}{8 \times 8} \right]^{1/2}$$

-0.032±0.672

$]-0.704, 0.643[$ Contrains zero, there is no statistical difference

Test for difference between tow means A & C:

Ra =1.758, $S_1 = 0.479$, $S_1^2 = 0.229$ $N_1 = 8$

R_C *=1.44,* $S_1 = 0.172$, $S_1^2 = 0.0029$ $N_2 = 8$

$$\bar{x}_1 - x_2 \pm t_2 \left[\frac{n_1 S_1^2 + \times n_2 S_2^2}{n_1 + n_2} \times \frac{N_1 + N_2}{N_1 N_2} \right]^{1/2}$$

$$1.758 - 1.44 \pm 2.36 \left[\frac{7 \times 0.229 + 7 \times 0.479}{7 + 7} \times \frac{8 + 8}{8 \times 8} \right]^{1/2}$$

- 0.318 + 0.702

$]-0.384, 1.02[$ Contrains zero,there is no statistical difference

Test for difference between tow means B & D:

R_B *=1.79,* $S_1 = 0.650$, $S_1^2 = 0.422$ $N_1 = 8$

R_D *=1.5,* $S_2 = 0.23$ $S_2^2 = 0.052$ $N_2 = 8$

$$\bar{x}_1 - x_2 \pm t_2 \left[\frac{n_1 S_1^2 + \times n_2 S_2^2}{n_1 + n_2} \times \frac{N_1 + N_2}{N_1 N_2} \right]^{1/2}$$

$$1.79 - 1.5 \pm 2.36 \left[\frac{7 \times 0.650 + 7 \times 0.052}{7 + 7} \times \frac{8 + 8}{8 \times 8} \right]^{1/2}$$

- 0.29 ⊥ 2.36 x 0.296

$]-0.4, 0.9[$ Contrains zero,there is no statistical difference.

Test for difference between tow means C& D:

R_C *=1.44,* $S_1 = 0.172$, $S_1^2 = 0.029$ $N_1 = 8$

R_D *=1.5,* $S_2 = 0.23$ $S_2^2 = 0.052$ $N_2 = 8$

$$\bar{x}_1 - x_2 \pm t_2 \left[\frac{n_1 S_1^2 + \times n_2 S_2^2}{n_1 + n_2} \times \frac{N_1 + N_2}{N_1 N_2} \right]^{1/2}$$

$$1.44 - 1.5 \pm 2.36 \left[\frac{0.029 + 0.052}{2} \times \frac{1}{4} \right]^{1/2}$$

$$- \quad 0.06 \pm 2.37$$

$$]-0.297, 0.177[$$ Contrains zero, there is no statistical difference.

Material	A	B	C	D
AB2	360	328	341	308
AC2	375	357	459	359
AD2	349	305	393	368
AA2	392	340	348	289
DA1	513	305	471	312
DB1	420	333	335	271
DC1	343	333	353	296
DA3	179	312	529	320

The calculation is as follows:

(i) $\sum x$: 2931 2613 3229 2523

(ii) *M = mean of each :* $= \sum \frac{x}{n} =$

366.37 326.62 403.62 315.70

(iii) σ^2_e *=Estimate of variability in each :*

$= \frac{\Sigma(x-m)^2}{n-1} =$

8729 333.4 3161.53 114.26

(iii) *Mean of the means:*

$$\sum \frac{m}{4} = \bar{m} = \frac{366.37+326.62+403.62+315.37}{4}$$

(iv) Variability between Means:

$$\frac{(366.37-352.99)^2+(403.62-352.99)^2+(326.62-352.99)^2+(315.37-352.99)^2}{n-1}$$

$$\frac{(179.02 + 2563.39 + 695.57 + 1415.26)}{3} = 1617.68$$

(vi) Estimate of population variance from variance of means:

8 x 1617.68

(vii) Estimate of population variance from within variance:

$$\frac{\Sigma(x_1 - m_1)^2 + \Sigma(x_2 - m_2)^2 + \Sigma x_3 - m_3)^2 + \Sigma x_4 - m_4)^2 \ldots\ldots\ldots}{(n-1) + (n-1) + (n-1) \ldots\ldots\ldots.}$$

$$\frac{61103.47+2333.84+22130.76+7799.82}{7+7+7+7.} = \frac{93367.89}{28} = 3334.56$$

For ν = 28

(viii) Test the two values of the population variance for a significant difference using the F distribution:

$$F = \frac{12941.28}{3980.28} = 3.25$$

$$F_{28}^{3} = \frac{12941.28}{3980.28} = 3.25$$

From the tables F_{28}^{3} for P = 5% F = 2.95

The value of the F significant. Therefore there is difference.

Material	A	B	C	D
AB2	1.181	1.522	1.486	1.351
AC2	1.393	1.426	1.516	1.904
AD2	2.413	1.760	1.357	1.497
AA2	2.187	3.248	1.165	1.522
DA1	1.219	1.760	1.332	1.602
DB1	1.961	1.185	1.369	1.636
DC1	2.154	1.356	1.758	1.359
DA3	1.556	2.072	1.615	1.130

The calculation is as follows:

(i) Σx : 14.06 14.32 11.598 12.001

(ii) m = mean of each $\Sigma \frac{x}{n}$:

1.758 1.79 1.44 1.500

(iii) σ^2_e *=Estimate of variability in each :*

$$= \frac{\Sigma(x-m)^2}{n-1} =$$

0.226 0.418 0.034 0.052

(iv) *Mean of the means:*

$$\sum \frac{m}{4} = \bar{m} = \frac{1.758+1.79+1.44+1.5}{4}$$

$$\bar{m} = 1.622$$

(v) *Variability between Means:*

$$\frac{(1.758-1.622)^2 + (1.79-1.622)^2 + (1.44-1.622)^2 + (1.5-1.622)^2}{n-1}$$

$$\frac{(179.02 + 2563.39 + 695.57 + 1415.26)}{3} = 1617.68$$

(v) Estimate of population variance from variance of means :

$$(\frac{\sigma^2}{8}) = 0.03$$

There for $\sigma^2 = 8 \times 0.03 = 0.24$

(vii) Estimate of population variance from within sample variance:

$$\frac{\Sigma(x_1-m_1)^2+\Sigma(x_2-m_2)^2+\Sigma x_3-m_3)^2+\Sigma x_4-m_4)^2 \dots\dots\dots}{(n-1)+(n-1)+(n-1)\dots\dots\dots.}$$

$$\frac{1.584+0.239+.366+2.93}{7} = 0.182$$

(viii) Test the two values of the population variance for a significant difference using the F distribution:

$$F_{28}^3 = \frac{0.24}{0.132} = 1.31$$

F_{28}^3

$F_{28}^3 = 2.95$ for $P = 5\%$

Our value is well below this, so our hypothesis has not been disproved.

That is, there is no evidence to show any difference.

:

Material	F_S/R_a(A)	F_S/R_A(C)	F_S/R_{suba}(B)	F_S/R_a(D)
AB2 A	360.72/1.181	341.21/1.486	328.92/1.52	308.57/1.351
AC2 A	375.04/1.393	459.36/1.516	357.48/1.42	359.24/1.904
AD2 A	349.45/2.413	343.23/1.357	305.41/1.76	365.69/1.497
AA2 A	392.78/2.187	348.08/1.165	340.9/3.24	289.92/1.522
DA1 A	513.3/1.219	471.46/1.332	305.41/1.76	312.95/1.602
DB1 A	420.57/1.961	335.44/1.369	333.42.1.18	271/1.636
DC1 A	343.39/2.154	353.32/1.758	333.02/1.35	296.67/1.359
DA3 A	179.47/47/1.556	529.09/1.615	312.47/2.07	320.36/1.130

The calculation is as follows:

(i) $\sum x$:

2931 3229 2613 2523

(ii) mean of each:

$m = \sum \frac{x}{n}$:

366.37 403.62 326.62 315.36

(iii) σ^2_e *=Estimate of variability in each :*

$= \frac{\Sigma(x-m)^2}{n-1} =$

8726 5389

334.9 1470.37

(iv) Mean of the means:

$$\sum \frac{m}{4} = \bar{m} = \frac{366.37+403.62+326.62+315.37}{4}$$

$$\bar{m} = 352.99$$

(v) Variability between Means:

$$\frac{(366.37-352.99)^2 + (403.62-352.99)^2 + (326.62-352.99)^2 + (315.37-352.99)^2}{n-1}$$

$$\frac{(179.02 + 2563.39 + 695.57 + 1415.26)}{3} = 1617.68$$

(vi) Estimate of population variance from variance of means:

= 8 x 1617.68 = 12941

(vii) Estimate of population variance from within sample variance:

ν = 28

$$\frac{\Sigma(x_1 - m_1)^2 + \Sigma(x_2 - m_2)^2 + \Sigma x_3 - m_3)^2 + \Sigma x_4 - m_4)^2 \ldots\ldots\ldots}{(n-1) + (n-1) + (n-1) \ldots\ldots\ldots.}$$

8729 333.4 3161.53 1114.26

(viii) Test the two values of the population variance for a significant difference using the F distribution:

$$F_{28}^{3} = \frac{12941.44}{3334.36} = 3.88$$

$F_{28}^{3} = 3.88$

From the table F_{28}^{3} r P = 5% is 2.95

From the table F_{28}^{3} r P = *1*% is 4.57

Table 11: 247165 Cold Drawn and Annealed Material

Material : 247165 AC2										
HSC	15	16	15	15	17	17	15.83	*Fc*	305/290	97 .5(N)
SM	252.9	243.2	240.9	252.0	234.9	226.8	241.78	F_f	130/120	125(N)
ΛQ	54.98	53.93	48.24	47.20	47.48	47.01	49.80			
Δ*Q*	0.161	0.169	0.196	0.188	0.196	0.189	0.183			
RMAX	6.867	7.660	7.431	6.467	7.254	6.696	7.06			
R3TM	5.197	4.922	5.742	5.547	5.859	5.586	5.475			
RTM	6.309	6.435	6.772	6.074	6.787	6.392	6.461			
RP	4.694	5.103	4.499	3.717	3.340	4.108	4.410			
RT	7.623	8.234	7.639	6.677	7.272	7.056	7.416			
RSK	0.699	0.790	0.411	0.770	0.851	0.769	0.715			
RQ	1.409	1.453	1.504	1.412	1.479	1.412	1.444			
RA	1.140	1.159	1.227	1.120	1.160	1.121	1.154	*Fc*		297.5(N)
	Material : 247165 AD2									
HSC	16	16	17	15	16	16	16	*Fc*	230/215	1222.5(N)
SM	243.9	242.5	228.0	258.9	242.1	242.5	242.98	F_f	100190	95(N)
ΛQ	77.28	73.08	70.45	83.46	72.85	70.68	74.63			
Δ*Q*	0.176	0.168	0.180	0.191	0.177	0.176	0.178			
RMAX	13.57	8.856	9.054	20.35	9.448	8.508	11.63			
R3TM	6.602	6.602	7.070	5.518	6.719	6.797	6.551			
RTM	8.794	7.930	8.203	10.56	8.564	7.817	8.644			
RP	7.886	5.142	5.532	10.18	5.347	4.772	6.476			
RT	13.57	8.927	9.251	20.35	9.449	8.509	11.67			
RSK	0.462	0.243	0.224	0.042	0.501	0.491	0.327			
RQ	2.167	1.955	2.022	2.531	2.056	1. 977	2.118			
RA	1.831	1.698	1.747	1. 998	1.759	1.700	1.788	*Fc*		222.5(N)

Table 12: 247165 Annealed & Cold drawn Material

Speed = 150 rn/min						Speed = 200 rn/min				
HSC	15	15	15	15	15	15	15	15	15	15
SM	247.6	256.9	245.7	251.5	250.42	245.1	252.3	242.8	247.6	246.95
ΛQ	92.80	99.89	96.63	103.6	98.23	97.05	118.0	113.5	100.1	107.16
ΔQ	0.109	0.1 03	0.102	0.097	0.102	0.113	0.102	0.098	0.111	0.106
RMAX	6.659	6.519	6.452	6.299	6.482	8.599	10.06	8.447	9.030	9.034
R3TM	5.195	5.312	5.156	4.687	5.087	6.094	4.980	5.742	5.625	5.610
RTM	6.147	6.245	5.903	6.113	3.102	7.959	8.452	7.764	8.320	8.123
RP	4.108	4.102	3.717	3.760	3.921	4.694	4.907	4.688	5.078	4.841
RT	6.891	6.885	6.647	6.714	6.784	8.799	10.06	8.593	9.223	9.168
RSK	0.429	0.454	0.442	0.329	0.413	0.476	0.435	0.494	0.307	0.428
RQ	1.605	1.635	1.571	1.594	1.601	1.738	1.908	1.772	1.767	1. 796
RA	1.372	1.390	1.345	1.357	1.366	1.434	1.543	1.467	1.461	1.476
Speed = 300 rn/min						**Speed = 250 rn/min**				
303 S21 ø75						**304 SC ø100**				
HSC	16	15	15	15	15.25	15	15	16	15	15.25
SM	242.2	251.2	244.8	253.9	248.02	250.7	255.6	242.4	253.9	250.65
ΛQ	71.27	73.35	69.88	71.63	71.53	69.65	80.54	70.43	72.71	73.33
ΔQ	0.167	0.157	0.168	0.165	0.164	0.131	0.116	0.125	0.121	0.123
RMAX	8.434	7.831	8.313	8.621	8.299	8.835	9.521	9.613	8.428	9.09
R3TM	7.031	6.914	7.227	7.147	7.08	5.078	3.906	4.531	5.117	5.078
RTM	8.100	7.720	7.891	8.183	7.973	8.354	8.022	7.988	7.519	7.970
RP	3.9311	3.912	3.906	4.126	3.968	6.839	6.665	7.074	6.256	6.708
RT	8.435	8.027	8.484	8.621	8.391	9.403	9.839	9.613	8.430	9.321
RSK	0.263	0.323	0.280	0.248	0.278	1.300	1.193	1.330	1.307	1.282
RQ	1.896	1.837	1.867	1.882	1.870	1.454	1.491	1.396	1.404	1.436
RA	1.610	1.563	1.590	1.603	1.591	1.110	1.142	1.085	1.089	1.106

Table 13 : Summary Table

Material	RQ	Ra (µm)	Fc (N)	F_f(N)	Comments
247165A(A2)	2.454	1.889	335	130	**Very high force and R_a (Poor)**
247165A(B2)	1.275	1.025	265	112.5	**Low force and low R_a (Best)**
247165A(C2)	0.715	1.444	297.5	125	**(Better)**
247165A(D2)	2.118	1.788	222.5	95	**High force and low *Ra***
247165D(Al)	2.234	1.872	340	150	**High force and *Ra* (Poor)**
247165D(A3)	1.869	1.494	322.5	140	**-**
247165D(Bl)	1.798	1.473	237.5	137.5	**(Better)**
247165D(Cl)	1.549	1.255	232.5	135	**(Best)**

Table 14 :

Material	*Fs*	*Ra*	M	*Fs*	*Ra*	M	*Fs*	*Ra*	M	*Fs*	*Ra*
AB2A	360.72	1.181	AB2C	341021	1.486	AB2B	328.92	1.522	AB2D	308.57	1.351
AC2A	375.04	1.393	AC2C	459.36	1.516	AC2B	357.48	1.426	AC2D	359.24	1.904
AD2A	349.35	2.413	AC2C	393.23	1.357	AD2B	305.41	1.760	AD2D	368.69	1.497
AA2A	392.78	2.187	AA2C	348.08	1.165	AA2B	340.96	3.248	AA2D	289.92	1.522
DAIA	513.3	1.219	DA1C	471.46	1.332	DA1B	305.41	1.760	DA1D	312.95	1.602_
DB lA	420.57	1.961	DB1C	355.44	1.369	DB1B	333.1	1.185	DB ID	271	1.636
DC1A	343.39	2.154	DC1C	353.32	1.758	DC1B	333.02	1.356	DC1D	296.67	1.359
DA3A	179.47	1.556	DA3C	529.09	1.615	DA3B	312.47	2.072	DA3D	320.36	1.130

Table 15: Chip thickness, shear plane angle and forces

Material :	Fc	F_f	t_2	t_1	θ	Fc	Fs	N	Ra
247165AA2	390	130	0.428	0.25	22.9	309.66	268.32	94.38	1.889
247165AB2	265	112.5	0.371	0.25	26.06	188.58	217.36	84.26	1.025
247165AC2	297.5	125	0.364	0.25	26.6	210.09	247.23	93.31	1.444
247165AD2	222.5	95	0.272	0.25	33	134.77	200.65	71.29	1.788
247165DAI	390	160	0.375	0.25	25.81	281.4	313.65	113.74	1.872
247165DA3	322.5	140	0.326	0.25	29.81	210.02	281.66	105.62	1.494
247165DBl	237.5	137.5	0.28	0.25	33.23	123.2	247.98	111.97	1.473
247165DCl	232.5	135	0.294	0.25	30.91	129.99	234.96	110.01	1.255

Table 16 :

Material :	T2.1	$T_{2.2}$	$T_{2.3}$	$T_{2.4}$	$T_{2.4}$	$T_{2.5}$	T_2	t_1	F_f	Fc
247165 AC2A	0.27	0.27	0.27	0.275	0.25	0.267	0.25	180	340	34.55
247165 AC2C	0.265	0.26	0.265	0.26	0.265	0.263	0.25	240	400	35.06
247165 AD2A	0.28	0.27	0.275	0.28	0.28	0.277	0.25	125	350	33.61
247165 AD2C	0.255	0.25	0.26	0.255	0.25	0.254	0.25	187.5	360	36.03
247165 AA2A	0.28	0.256	0.265	0.255	0.27	0.265	0.25	190	355	34.85
247165 AA2C	0.245	0.26	0.24	0.26	0.245	0.25	0.25	135	347.5	36.51
247165 AB2A	0.27	0.27	0.255	0.255	0.26	0.262	0.25	130	365	35.17
247165 AB2C	0.27	0.275	0.28	0.28	0.27	0.275	0.25	125	340	33.81
247165 DAIA	0.24	0.23	0.235	0.23	0.23	0.233	0.25	317.5	407.5	38.56
247165 DA1C	0.23	0.23	0.23	0.21	0.215	0.223	0.25	292.5	375	39.86
247165 DA3A	0.145	0.145	0.14	0.13	0.145	0.141	0.25	80	205	53.8
247165 DA3C	0.255	0.25	0.4	0.2265	0.24	0.25	0.25	0.275	465	36.51
247165 DB lA	0.22	0.22	0.23	0.23	0.225	0.225	0.5	230	365	39.60
247165 DBIC	0.23	0.20	0.205	0.21	0.15	0.212	0.25	150	330	41.38
247165 DCIA	0.215	0.20	0.205	0.205	0.22	0.209	0.25	180	310	41.81
247165 DCIC	0.22	0.235	0.22	0.21	0.23	0.223	0.25	180	320	39.77

Table 17 :

Material :	T_2	T_1	θ	Ff	Fc	F_{C1}	N	F_s	Ra
AB2A	0.262	0.25	35.17	130	365	3.3	91.26	316.45	1.181
AB2C	0.275	0.25	33.81	125	340	213.45	87.33	290.75	1.486
AC2A	0.67	0.5	34.64	180	340	177.24	143.56	341.08	1.393
AC2C	0.263	0.25	35.06	240	400	189.44	196.96	542.92	1.516
AD2A	0.277	0.25	33.61	125	350	222	87.85	297.55	2.413
AD2C	0.254	0.25	36.05	187.5	360	180.63	148.93	363.18	1.357
AA2A	0.265	0.25	34.85	190	355	182.04	151. 94	359.57	2.187
AA2C	0.25	0.25	36.51	135	347.5	198.85	133.1	314.82	1.165
DAIA	0.233	0.25	38.56	317.5	407.5	120.45	273.21	501.84	1.219
DA1C	0.223	0.25	39.86	292.5	375	100.42	251.74	464.34	1.332
DB lA	0.225	0.25	39.60	230	365	134.54	190.66	409.6	1.961
DBIC	0.212	0.25	41.38	135	345	169.51	98.31	329.29	1.369
DCIA	0.209	0.25	41.81	180	310	111.07	146.68	340.56	2.154
DCIC	0.223	0.25	39.86	180	320	130.24	145.64	342.86	1.758
DA3A	0.141	0.25	53.8	80	205	56.47	58.2	212.43	1.556
DA3C	0.25	0.25	36.51	275	465	210.04	224.99	497.03	1.615

Table 18 :

Material :	*T2.1*	*T2.2*	*T2.3*	*T24*	*T2.5*	*T2.6*	*T2av*
247165 AB2B	0.29	0.28	0.29	0.27	0.27	0.28	0.28
247165 AA2D	0.21	0.22	0.22	0.26	0.21	0.23	0.225
247165 AA2B	0.29	0.26	0.265	0.27	0.28	0.29	0.275
247165 AB2D	0.30	0.285	0.28	0.31	0.295	0.285	0.2925
247165 AC2B	0.30	0.285	0.285	0.30	0.29	0.29	0.291
247165 AD2D	0.255	0.275	0.28	0.28	0.275	0.28	0.274
247165 AD2B	0.275	0.27	0.26	0.27	0.27	0.255	0.266
247165 DAIB	0.24	0.22	0.23	0.24	0.23	0.23	0.231
247165 DAID	0.205	0.21	0.215	0.205	0.20	0.21	0.207
247165 DA3B	0.22	0.22	0.24	0.245	0.23	0.235	0.231
247165 DA3D	0.225	0.24	0.24	0.23	0.24	0.23	0.234
247165 DBIB	0.23	0.21	0.24	0.21	0.23	0.25	0.228
247165 DBAD	0.24	0.22	0.20	0.22	0.205	0.215	0.216
247165 DCIB	0.22	0.215	0.21	0.21	0.205	0.195	0.206
247165 DCID	0.215	0.21	0.21	0.21	0.215	0.20	0.21

Table 19 :

Material :	Fc	Ff	t_2	t_1	θ	Fc	Fs	N	Ra
247165 AA2B	335	130	0.275	0.25	33.81	205.77	294.16	94.38	3.248
247165 AA2D	290	120	0.225	0.25	39.60	146.86	277 .13	89.12	1.522
247165 AB2B	322	125	0.28	0.25	33.32	200.24	281.15	90.76	1.546
247165 AB2D	310	110	0.275	0.25	33.81	196.14	263.66	77.1	1.351
247165 AC2B	345	140	0.291	0.25	32.27	216.90	302.18	103.28	1.426
247165 AC2B	355	130	0.292	0.25	32.17	231.17	298.84	92.3	1.904
247165 AD2B	325	140	0.266	0.25	34.74	204.23	329.41	75.54	1.162
247165 AD2D	367.5	135	0.274	0.25	33.83	229.96	316.38	95.97	1.497
247165 DA1B	305	130	0.231	0.25	38.82	156.21	292.2	98.02	1.760
247165 DA1D	320	130	0.207	0.25	42.1	149.7	310.73	95.94	1.602
247165 DA3B	305	135	0.231	0.25	38.82	153.08	296.09	102.47	2.072
247165 DA3D	320	130	0.234	0.25	38.43	169.83	300.51	95.94	1.130
247165 DB1B	330	140	0.228	0.25	39.2	166.94	316.92	104.84	1.185
247165 DBAD	277.5	110	0.216	0.25	40.82	137.96	264.36	80.48	1.636
247165 DC1B	317.5	160	0.206	0.25	42.25	127.43	331.76	126.02	1.356
247165 DC1D	300	125	0.21	0.25	41.66	141.1	292.57	93.05	1.359

Table 20: 247165 Cold Drawn and Annealed Material

Material : 247165 A									
HSC	16	16	15	15	15	15	15.33		A_2
SM	244.2	249.4	250.5	250.3	250	252.0	249.4		
Λ Q	86.60	91.04	94.31	91.37	91.90	86.04	90.21		
Δ Q	.190	0.178	0.172	0.167	0.167	0.151	0.170		
RMAX	21.12	20.42	19.07	0.56	20.73	17.0	19.81		
R3TM	7.070	6.055	5.039	6.445	6.494	6.152	6.209		
RTM	12.38	12.88	Il.38	10.22	10.91	9.126	11.14		
RP	Il.52	11.74	9.985	11.53	13.09	10.75	11.43		
RT	21.12	20.42	19.07	20.56	20.73	17.0	19.81		
RSK	0.437	0.659	0.446	0.564	0.966	0.685	0.626		
RQ	2.617	2.584	2.586	2.425	2.447	2.066	2.454	Fc	335(N)
RA	2.020	1. 996	.014	1.848	1.816	1.644	1.889	Fsumf	BON
	Material : 247165 Dl								
HSC	16	15	16	15	15	17	15.33		A_1
SM	237.0	252.1	247.9	250.9	250.7	21.5	243.35		
Λ Q	74.62	7.53	76.90	76.89	79.49	85.54	77.66		
Δ Q	0.178	0.181	0.176	0.177	0.175	0.197	0.180		
RMAX	9.406	9.384	9.496	10.24	9.644	20.03	11.36		
R3TM	8.203	8.047	8.125	7.734	7.812	8.242	8.027		
RTM	9.258	9.243	9.385	9.502	9.448	12.11	9.824		
RP	3.931	3.949	4.126	4.407	4.297	11.92	5.438		
RT	9.601	9.620	9.876	10.24	10.31	20.03	11.61		
RSK	0.151	..0.054	0.102	0.051	0.184	0.887	0.220	Fc	(340N)
RQ	.109	2.095	2.150	2.165	2.211	2.678	2.234	F_f	(150N)
RA	1.785	1. 799	1.831	1.858	1.88	2.078	1.872		

Table 20 (cont) :

Material : 303 S21									
HSC	15	15	15	15	15	15	15		
SM	254.0	254.5	253.3	250.1	252	250.8	252.45		
ΛQ	129.4	122.7	117.1	126.0	112.1	122.0	121.55		
ΔQ	0.108	0.114	0.122	0.115	0.128	0.117	0.117		
RMAX	7.836	7.822	7.739	7.849	8.307	7.828	7.896		
R3TM	6.250	6.250	6.641	6.406	6.797	6.602	6.491		
RTM	7.422	7.432	7.451	7.558	7.739	7.539	7.523		
RP	4.297	4.340	4.419	4.108	4.495	4.174	4.305		
RT	7.837	7.861	8.008	8.027	8.603	7.910	8.041		
RSK	0.292	0.262	0.239	0.279	0.151	0.206	0.238		
RQ	2.214	2.234	2.283	2.306	2.283	2.277	2.266	*Fe*	295(N)
RA	1.957	1.982	2.036	2.054	2.036	2.033	2.016	*FI*	110(N)
	Material : 304 SC								
HSC	15	16	15	17	15	15	15.5		
SM	255.7	244.6	255.3	231.5	259.6	258.4	250.85		
ΛQ	83.94	87.19	76.40	76.35	76.80	82.04	7.45		
ΔQ	0.127	0.123	0.139	0.139	0.139	0.128	0.132		
RMAX	7.276	6.33	7.703	7.031	7.306	7.064	7.119		
R3TM	5.430	5.703	5.234	5.586	6.055	5.664	5.612		
RTM	6.680	6.01	6.038	6.567	6.924	6.401	6.468		
RP	4.126	3.754	4.535	4.297	4.557	4.126	4.2325		
RT	7.257	6.503	7.703	7.242	7.321	7.065	7.184		
RSK	0.651	0.755	0.831	0.538	0.865	0.799	0.739		
RQ	1. 701	1.713	1.693	1.684	1.697	1.665	1.69	*Fe*	355(N)
RA	1.426	1.431	1.390	1.433	1.388	1.372	1.406	F_I	155(N)

Table 21 : Position of cut

Material: 303 S21-Annealed-Free-cutting Austenite										
HSC	16	15	16	16	16	15.66	*Fe*	32.5N	Beg	
SM	241.0	249.0	251.6	243.5	243.2	243.2	245.25	*Fe*	340(N)	M
ΛQ	70.10	74.02	76.21	74.39	72.49	69.91	72.85	*FI*	115(N)	Beg
Δ Q	0.165	0.156	0.150	0.1522	0.165	0.169	0.159	*FI*	115(N)	M
RMAX	9.009	8.032	8.060	8.008	8.4722	8.597	8.363	*Fe*	346(N)	B
R3TM	6.719	6.758	6.836	6.523	7.109	7.187	6.855	*Fe*	340(N)	M
RTM	8.096	7.617	7.617	7.598	8.105	8.213	7.874	*FI*	136(N)	B
RP	4.517	3.955	4.346	3.717	3.912	4.108	4.092	*FI*	BON	M
RT	9.009	8.057	8.268	8.014	8.603	8.603	8.425	*Fe*	338(N)	B
RSK	0.387	0.456	0.362	0.367	0.216	0.286	0.341	*Fe*	346(N)	M
RQ	1.836	1.833	1.815	1.805	1. 907	1.881	1.846	*FI*	140(N)	B
RA	1.543	1.547	1.549	1.528	1.631	1.599	1.599	*FI*	135(N)	M
Material : 304 SC - Annealed										
HSC	4	9	14	14	15	15	Il.83	*Fe*	95(N)	B
SM	821.0	389.5	274.8	254.3	261.2	252.5	357.55	*Fe*	345(N)	M
ΛQ	219.6	130.9	79.54	79.54	84.39	67.26	110.17	*FI*	-	B
ΔQ	0.104	0.098	0.117	0.105	0.115	0.130	0.111	*FI*	142.5(N)	M
RMAX	17.41	13.10	9.279	7.714	9.647	8.814	10.99	*Fe*	335(N)	B
R3TM		1.562	4.883	4.727	3.867	4.785	3.304	*Fe*	370(N)	M
RTM	13.86	10.92	7.285	6.479	8.135	7.871	10.02	*FI*	140(N)	B
RP	9.57	7.819	7.105	5.22	7.034	6.446	7.216	*FI*	156(N)	M
RT	17.60	13.29	10.24	7.715	10.36	8.814	11.33	*Fe*	327.5(N)	B
RSK	0.207	0.332	0.880	0.958	1.171	1.251	0.799	*Fe*	337.5(N)	M
RQ	3.643	2.171	1.479	1.333	1.539	1.395	1. 926	*FI*	150(N)	B
RA	33.054	1.677	1.173	1.061	1.168	1.079	1.535	*FI*	140(N)	M

Table 21 : Position of cut

Material : 247165 A										
HSC	16	15	15	16	15	15	15.33	Fc	335.5(N)	B
SM	243.9	254.3	256	243.6	51.8	257.7	251.2	Fc	335(N)	M
ΛQ	105.5	103.6	96.48	98.46	92.72	99.03	99.298	F_f	136(N)	B
ΔQ	0.095	0.097	0.106	0.103	0.105	0.103	0.101	F_f	135(N)	M
RMAX	6.494	6.256	7.242	6.839	6.281	6.842	6.659	Fc	347(N)	B
R3TM	4.931	5.312	5.117	5.078	5.312	5.312	5.17	Fc	350(N)	M
RTM	6.113	6.16	6.333	6.313	6.152	6.362	6.248	S_f	146(N)	B
RP	3.931	3.910	4.116	3.006	3.735	4.303	3.833	F_f	149(N)	M
RT	6.714	6.839	7.42	6.839	6.281	7.239	6.859	Fc	342.5(N)	B
RSK	0.436	0.362	0.372	0.482	0.389	0.389	0.405	Fc	357.5(N)	M
RQ	1.589	1.591	1.623	1.612	1.556	1.622	1.598	F_f	150(N)	B
RA	1.348	1.351	1.396	1.371	1.334	1.383	1.363	F_f	140(N)	M
Material : 247165 CD										
HSC	15	15	16	15	14	15	15	Fc	357.5(N)	B
SM	252.3	251.8	243.9	241. 7	253.1	244.7	247.9	Fc	327.5(N)	M
ΛQ	10.6	109.3	103.7	101.1	99.91	101.9	102.91	F_f	162.5(N)	B
ΔQ	0.116	0.100	0.104	0.107	0.108	0.107	0.107	F_f	150(N)	M
RMAX	11.25	8.234	8.057	8.167	8.691	8.615	8.835	Fc	340(N)	B
R3TM	5.977	6.094	5.859	6.133	6.211	5.859	6.031	Fc	-	M
RTM	5.977	7.695	7.59	7.563	8.086	7.807	7.748	Fc	-	M
RP	8.628	4.932	4.499	4.407	4.932	4.300	4.614	F_f	165(N)	B
RT	7.105	9.253	8.448	8.167	9.098	9.003	8.793	F_f	-	M
RSK	Il.25	0.388	0.481	0.496	0.392	0.469	0.445	Fc	330(N)	B
RQ	1.875	1.744	1.716	1.729	1.714	1.743	1.753	Fc	327(N)	M
RA	1.533	1.453	1.423	1.435	1.414	1.430	1.448	F_f	146(N)	M

Table 22: Stainless Steel Machined, using ground tool.

Material : 247165 A2					Material: 247165 DA3			
HSC	15	14	15	14.66	15	15	14	14.66
SM	249.9	253.7	253.5	252.3	253.0	249.7	256.7	253.13
ΛQ	204.1	194.1	206.7	201.63	215.4	196.3	225.1	212.26
ΔQ	0.792	0.808	0.799	0.799	0.709	0.834	0.699	0.747
RMAX	98.05	93.35	97.80	96.4	93.51	96.23	78.24	89.32
R3TM	56.41	72.81	68.59	65.93	64.22	67.03	66.89	66.04
RTM	88.25	81.87	84.99	85.03	78.60	90.24	76.05	81.63
RP	47.27	43.75	45.75	45.59	43.85	44.97	41.50	43.44
RT	98.05	94.92	97.80	96.92	95.07	96.59	79.02	90.22
RSK	0.316	0.260	0.889	0.218	0.277	0.044	0.207	0.176
RQ	25.72	4.95	26.29	25.65	4.30	26.05	25.04	5.13
RA	22.96	22.19	23.45	22.86	21.68	23.17	22.56	22.47
Material : 247165 CI					**Material : 303 S21**			
HSC	14	15	15	14.66	15	15	15	15
SM	256.4	250.4	249.3	252.0	255.6	254.3	253.6	254.5
ΛQ	212.8	201.7	185.7	200	210.7	217.8	218.1	215.53
ΔQ	0.758	0.818	0.906	0.827	0.664	0.684	0.709	0.685
RMAX	93.46	94.63	97.90	95.33	72.46	78.52	81.36	77.44
R3TM	79.56	73.12	71.95	74.87	64.06	67.09	69.14	66.76
RTM	83.21	90.34	92.58	88.71	69.76	96.30	78.43	74.83
RP	42.73	43.76	46.49	44.32	39.06	44.92	45.72	43.23
RT	93.60	95.33	98.15	95.69	72.81	80.47	81.36	78.21
RSK	0.222	0.166	0.105	0.164	0.216	0.294	0.273	0.261
RQ	25.67	26.26	26.77	26.33	22.26	23.69	24.59	23.51
RA	1'(2.93)	23.47	23.81	23.40	19.79	21.04	21.96	20.93

Table 22(Cont.): Stainless Steel Machined, using ground tool.

Material: 247165 DA1					Material : 247165 DBl			
HSC	15	15	15	15	15	15	15	15
SM	252.1	251.2	250.9	251.4	253.3	254.7	252.8	253.6
ΛQ	215.0	213.2	204.3	210.83	221.0	223.5	209.8	218.1
Δ Q	0.729	0.717	0.768	0.738	0.692	0.680	0.768	0.713
RMAX	92.33	91.81	92.63	92.25	78.91	74.76	97.17	83.61
R3TM	65.55	66.56	66.70	66.27	67.77	64.94	65.53	66.08
RTM	79.54	76.78	82.81	79.71	74.89	72.7	85.28	77.63
RP	44.24	41.11	44.14	43.16	43.07	49.85	45.36	43.32
RT	95.17	92.67	95.57	94.45	79.41	76.76	97.17	84.44
RSK	0.32	0.301	0.168	0.233	0.301	0.223	0.149	0.224
RQ	24.94	24.31	24.97	24.74	24.36	24.19	25.57	24.70
RA	22.27	21.77	22.1	22.08	21.81	21.67	22.79	22.09
Material: 247165 AD2					**Material : 247165 AB2**			
HSC	15	15	15	15	15	15	15	15
SM	251.3	250.5	250.7	250.83	253.2	254.9	254.1	254.06
Λ Q	216.2	199.7	187.5	201.13	214.3	218.6	203.8	212.23
Δ Q	0.716	0.799	0.867	0.794	0.749	0.745	0.804	0.766
RMAX	93.35	97.46	99.33	96.71	93.74	94.97	95.38	94.69
R3TM	67.81	67.19	70.94	68.64	71.64	72.85	76.17	73.55
RTM	80.09	81.60	88.55	83.41	83.91	81.94	81.24	82.36
RP	43.76	46.24	48.05	46.01	43.75	43.76	43.37	43.62
RT	93.38	97.46	99.62	96.82	95.07	96.11	95.38	95.52
RSK	0.322	0.172	0.162	0.218	0.216	0.254	0.181	0.17
RQ	24.62	25.39	25.88	25.29	25.53	25.91	26.08	25.84
RA	22.04	22.56	23.0	22.53	22.81	23.13	23.13	

Table 23 :

aterial : 247165 AD2														
Speed = 200 m/min (Chamfer)								Speed = 250 m/min (Chamfer)						
HSC	15	14	15	15	15	15	14.83	14	14	14	15	15	14	14.33
SM	250.4	254.6	250.5	253.9	255.1	253.2	252.95	253.7	253.7	255.6	252.9	252.3	253.4	253.58
ΛQ	196.7	197.0	200.5	196.4	204.3	204.3	199.88	198.7	200.3	200.8	200.3	197.2	202.1	199.9
Δ *Q*	0.714	0.674	0.719	0.703	0.731	0.728	0.711	0.724	0.725	0.727	0.694	0.741	0.746	0.726
RMAX	0.079	0.079	0.087	0.083	0.091	0.092	0.085	0.083	0.083	0.081	0.083	0.087	0.097	0.085
R3TM	0.062	0.060	0.059	0.062	0.063	0.062	0.061	0.065	0.060	0.065	0.059	0.061	0.064	0.062
RTM	0.076	0.073	0.078	0.076	0.082	0.080	0.072	0.076	0.081	0.076	0.075	0.078	0.077	0.077
RP	0.044	0.048	0.052	0.044	0.049	0.047	0.047	0.046	0.047	0.044	0.047	0.049	0.049	0.047
RT	0.079	0.080	0.090	0.083	0.092	0.093	0.086	0.084	0.086	0.082	0.083	0.088	0.097	0.073
RSK	0.291	0.314	0.261	0.395	0.376	0.164	0.300	0.217	0.300	0.275	0.310	0.284	0.153	0.250
RQ	22.36	21.13	22.96	21.96	23.78	23.67	22.64	22.89	23.12	23.24	22.13	23.26	24.0	23.09
RA	19.76	18.56	20.11	19.25	20.81	20.76	19.87	20.09	20.30	20.66	19.54	20.46	21.13	20.36
Material : 247165 DA3														
Speed = 200 m/min(Chamfer)								**Speed = 250 m/min(Chamfer)**						
HSC	15	15	15	15	15	15	15	15	14	15	15	15	15	14.83
SM	251.6	249.7	253.7	252.3	253.7	254.5	252.58	255.1	255.3	250.7	250.3	250.5	253.5	252.56
ΛQ	190.6	189.0	194.8	200.1	189.2	200.1	193.96	193.7	194.6	190.7	194.0	188.9	196.5	193.06
ΔQ	0.653	0.656	0.671	0.699	0.669	0.693	0.673	0.683	0.666	0.691	0.710	0.674	0.684	0.684
RMAX	0.072	0.071	0.079	0.082	0.074	0.079	0.076	0.077	0.079	0.077	0.079	0.079	0.077	0.078
R3TM	0.061	0.060	0.060	0.061	0.060	0.057	0.059	0.060	0.062	0.056	0.060	0.058	0.061	0.0595
RTM	0.069	0.068	0.072	0.077	0.069	0.076	0.071	0.072	0.073	0.072	0.073	0.068	0.069	0.071
RP	0.043	0.041	0.047	0.049	0.044	0.045	0.044	0.047	0.044	0.044	0.047	0.040	0.041	0.043
RT	0.074	0.071	0.079	0.085	0.074	0.079	0.077	0.084	0.081	0.078	0.080	0.073	0.078	0.078
RSK	0.415	0.455	0.369	0.460	0.435	0.348	0.413	0.385	0.447	0.352	0.346	0.319	0.384	0.372
RQ	19.80	19.71	20.82	22.25	20.15	22.08	20.80	21.06	20.63	20.97	21.91	20.26	21.39	21.03
RA	17.16	17.03	18.10	19.36	17.47	19.35	18.07	18.41	18.21	19.30	17.74	18.76		18.48

Table 23(Cont...):

Material : 247165 DBI														
Speed = 200 M/Min, 0=1.27mm								Speed = 250 M/Min, 0=1.27mm						
HSC	3	3	5	5	4	4	4	15	16	13	16	13	15	14.66
SM	720.6	928.0	706.8	748.8	715.0	495.5	725.1	257.3	246	278.3	246.6	270.4	253.3	258.65
ΛQ	43.04	40.12	41.24	41.90	46.58	43.61	42.74	73.25	71.74	74.07	72.30	75.15	74.23	73.45
ΔQ	0.257	0.266	0.264	0.270	0.257	0.252	0.261	0.279	0.276	0.274	0.280	0.273	0.287	0.278
RMAX	0.009	0.010	0.009	0.010	0.012	0.010	0.01	0.013	0.013	0.015	0.014	0.015	0.014	0.014
R3TM	0.006	0.006	0.006	0.006	0.007	0.007	0.006	0.011	0.010	0.011	0.011	0.011	0.012	0.011
RTM	0.008	0.008	0.008	0.009	0.009	0.009	0.0085	0.012	0.012	0.013	0.013	0.014	0.014	0.013
RP	0.006	0.005	0.005	0.006	0.008	0.006	0.006	0.007	0.008	0.009	0.008	0.009	0.009	0.0083
RT	0.010	0.010	0.009	0.010	0.012	0.010	0.010	0.013	0.013	0.016	0.014	0.016	0.016	0.014
RSK	0.243	0.395	0.194	0.509	0.537	0.186	0.344	0.173	0.832	0.961	0.279	1.035	1.070	0.725
RQ	1.759	1.699	1.731	1.798	1.905	1.751	1.773	3.258	3.144	3.226	3.225	3.269	3.386	3.25
RA	1.416	1.362	1.390	1.439	1.528	1.384	1.419	2.768	2.590	2.613	2.726	2.637	2.732	2.677
Material : 247165 AB2														
Speed = 200 m/min, 0= 1.27mm								Speed = 250m/min, 0= 1.27mm						
HSC	3	6	5	-	4	1	3.8	3	3	-	5	4	-	4.5
SM	1.257	569.0	612.0	-	683.5	256.0	530.1	674.7	911.3	-	625.6	907.0	-	805.98
ΛQ	42.92	44.90	40.85	41.32	39.82	40.78	41.77	42.13	42.24	-	40.91	42.06	43.21	42.13
ΔQ	0.259	0.270	0.262	0.263	0.274	0.261	0.264	0.274	0.268	-	0.278	0.276	0.267	0.271
RMAX	0.009	0.014	0.012	0.008	0.010	0.008	0.010	0.009	0.010	-	0.011	0.011	0.010	0.010
R3TM	0.006	0.007	0.007	0.006	0.007	0.006	0.006	0.007	0.007	-	0.007	0.006	0.006	0.0066
RTM	0.008	0.010	0.008	0.007	0.008	0.008	0.0081	0.009	0.009	-	0.009	0.009	0.009	0.009
RP	0.005	0.010	0.009	0.005	0.005	0.005	0.0065	0.006	0.006	-	0.008	0.006	0.007	0.0075
RT	0.010	0.014	0.013	0.008	0.010	0.009	0.010	0.010	0.011	0.011	0.012	0.011	0.011	0.011
RSK	-0.127	1.227	1.245	1.250	-0.117	1.185	0.816	0.237	0.116	0.116	0.081	-0.110	1.473	0.355
RQ	1.772	1.930	1.706	1.732	1.737	1.697	1.762	1.835	1.803	1.803	1.811	1.849	1.836	1.822
RA	1.453	1.451	1.296	1.308	1.435	1.298	1.373	1.479	1.470	1.470	1.469	1.510	1.338	1.456

Table 24:

Material : 247165 DA3								Material : 247165 DBI			
HSC	15	15	14	15	15	15	15	16	15	15	15.33
SM	254.0	250.9	251.4	253.3	253.5	257.3	253.4	245.4	253.5	252.8	250.56
ΛQ	135.6	136.7	136.2	140.0	131.9	141.1	136.9	130.1	141.6	142.8	138.16
ΔQ	0.182	0.178	0.186	0.176	0.195	0.174	0.181	0.258	0.253	0.250	0.253
RMAX	19.32	12.99	16.55	13.68	23.96	14.56	16.84	22.78	22.27	21.14	22.06
R3TM	Il.04	10.35	10.64	9.219	9.896	10.74	10.31	17.58	18.52	18.59	18.23
RTM	13.98	12.47	13.81	12.69	15.05	12.87	13.47	20.64	20.82	20.50	20.65
RP	8.301	7.910	10.21	8.203	14.45	9.081	9.692	11.43	Il.33	11.34	Il.36
RT	19.32	14.21	16.55	14.11	23.96	14.99	17.19	22.78	22.66	21.15	22.19
RSK	0.449	0.367	0.190	0.206	0.461	0.324	0.332	0.429	0.403	0.265	0.365
RQ	3.926	3.873	4.042	3.930	4.086	3.909	3.961	5.663	5.700	5.681	5.681
RA	3.473	3.433	3.395	3.509	3.548	3.482	3.473	4.718	4.762	4.797	4.759
Material : 247165 C2								**Material : 247165 AB2**			
HSC	14	16	15	15	-	-	-	11	15	15	13.66
SM	256.6	241.1	253.3	250.3	-	-	-	317.6	251.5	252.1	273.73
ΛQ	78.90	75.22	76.54	76.88	-	-	-	92.45	82.27	81.61	85.44
ΔQ	0.221	0.239	0.245	0.235	-	-	-	0.155	0.177	0.179	0.170
RMAX	13.34	12.60	14.12	12.35	-	-	-	10.22	9.473	8.605	9.432
R3TM	10.39	Il.09	10.78	10.75	-	-	-	5.937	6.562	6.953	6.484
RTM	11.76	12.39	13.13	12.4	-	-	-	9.336	8.252	7.851	8.474
RP	8.252	9.069	8.997	8.772	-	-	-	9.336	5.518	5.127	6.660
RT	13.34	12.60	14.37	13.43	-	-	-	10.99	9.473	8.654	9.205
RSK	1.613	1.637	1.534	1.594	-	-	-	0.378	0.641	1.108	0.709
RQ	2.774	2.864	2.983	2.873	-	-	-	2.281	2.313	2.320	2.304
RA	2.033	2.094	2.191	2.106	-	-	-	1.896	1.952	1.868	1.905

Table 24(Cont) :

	Material: 247165 A2				Material : 247165 CI			
HSC	14	14	16	14.66	13	10	14	12.33
SM	256.1	254.0	242.7	250.93	283.5	345.0	267.8	298.7
ΛQ	56.94	65.71	66.17	62.94	57.84	64.06	58.52	60.14
ΔQ	0.188	0.163	0.176	0.175	0.134	0.149	0.137	0.140
RMAX	7.831	7.831	9.046	8.236	6.787	8.643	6.665	7.365
R3TM	6.641	6.562	6.172	6.458	4.375	5.078	4.531	4.661
RTM	7.441	7.510	8.096	7.682	6.289	7.148	5.986	6.474
RP	5.090	5.129	5.127	5.114	3.955	5.469	3.955	4.459
RT	7.831	7.868	9.436	8.378	6.787	8.643	6.802	7.377
RSK	1.134	1.189	0.656	0.993	1.103	1.061	0.862	1.008
RQ	1.706	1.704	1.849	1.753	1.236	1.519	1.279	1.344
RA	1.358	1.344	1.507	1.403	0.922	1.119	0.986	1.009
Material: 247165 DAI					**Material : 247165 AD2**			
HSC	15	15	15	15	15	15	15	15
SM	254.4	245.3	252.1	250.6	256.3	253.7	254.1	254.7
ΛQ	106.8	101.0	100.3	102.6	69.85	63.58	65.19	66.20
ΔQ	0.294	0.303	0.314	0.303	0.158	0.169	0.175	0.167
RMAX	20.13	19.68	20.41	20.07	10.74	7.190	11. 73	9.886
R3TM	17.66	17.19	17.97	17.60	5.234	5.937	5.859	5.676
RTM	19.37	18.83	19.75	19.31	7.725	6.797	7.754	7.425
RP	9.778	9.473	9.315	9.522	6.787	4.443	7.422	6.217
RT	20.32	19.68	20.41	20.13	10.74	7.190	11. 73	9.886
RSK	-0.108	-0.167	0.025	-0.083	0.779	0.626	0.696	0.700
RQ	4.989	4.876	5.010	4.958	1.760	1. 707	1.818	1.761
RA	4.229	4.129	4.217	4.191	1.472	1.460	1.534	1.488

Table 25 :

Material : 247165 AC2								
Speed = 300 m/min					Speed = 350 m/min			
HSC	10	11	11	10.66	11	11	11	11
SM	254.8	251.6	254.0	253.4	251.3	250.9	251.6	251.26
ΛQ	166.1	178.5	183.5	176.03	158.1	163.2	165.1	162.13
ΔQ	0.610	0.623	0.632	0.621	0.598	0.625	0.630	0.617
RMAX	0.053	0.066	0.069	0.0626	0.056	0.055	0.056	0.055
R3TM	-	-	-	-	-	-	-	-
RTM	0.047	0.053	0.053	0.051	0.047	0.048	0.050	0.048
RP	0.028	0.028	0.029	0.028	0.026	0.028	0.028	0.027
RT	0.055	0.066	0.069	0.063	0.057	0.057	0.058	0.057
RSK	0.245	0.046	0.246	0.179	0.214	0.338	0.179	0.223
RQ	16.12	17.68	18.45	17.41	15.05	16.22	16.55	15.94
RA	14.64	15.91	16.72	15.75	13.27	14.25	14.81	14.11
Material : 247165 DA1								
Speed = 350 m/min					Speed = 300 m/min			
HSC	11	11	11	11	11	10	11	10.66
SM	248.2	249.1	247.4	248.23	252.2	253.0	252.9	252.7
ΛQ	179.8	189.7	193.2	187.56	188.8	183.1	194.4	188.76
Δ Q	0.552	0.560	0.631	0.581	0.628	0.639	0.647	0.638
RMAX	55.32	56.26	0.068	37.21	0.063	0.062	0.070	0.065
R3TM	-	-	-	-	-	-		
RTM	46.92	49.83	0.058	32.26	0.054	0.052	0.058	0.054
RP	26.95	27.39	0.030	18.12	0.030	0.028	0.031	0.029
RT	57.04	59.42	0.069	38.84	0.069	0.063	0.074	0.068
RSK	0.195	0.136	0.	0.127	0.013	0.183	0.068	0.088
RQ	15.78	16.90	19.42	17.36	18.86	18.61	20.01	19.16
RA	14.07	15.37	17.61	15.68	17.25	17.11	18.24	17.53

Ideal values of Ra

Feed	N R (mm)					
(mm)	0.1	0.25	0.5	0.75	1.0	2.0
0.5	0.64	0.4	16	36	64	256
1.0	0.32	2	8	18	32	128
1.2	0.266	5.748	6.66	15	26.6	106.0
1.5	0.213	1.33	5.33	12	21.33	85.3
1.6	0.2	1.25	5	11.25	20	80